

**FACULTY  
OF MATHEMATICS  
AND PHYSICS**  
Charles University

**MASTER THESIS**

Bc. Jiří Ryzner

**Physical interpretation of special  
solutions of Einstein-Maxwell equations**

Institute of Theoretical Physics

Supervisor of the master thesis: RNDr. Martin Žofka, Ph.D.

Study programme: Physics

Study branch: Theoretical Physics

Prague 2016



I declare that I carried out this master thesis independently, and only with the cited sources, literature and other professional sources.

I understand that my work relates to the rights and obligations under the Act No. 121/2000 Sb., the Copyright Act, as amended, in particular the fact that the Charles University has the right to conclude a license agreement on the use of this work as a school work pursuant to Section 60 subsection 1 of the Copyright Act.

In ..... date .....

signature of the author

Title: Physical interpretation of special solutions of Einstein-Maxwell equations

Author: Bc. Jiří Ryzner

Department: Institute of Theoretical Physics

Supervisor: RNDr. Martin Žofka, Ph.D., Institute of Theoretical Physics

Abstract: In Newtonian physics, it is possible to establish static equilibrium in a system, which consists of extremal sources of gravitational and electromagnetic field. Surprisingly, this situation can occur in general relativity for black holes, too. This work examines a special case involving an infinitely long, straight, extremally charged string, studies its geometry, electrogeodesics, properties of the source and compares the solution to Newtonian physics. We also investigate an analogous situation in a dynamic spacetime with cosmological constant, and we compare it to the static version. Finally, we investigate a periodical solution of Laplace's equation corresponding to infinitely many extremal point sources distributed at regular intervals along a straight line. We study the properties of the electrostatic potential and show that in the limit of large distances from the axis formed by the sources, the solution approaches the charged string.

Keywords: general relativity, Einstein-Maxwell equations, black hole, electrogeodesic, naked singularity, classification of spacetimes, periodical spacetime

I thank everyone who supported me in this work. My biggest thanks goes to my thesis supervisor RNDr. Martin Žofka Ph.D. for a number of valuable advice, guidance and much time that we spent on consultations.



# Contents

Introduction . . . . .	3
<b>1 Charged string in classical mechanics</b>	<b>5</b>
1.1 Static solution . . . . .	6
1.2 Cylindrical radial motion . . . . .	6
1.3 Circular orbit . . . . .	7
1.4 Axial motion . . . . .	9
<b>2 Geometry of ECS</b>	<b>11</b>
2.1 Algebraic classification . . . . .	13
2.2 Symmetries . . . . .	15
2.3 Proper length, surface and volume . . . . .	15
2.3.1 Proper lengths . . . . .	15
2.3.2 Proper surface . . . . .	16
2.3.3 Proper volume . . . . .	17
<b>3 Mass, energy and charge of ECS</b>	<b>19</b>
3.1 Introduction . . . . .	19
3.2 C-energy . . . . .	20
3.3 Landau-Lifshitz . . . . .	22
3.4 Brown-York mass . . . . .	23
3.5 Komar mass . . . . .	24
3.6 Charge of cylinder . . . . .	24
3.7 Summary of results for mass and charge . . . . .	25
<b>4 Equations of motion</b>	<b>27</b>
4.1 Static electrogeodesics . . . . .	28
4.2 Radial electrogeodesics . . . . .	30
4.2.1 Photon motion . . . . .	30
4.2.2 Electrogeodesic . . . . .	31
4.3 Circular electrogeodesics . . . . .	35
4.3.1 Photon motion . . . . .	35
4.3.2 Charged mass particle . . . . .	36
4.4 Electrogeodesics parallel to $z$ -axis . . . . .	41
<b>5 The Newtonian limit</b>	<b>45</b>
5.1 $K < 0$ . . . . .	45
5.2 $K > 0$ . . . . .	45
<b>6 Summary of ECS</b>	<b>47</b>
<b>7 Geometry of ECS with a cosmological constant</b>	<b>49</b>
7.1 Algebraic classification . . . . .	50
7.2 Mass . . . . .	51
7.2.1 Landau-Lifschitz . . . . .	51
7.2.2 Charge . . . . .	52

<b>8 Grid spacetime</b>	<b>53</b>
8.1 Superposition of point charges . . . . .	53
8.1.1 Convergence . . . . .	54
8.2 Separated potential . . . . .	55
8.2.1 Convergence . . . . .	57
<b>Conclusion</b>	<b>61</b>
<b>Appendix</b>	<b>63</b>
<b>Bibliography</b>	<b>83</b>



# Introduction

One of important analytical solutions of Einstein-Maxwell equations is the Majumdar-Papapetrou solution [1], [2], which represents an arbitrary finite set of stationary, extremally charged black holes in equilibrium. The spacetime is described by a single function, which is a solution of Laplace's equation. Hartle and Hawking [3] assumed a flat spatial infinity and showed that any solution to the Laplace equation with non point-like sources must contain a naked singularity. There are, however, interesting classes of solutions of different asymptotics. In this thesis we assume a line source that extends to infinity along a straight line and we thus do not have a flat spatial infinity. Our goal is to interpret this spacetime and its parameters.

We first investigate an analogous solution in classical physics. Then we calculate electrogeodesic motion of charged test particles and trajectories of photons and look for horizons. We also find the properties of the singularities and at the end we investigate the Newtonian limit.

Kastor and Traschen [4] found that the static Majumdar-Papapetrou solution with a discrete number of black holes can be extended to a non-static case with a positive cosmological constant. We generalize the extremal charged line, too, investigate its geometry and compare it to the static case. Finally, we study a spacetime constructed of an infinite number of extremal point sources. We look at its geometry and compare it to the line source.

## Conventions

We use formalism of general relativity, Einstein summation convention is used. Greek indices have values from 0 to 3 and can be also labelled by coordinates. The spacetime metric tensor is denoted as  $g_{\mu\nu}$  and has signature  $(-, +, +, +)$ . Tetrad components are written using round brackets, e.g.  $A_{(t)}$ . Symmetrization of two or more indices is denoted with round brackets and antisymmetrization with square brackets:

$$B_{(\mu\nu)} = \frac{1}{2} (B_{\mu\nu} + B_{\nu\mu}), B_{[\mu\nu]} = \frac{1}{2} (B_{\mu\nu} - B_{\nu\mu}). \quad (1)$$

Partial derivatives are denoted by  $\partial$  or a comma,

$$\frac{\partial f}{\partial x} = \partial_x f = f_{,x}. \quad (2)$$

In classical physics the dot denotes derivative with respect to time  $t$ , in GR it denotes derivative with respect to affine parameter  $\tau$ . Covariant derivative is denoted with semicolon and is chosen so that it annihilates the metric and is torsion-free. Christoffel symbols  $\Gamma$  are defined as

$$\Gamma_{\mu\nu\lambda} = \frac{1}{2} (g_{\mu\nu,\lambda} + g_{\lambda\mu,\nu} - g_{\nu\lambda,\mu}). \quad (3)$$

The Riemann tensor is defined as the commutator of the second covariant derivatives of a vector field:

$$v^\mu{}_{;\nu\lambda} - v^\mu{}_{;\lambda\nu} = R^\mu{}_{\alpha\lambda\nu} v^\alpha, \quad (4)$$

or, explicitly

$$R_{\mu\nu\kappa\lambda} = \frac{1}{2} (g_{\mu\lambda,\nu\kappa} + g_{\nu\kappa,\mu\lambda} - g_{\mu\kappa,\nu\lambda} - g_{\nu\lambda,\mu\kappa}) + g_{\alpha\sigma} \left( \Gamma_{\mu\lambda}^{\alpha} \Gamma_{\nu\kappa}^{\sigma} - \Gamma_{\mu\kappa}^{\alpha} \Gamma_{\nu\lambda}^{\sigma} \right). \quad (5)$$

Ricci tensor and Ricci scalar are defined

$$Ric_{\alpha\beta} = R^{\mu}_{\alpha\mu\beta}, R = Ric^{\alpha}_{\alpha}. \quad (6)$$

The Weyl tensor is defined as

$$\begin{aligned} C_{\kappa\lambda\mu\nu} &= R_{\kappa\lambda\mu\nu} + \frac{1}{2} (Ric_{\lambda\mu} g_{\kappa\nu} + Ric_{\kappa\nu} g_{\lambda\mu} - Ric_{\lambda\nu} g_{\kappa\mu} - Ric_{\kappa\mu} g_{\lambda\nu}) + \\ &+ \frac{R}{6} (g_{\kappa\mu} g_{\lambda\nu} - g_{\kappa\nu} g_{\lambda\mu}). \end{aligned} \quad (7)$$

Einstein equations with a cosmological constant  $\Lambda$  are of the form

$$Ric_{\mu\nu} - \frac{R}{2} g_{\mu\nu} + \Lambda g_{\mu\nu} = 8\pi T_{\mu\nu}. \quad (8)$$

We use stress energy  $T$  tensor of electromagnetic field  $F$  constructed from four-potential  $A$

$$F = dA \Leftrightarrow F_{\mu\nu} = A_{\nu;\mu} - A_{\mu;\nu}. \quad (9)$$

Maxwell equations with source current  $J^{\mu}$  for electromagnetic tensor read

$$F^{\mu\nu}_{;\nu} = 4\pi J^{\mu}, F_{\mu\nu;\lambda} + F_{\lambda\mu;\nu} + F_{\nu\lambda;\mu} = 0. \quad (10)$$

Finally, stress energy tensor of electromagnetic field is defined as

$$T^{\mu\nu} = \frac{1}{4\pi} \left( F^{\mu}_{\beta} F^{\nu\beta} - \frac{\mathcal{F}}{4} g_{\mu\nu} \right), \mathcal{F} = F_{\mu\nu} F^{\mu\nu}. \quad (11)$$

Hodge dual is denoted with  $*$  and, for a totally antisymmetric form  $\sigma$  of order  $p$ , it is defined as

$$(*\sigma)_{\beta_1 \dots \beta_{d-p}} = \frac{1}{p!} \sigma^{\alpha_1 \dots \alpha_p} \epsilon_{\alpha_1 \dots \alpha_p \beta_1 \dots \beta_{d-p}}. \quad (12)$$

## Congruences

To investigate (electro-)geodesics, we calculate the properties of congruences. For a timelike congruence with a tangent unit vector field  $u^{\mu}$  (it does not need to be geodesic) we define

$$\Theta_{\mu\nu} \equiv u_{(\mu;\nu)} + a_{(\mu} u_{\nu)}, \Omega_{\mu\nu} \equiv u_{[\mu;\nu]} + a_{[\mu} u_{\nu]}, h_{\mu\nu} \equiv g_{\mu\nu} + u_{\mu} u_{\nu}, \quad (13)$$

$$\sigma_{\mu\nu} \equiv \Theta_{\mu\nu} - \frac{1}{3} \Theta h_{\mu\nu}, \Theta \equiv \Theta^{\mu}_{\mu}, \Omega^2 \equiv \frac{1}{2} \Omega_{\mu\nu} \Omega^{\mu\nu}, \sigma^2 \equiv \frac{1}{2} \sigma_{\mu\nu} \sigma^{\mu\nu}, \quad (14)$$

where  $\Theta$  is expansion scalar,  $\sigma_{\mu\nu}$  is shear tensor,  $\Theta_{\mu\nu}$  is expansion tensor,  $\Omega_{\mu\nu}$  is vorticity tensor and  $h_{\mu\nu}$  is metric on three-surfaces perpendicular to  $u^{\mu}$  and with the acceleration  $a^{\mu}$ . For null geodesic congruence of velocity  $k^{\mu}$ , using arbitrary null field  $l^{\mu}$  such as  $k^{\mu} k_{\mu} = l^{\mu} l_{\mu} = 0, k^{\mu} l_{\mu} = -1$ , we can define these quantities in similar way:

$$h_{\mu\nu} \equiv g_{\mu\nu} + k_{\mu} l_{\nu} + l_{\mu} k_{\nu}, \sigma_{\mu\nu} \equiv \Theta_{\mu\nu} - \frac{1}{2} \Theta h_{\mu\nu}, \quad (15)$$

$$\Theta_{\mu\nu} \equiv h^{\alpha}_{(\mu} h^{\beta}_{\nu)} k_{\alpha;\beta}, \Omega_{\mu\nu} \equiv h^{\alpha}_{[\mu} h^{\beta}_{\nu]} k_{\alpha;\beta}. \quad (16)$$

Here  $h_{\mu\nu}$  is metric on two-surfaces perpendicular to  $k^{\mu}$  and  $l^{\mu}$ . Quantities  $\Omega^2, \sigma^2, \Theta$  are defined in the same way as in timelike case.

# 1. Charged string in classical mechanics

Our classical system consists of static infinite rod, which has constant linear mass and charge densities. It is located along the  $z$ -axis. To find the electric and gravitational potentials of the rod, we have to solve Poisson's equation (outside of the source)

$$\varphi_{,xx} + \varphi_{,yy} + \varphi_{,zz} = 0, \quad (1.1)$$

for both potentials. Assuming cylindrical symmetry, we obtain solutions

$$\varphi_G = \mu \ln \frac{x^2 + y^2}{P_1^2}, \varphi_E = -\lambda \ln \frac{x^2 + y^2}{P_2^2}, \quad (1.2)$$

where constant  $\mu$  is mass per unit length,  $\lambda$  is charge per unit length,  $\varphi_G$  is gravitational potential and  $\varphi_E$  is electrostatic potential. The constants  $P_1, P_2$  determine the surfaces of vanishing potentials. However, we can rewrite  $P_2$  using  $P_1$ , so a new constant term appears in one of the potentials, which will not affect Euler-Lagrange equations governing test-particle motion. Thus we take without loss of generality  $P_1 = P_2 \equiv P$ . From this point, we will use dimensionless coordinates, with  $x_i/P \rightarrow x_i$ , and we will work in the CGS unit system. Before writing the Lagrangian, we introduce cylindrical coordinates

$$\rho \equiv \sqrt{x^2 + y^2}, \phi \equiv \arctan \frac{y}{x}. \quad (1.3)$$

Then the gravitational potential  $\varphi_G$  and electrostatic potential  $\varphi_E$  read

$$\varphi_G = 2\mu \ln \rho, \varphi_E = -2\lambda \ln \rho. \quad (1.4)$$

Now it can be easily seen that  $\lambda$  is indeed the linear charge density:

$$\frac{Q}{\epsilon_0} = \oint_S E^i n_i dS = - \oint_S \varphi_{E,i} n^i dS = \int_0^{2\pi} \int_0^h 2\lambda d\phi dz = 4\pi\lambda h. \quad (1.5)$$

The classical Lagrangian per unit mass and divided by  $P^2$  for test massive charged particle with charge-to-mass ratio  $q$  is

$$\mathcal{L} = \frac{1}{2} \left( \dot{\rho}^2 + \rho^2 \dot{\phi}^2 + \dot{z}^2 \right) - (q\varphi_E + \varphi_G). \quad (1.6)$$

The Lagrangian does not depend on  $\phi, z$  and does not explicitly depend on  $t$ , so we have the following integrals of motion:

$$E \equiv \sum_i \frac{\partial \mathcal{L}}{\partial \dot{q}_i} \dot{q}_i = \frac{1}{2} \left( \dot{\rho}^2 + \rho^2 \dot{\phi}^2 + \dot{z}^2 \right) + \varphi_G + q\varphi_E = \quad (1.7)$$

$$= \frac{1}{2} \left( \dot{\rho}^2 + \rho^2 \dot{\phi}^2 + \dot{z}^2 \right) + 2\mathcal{A} \ln \rho,$$

$$L_z \equiv \frac{\partial \mathcal{L}}{\partial \dot{\phi}} = \rho^2 \dot{\phi}, \quad (1.8)$$

$$p_z \equiv \frac{\partial \mathcal{L}}{\partial \dot{z}} = \dot{z}, \quad (1.9)$$

where we defined

$$\mathcal{A} \equiv \mu - q\lambda. \quad (1.10)$$

Thanks to the integrals of motion, the equation for  $\rho$  reads

$$\rho^2 \dot{\phi}^2 - \rho \ddot{\rho} - 2\mathcal{A} = 0, \quad (1.11)$$

and it is time derivative of (1.7) if we put in definitions of integrals of motion.

## 1.1 Static solution

For simplicity we search for static solutions first. By setting coordinate derivatives to zero, we obtain the condition

$$\mathcal{A} = E = p_z = L_z = 0, \quad (1.12)$$

which can be seen from eq. (1.7) - (1.11). The first condition is derived from (1.11) and is restriction for charge-to-mass ratio  $q$  of the test particle. We see that if the rod is charged extremally, i.e.,  $\mu = \lambda$ , the test particle has to be charged extremally, too. We use the term ‘extremal’ due to the fact that a Reissner-Nordström black hole with  $Q = M$  has a degenerate, extremal horizon and adding any further charge will produce a naked singularity.

## 1.2 Cylindrical radial motion

In case of cylindrical radial motion, where  $z$  and  $\phi$  are constant, we obtain

$$E = \frac{1}{2} [\dot{\rho}^2 + 4\mathcal{A} \ln \rho], L_z = p_z = 0, \quad (1.13)$$

where the equation for  $\rho$  can be rewritten as

$$\dot{\rho}^2 = 2 [E - 2\mathcal{A} \ln \rho], \quad (1.14)$$

where the right-hand side can be understood as effective potential. The motion then is possible if and only if the right side is non-negative. If the motion is not free, i.e.,  $\mathcal{A}$  does not vanish, there exists a turning point, which can be found by solving  $\dot{\rho} = 0$ :

$$\rho_{tp} = \exp \frac{E}{2\mathcal{A}}. \quad (1.15)$$

It is not possible to be static there, since radial acceleration for non-free solution reads

$$\mathcal{A} \neq 0 \Rightarrow \ddot{\rho} = -\frac{2\mathcal{A}}{\rho} \neq 0. \quad (1.16)$$

Thus if  $\mathcal{A} < 0$ , the radial acceleration is greater than zero and forces the particle to escape to infinity. Rewriting the radius as  $\rho(t) = \rho_{tp} \exp [\mathcal{R}(t)]$ , we have

$$\rho_{tp}^2 \exp [\mathcal{R}(t)] \dot{\mathcal{R}}^2(t) = -4\mathcal{A}\mathcal{R}(t) \Rightarrow \mathcal{A}\mathcal{R}(t) \leq 0, \quad (1.17)$$

so the motion for  $\mathcal{A} < 0$  is possible only above the turning radius, as  $\mathcal{R} \geq 0$  and thus  $\rho \geq \rho_{tp}$ . The same argument is used for  $\mathcal{A} > 0$ , where the acceleration is

negative and forces the particle to fall upon the charged string, and from previous equation we see that motion is possible only for  $\mathcal{R} \leq 0$ . From the expressions of radial velocity and acceleration we see that velocity increases when particle moves from charged string, but the acceleration decreases. So there exist three solutions, which are summarized in Table 1.1.

$E$	$\mathcal{A}$	$\rho$	Description of motion	End of motion ( $\rho$ )
$E \in \mathbb{R}$	$\mathcal{A} < 0$	$\rho \geq \rho_{tp}$	Away from rod	$\infty$
$E \geq 0$	$\mathcal{A} = 0$	$\rho > 0$	Free motion	0 or $\infty$
$E \in \mathbb{R}$	$\mathcal{A} > 0$	$\rho \leq \rho_{tp}$	Vicinity of rod	0

Table 1.1: Regions, where classical cylindrical radial motion is possible.

At the end we present analytical solutions in each region, using parametrization  $\rho(t) = \rho_{tp} \exp \mathcal{R}(t)$  for non-free solutions:

$$\mathcal{R}(t) = \begin{cases} \left[ \operatorname{erfi}_{-1} \left( \sqrt{-\frac{\mathcal{A}}{\pi}} \frac{2(t_0-t)}{\rho_{tp}} \right) \right]^2, & \mathcal{A} < 0, \\ - \left[ \operatorname{erf}_{-1} \left( 1 - \sqrt{\frac{\mathcal{A}}{\pi}} \frac{2(t-t_f)}{\rho_{tp}} \right) \right]^2, & \mathcal{A} > 0, \end{cases}$$

where  $\operatorname{erf}(x)$  is the error function (A.1) and  $\operatorname{erfi}(x)$  is the imaginary error function (A.2). We can check the consistency of non-free solutions.

First let us check region  $\rho \leq \rho_{tp}$ . Argument of  $\operatorname{erf}_{-1}(x)$  is equal to minus one for

$$t_i = t_f - \sqrt{\frac{\mathcal{A}}{\pi}} \rho_{tp}, \lim_{t \rightarrow t_i} \rho(t) = 0, \quad (1.18)$$

which would correspond to particle emitted by charged string. Argument of  $\operatorname{erf}_{-1}(x)$  is one for  $t = t_f$ , for which  $\lim_{t \rightarrow t_f} \rho(t) = 0$  and corresponds to final time, at which particle ends in charged string. In the region  $\rho \geq \rho_{tp}$  the time  $t \rightarrow \pm\infty$  corresponds to  $\rho \rightarrow \infty$  and  $t = t_0$  corresponds to  $\rho = \rho_{tp}$ .

### 1.3 Circular orbit

For a circular orbit, where  $\rho$  and  $z$  are constant, we obtain the following equations of motion

$$2\mathcal{A} = \rho^2 \dot{\phi}^2, \quad (1.19)$$

$$L_z = \rho^2 \dot{\phi}, p_z = 0, \quad (1.20)$$

$$E = \frac{1}{2} \left[ \rho^2 \dot{\phi}^2 + 4\mathcal{A} \ln \rho \right]. \quad (1.21)$$

Since  $L_z$  is constant, it is clear that  $\dot{\phi}$  has to be time-independent, too. We denote  $\omega = \dot{\phi}$ . Then we express  $\omega$  and substitute in the first equation, from which we obtain dependence of radius on particle parameters. The solution can be summarized as

$$\phi = \omega t + \phi_0, \rho^2 = \frac{L_z^2}{2\mathcal{A}}, \mathcal{A} > 0, \quad (1.22)$$

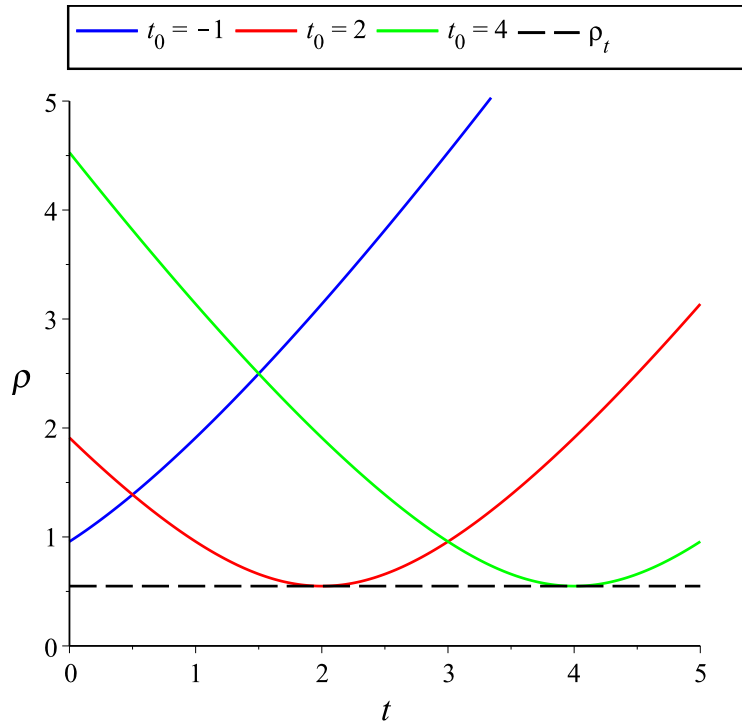


Figure 1.1: Cylindrical radial motion - dependence of cylindrical radius on time for  $E = 0.3, q = 0.5, \mu = 0.25, \lambda = 1$  for various starting radii.

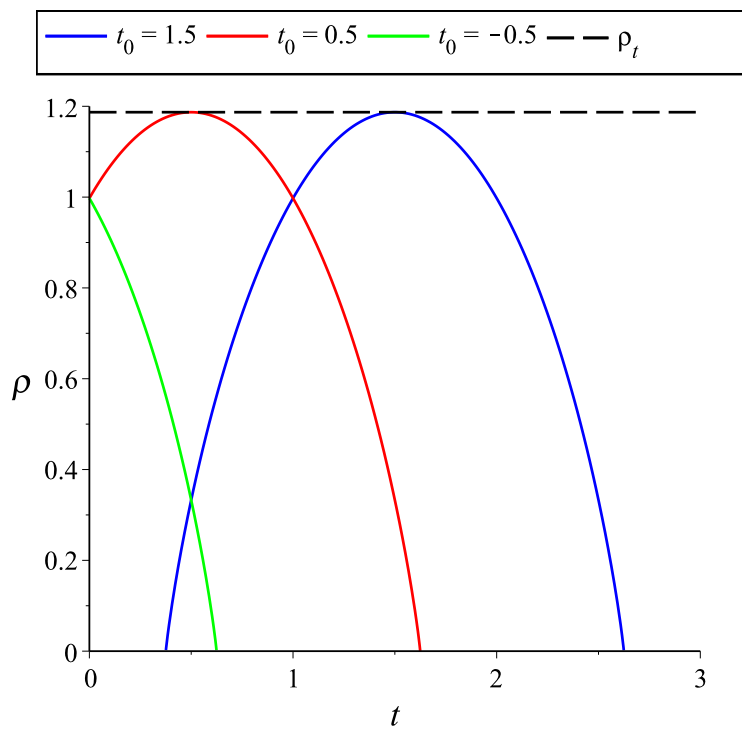


Figure 1.2: Cylindrical radial motion - dependence of cylindrical radius on time for  $E = 0.3, q = 0.5, \lambda = 0.25, \mu = 1$  for various starting radii.

where the angular velocity reads

$$\omega^2 = \frac{L_z^2}{\rho^4} = 4\frac{\mathcal{A}^2}{L_z^2} = 2\frac{\mathcal{A}}{\rho^2}, \mathcal{A} > 0. \quad (1.23)$$

For a neutral particle, i.e.,  $q = 0$ , we get  $\mathcal{A} = \mu$  and circular motion is possible if  $\mu > 0$ . The situation  $\mathcal{A} = 0$  corresponds to a static position in (1.12). We see from (1.19) that circular motion is not possible for  $\mu < q\lambda$ , i.e.  $\mathcal{A} < 0$ .

## 1.4 Axial motion

For pure motion along the  $z$ -axis ( $\rho$  and  $\phi$  are constant), we obtain equations

$$\mathcal{A} = 0, L_z = 0, p_z = \dot{z}. \quad (1.24)$$

The solution is

$$z(t) = p_z t + z_0, L_z = 0, \mathcal{A} = 0, E = \frac{p_z^2}{2}, \quad (1.25)$$

and does not depend on  $\rho$  or  $\phi$ . We see that only a particle, which is extremally charged, can move along the  $z$ -axis, and it moves as a free particle.





## 2. Geometry of ECS

In the previous section we constructed a massive charged infinite string in classical physics. If we put  $\lambda = \mu$ , we can translate this classical solution to general relativity, resulting in the Majumdar-Papapetrou solution interpreted by Hartle and Hawking in [3]. The electrostatic potential, denoted  $U$ , will enter the metric and four-potential in the following way

$$ds^2 = -U^{-2}dt^2 + U^2 d\vec{x} \cdot d\vec{x}, U = U(x, y), \quad (2.1)$$

and we assume cylindrical symmetry of function  $U$ . The electromagnetic four-potential is defined as

$$A = \frac{dt}{U}. \quad (2.2)$$

Given these tensors, we can proceed to compute Maxwell and Einstein equations. We get only one independent equation

$$U_{,xx} + U_{,yy} = 0 \Rightarrow U(x, y) = 1 + \frac{K}{2} \ln \frac{x^2 + y^2}{P^2}, \quad (2.3)$$

where  $K, P$  are constants. Constant  $P$  determines where  $U$  is zero and plays only the role of a dimensional factor, and  $K$  is the parameter we wish to interpret and which will play the main role in our interpretation of charge and mass of the field source. The constant 1 is chosen in such a way that the limit  $K \rightarrow 0$  represents a formal limit to Minkowski space. As in the previous section, we will work in dimensionless coordinates  $x^\mu \rightarrow x^\mu/P$  and use dimensionless metric element  $ds^2/P^2 \rightarrow ds^2$ . So the function  $U$  can be written

$$U(x, y) = 1 + \frac{K}{2} \ln(x^2 + y^2), \quad (2.4)$$

and we got rid of the parameter  $P$ . In Cartesian coordinates we have a coordinate basis

$$\mathbf{E}_{(t)} = \partial_t, \mathbf{E}_{(x)} = \partial_x, \mathbf{E}_{(y)} = \partial_y, \mathbf{E}_{(z)} = \partial_z, \quad (2.5)$$

and choose a normalized tetrad

$$\mathbf{e}_{(t)} = \sqrt{U^2} \mathbf{E}_{(t)}, \mathbf{e}_{(x)} = \frac{\mathbf{E}_{(x)}}{\sqrt{U^2}}, \mathbf{e}_{(y)} = \frac{\mathbf{E}_{(y)}}{\sqrt{U^2}}, \mathbf{e}_{(z)} = \frac{\mathbf{E}_{(z)}}{\sqrt{U^2}}, \quad (2.6)$$

where  $U$  is expressed in  $x, y$ . Since the metric is cylindrically symmetric, it is useful to transform to cylindrical coordinates

$$\rho = \sqrt{x^2 + y^2}, \phi = \text{arctg} \frac{y}{x}. \quad (2.7)$$

After the transformation we find

$$U(\rho) = 1 + K \ln \rho, \quad (2.8)$$

$$ds^2 = -\frac{dt^2}{U^2} + U^2 (d\rho^2 + \rho^2 d\phi^2 + dz^2), \quad (2.9)$$

$$F = \frac{U_{,\rho}}{U^2} dt \wedge d\rho, \mathcal{F} = F_{\mu\nu} F^{\mu\nu} = -2 \frac{U_{,\rho}^2}{U^4}, \quad (2.10)$$

$$T_{\mu\nu} = \frac{U_{,\rho}^2}{8\pi U^6} \text{diag}(1, -U^4, \rho^2 U^4, U^4), T_\mu^\mu = 0. \quad (2.11)$$

In the cylindrical coordinate system we have a coordinate basis

$$\mathbf{E}_{(t)} = \partial_t, \mathbf{E}_{(\rho)} = \partial_\rho, \mathbf{E}_{(\phi)} = \partial_\phi, \mathbf{E}_{(z)} = \partial_z, \quad (2.12)$$

and choose a tetrad

$$\mathbf{e}_{(t)} = \sqrt{U^2} \mathbf{E}_{(t)}, \mathbf{e}_{(\rho)} = \frac{\mathbf{E}_{(\rho)}}{\sqrt{U^2}}, \mathbf{e}_{(\phi)} = \frac{\mathbf{E}_{(\phi)}}{\rho \sqrt{U^2}}, \mathbf{e}_{(z)} = \frac{\mathbf{E}_{(z)}}{\sqrt{U^2}}, \quad (2.13)$$

where  $U$  is expressed in terms of  $\rho$ . The non-trivial independent components of Riemann tensor are

$$R_{\rho t \rho t} = \frac{K(1+3K+K \ln \rho)}{\rho^2(1+K \ln \rho)^4}, R_{\phi t \phi t} = -\frac{K(1+K+K \ln \rho)}{(1+K \ln \rho)^4}, \quad (2.14)$$

$$R_{\phi \rho \phi \rho} = K^2, R_{z t z t} = -\frac{K^2}{\rho^2(1+K \ln \rho)^4},$$

$$R_{z \rho z \rho} = \frac{K(1+K+K \ln \rho)}{\rho^2}, R_{z \phi z \phi} = -K(1+K+K \ln \rho),$$

and the tetrad components are

$$R_{(\rho)(t)(\rho)(t)} = \frac{K(1+3K+K \ln \rho)}{\rho^2(1+K \ln \rho)^4}, \quad (2.15)$$

$$R_{(\phi)(\rho)(\phi)(\rho)} = -R_{(z)(t)(z)(t)} = \frac{K^2}{\rho^2(1+K \ln \rho)^4},$$

$$R_{(z)(\rho)(z)(\rho)} = -R_{(\phi)(t)(\phi)(t)} = -R_{(z)(\phi)(z)(\phi)} = \frac{K(1+K+K \ln \rho)}{\rho^2(1+K \ln \rho)^4}.$$

We notice that all tetrad components of Riemann vanish for large  $\rho$ :

$$\lim_{\rho \rightarrow \infty} R_{(\alpha)(\beta)(\mu)(\nu)} = 0. \quad (2.16)$$

If we compute Kretschmann invariant  $\mathcal{K} = R_{\mu\nu\kappa\lambda} R^{\mu\nu\kappa\lambda}$  from Riemann tensor  $R$ , we obtain

$$\mathcal{K} = \frac{8K^2 \left[ 2K^2 \ln^2 \rho + 7K^2 + 2(3K+2)K \ln \rho + 6K + 2 \right]}{\rho^4 (K \ln \rho + 1)^8}. \quad (2.17)$$

From Kretschmann invariant  $\mathcal{K}$  and Maxwell invariant  $\mathcal{F}$  we can deduce two singularities. The inner singularity is located at radius  $\rho_i$  and the outer one at radius  $\rho_o$ , where

$$\rho_i = 0, \rho_o = e^{-1/K}. \quad (2.18)$$

It can be seen that the Kretschmann invariant also vanishes at large radii

$$\lim_{\rho \rightarrow \infty} R_{\mu\nu\kappa\lambda} R^{\mu\nu\kappa\lambda} = 0. \quad (2.19)$$

We also introduce two additional significant radii, which will be explained in the subsequent chapters

$$\rho_{ph} = e^{-2-1/K}, \rho_c = e^{-1-1/K}. \quad (2.20)$$

The Ricci tensor  $Ric_{\mu\nu}$  and Ricci curvature are given by formulae

$$Ric_{\mu\nu} = U^2_{,\rho} U^{-2} \text{diag} (U^{-4}, -1, \rho^2, 1), Ric_{\mu}{}^{\mu} = 0. \quad (2.21)$$

The non-trivial component of Levi-Civita pseudotensor density is

$$\epsilon_{t\rho\phi z} = \sqrt{-\det g_{\mu\nu}} = \rho U^2. \quad (2.22)$$

## 2.1 Algebraic classification

To determine the algebraic type of the spacetime, it is useful to use the Newman-Penrose formalism [5]. We set up a null tetrad consisting of two real null vector fields  $k^\mu, l^\mu$  and two complex null vector fields  $m^\mu, \bar{m}^\mu$ , where  $\bar{m}^\mu$  is complex conjugate of  $m^\mu$ . They are normalized as follows

$$k_\mu l^\mu = -1, \bar{m}^\mu m_\mu = 1, \quad (2.23)$$

with all other scalar products vanishing. We choose a null tetrad as

$$\begin{aligned} k^\mu &= \frac{1}{\sqrt{2}} \left( \mathbf{e}_{(t)}^\mu - \mathbf{e}_{(\rho)}^\mu \right), l^\mu = \frac{1}{\sqrt{2}} \left( \mathbf{e}_{(t)}^\mu + \mathbf{e}_{(\rho)}^\mu \right), \\ m^\mu &= \frac{1}{\sqrt{2}} \left( i \mathbf{e}_{(\phi)}^\mu - \mathbf{e}_{(z)}^\mu \right), \bar{m}^\mu = -\frac{1}{\sqrt{2}} \left( i \mathbf{e}_{(\phi)}^\mu + \mathbf{e}_{(z)}^\mu \right). \end{aligned} \quad (2.24)$$

Using Weyl tensor  $C_{\alpha\beta\mu\nu}$ , we can calculate Weyl scalars [5]

$$\psi_0 \equiv C_{\alpha\beta\mu\nu} k^\alpha m^\beta k^\mu m^\nu = \frac{U_{,\rho}}{2\rho U^3}, \quad (2.25)$$

$$\psi_1 \equiv C_{\alpha\beta\mu\nu} k^\alpha l^\beta k^\mu m^\nu = 0, \quad (2.26)$$

$$\psi_2 \equiv C_{\alpha\beta\mu\nu} k^\alpha m^\beta \bar{m}^\mu l^\nu = \frac{6\rho U_{,\rho}^2 + U(U_{,\rho} - 2\rho U_{,\rho\rho})}{6\rho U^4}, \quad (2.27)$$

$$\psi_3 \equiv C_{\alpha\beta\mu\nu} l^\alpha k^\beta l^\mu \bar{m}^\nu = 0, \quad (2.28)$$

$$\psi_4 \equiv C_{\alpha\beta\mu\nu} l^\alpha \bar{m}^\beta l^\mu \bar{m}^\nu = \frac{U_{,\rho}}{2\rho U^3}. \quad (2.29)$$

Or explicitly

$$\psi_0 = \psi_4 = \frac{K}{2\rho^2 (1 + K \ln \rho)^3}, \psi_2 = \frac{K(1 + 2K + K \ln \rho)}{2\rho^2 (1 + K \ln \rho)^4}. \quad (2.30)$$

We can see that all Weyl scalars vanish in limit  $\rho \rightarrow \infty$ , thus ECS will be conformally flat for  $\rho \gg 1$ . Indeed, if we transform to a new time coordinate  $\eta$

$$\eta(t, \rho) \equiv U^2(\rho) t \Rightarrow d\eta = U^2 dt + 2UU_{,\rho} d\rho, \quad (2.31)$$

the metric transforms as

$$ds^2 = U^2 \left[ -d\eta^2 - 2\eta \frac{U_{,\rho}}{U^5} d\rho d\eta + \left( 1 - \frac{\eta^2 U_{,\rho}^2}{U^8} \right) d\rho^2 + \rho^2 d\phi^2 + dz^2 \right]. \quad (2.32)$$

The non-diagonal term vanishes for large  $\rho$  and the metric becomes

$$ds^2 \approx U^2 [-d\eta^2 + d\rho^2 + \rho^2 d\phi^2 + dz^2], \rho \gg 1, \quad (2.33)$$

which is a conformally flat metric. The metric cannot be asymptotically flat, as along the  $z$ -direction the metric does not change. We can easily see that the hypersurface where  $\rho$  is constant (but  $\rho \neq 0, \rho_0$ ) is flat.

To find out the algebraic type we search for principal null directions of the gravitational field. If  $k^\mu$  is a principal null direction, then it satisfies the equation [5]

$$k_{[\alpha} C_{\beta]\mu\nu[\delta} k_{\kappa]} k^\mu k^\nu = 0. \quad (2.34)$$

It is known that this the requirement is equivalent to condition  $\psi_0 = 0$ . However, our chosen  $k^\mu$  does not satisfy this equation. By applying a transformation to the tetrad [5], which does not change the normalization conditions (2.23),

$$k'^\mu = k^\mu + Z\bar{m}^\mu + \bar{Z}m^\mu + Z\bar{Z}l^\mu, \quad (2.35)$$

$$l'^\mu = l^\mu, m'^\mu = m^\mu + Zl^\mu, \bar{m}'^\mu = \overline{(m'^\mu)}, Z \in \mathbb{C}, \quad (2.36)$$

we can find such  $Z$  that the new vector  $k'^\mu$  will be the principal null direction. The last ingredient is a transformation of  $\psi_0$ :

$$\psi'_0 = \psi_0 - 4Z\psi_1 + 6Z^2\psi_2 - 4Z^3\psi_3 + Z^4\psi_4. \quad (2.37)$$

Thus solving equation  $\psi'_0 = 0$  for  $Z$  will yield up to four different principal null directions. In our case the equation reads

$$1 + 2\alpha Z^2 + Z^4 = 0, \alpha \equiv \frac{\psi_2}{3\psi_0}, \quad (2.38)$$

where we divided by  $\psi_0 = \psi_4$ , which is always non-zero for finite  $\rho > 0$ . General solution is

$$Z_{1,2} = \pm\sqrt{-\alpha - \sqrt{\alpha^2 - 1}}, Z_{3,4} = \pm\sqrt{-\alpha + \sqrt{\alpha^2 - 1}}. \quad (2.39)$$

In general there are four complex roots, so there are four principal null directions and thus the ECS spacetime is **type I**. The roots can be degenerate, if one of following condition is satisfied:

$$\alpha^2 - 1 = 0 \vee -\alpha \pm \sqrt{\alpha^2 - 1} = 0. \quad (2.40)$$

The second one has no solution, the first one yields two different radii

$$\rho_{D1,2} = \exp\left(-\frac{3 \mp 1 \mp 2K}{K(3 \mp 1)}\right), \quad (2.41)$$

where the spacetime is **type D**. As we have shown above, the spacetime is **type 0** in cylindrical radial infinity, which can also be seen from Weyl scalars, which vanish in the limit  $\rho \rightarrow \infty$ . However, these three-surfaces have zero measure in the spacetime. The summary is in table (2.1).

Set	Type
$\rho = \rho_{D1}$	D
$\rho = \rho_{D2}$	D
$\rho = \infty$	0
almost everywhere	I

Table 2.1: Algebraic classification of the spacetime.

## 2.2 Symmetries

In cylindrical coordinates the metric is static and it is translationally invariant in  $t$ ,  $z$  and  $\phi$ . These symmetries are given by Killing vectors  $\xi_{(t)}, \xi_{(\phi)}, \xi_{(z)}$ ,

$$\xi_{(t)}^\mu = \mathbf{E}_{(t)}^\mu, \xi_{(\phi)}^\mu = \mathbf{E}_{(\phi)}^\mu, \xi_{(z)}^\mu = \mathbf{E}_{(z)}^\mu, \quad (2.42)$$

which satisfy Killing equation

$$\xi_{\mu;\nu} + \xi_{\nu;\mu} = 0. \quad (2.43)$$

If we prescribe the most general form of  $\xi$ , where all components are general functions of all coordinates, we find that there are no more independent non-trivial Killing vectors for  $K \neq 0$ .

## 2.3 Proper length, surface and volume

### 2.3.1 Proper lengths

Let us investigate, how proper length of some curves changes with  $\rho$ . Since the metric coefficients depend only on  $\rho$ , some expressions are straightforward. The proper lengths are obtained by integrating the differential spacetime interval. Let us begin with the proper circumference of circle with constant  $\rho$ , which is

$$dl_\phi^2 = \rho^2 U^2(\rho) d\phi^2 \Rightarrow l_\phi(\rho) = 2\pi\rho|1 + K \ln \rho|. \quad (2.44)$$

Similarly, proper length of coordinate segment  $(0, h)$  parallel to the  $z$ -axis is

$$dl_z^2 = U^2(\rho) dz^2 \Rightarrow l_z(\rho) = h|1 + K \ln \rho|. \quad (2.45)$$

Length of a radial cylindrical coordinate segment specified by the coordinate interval  $(0, \rho)$ , can be integrated from

$$dl_\rho^2 = U^2(\rho) d\rho^2 \Rightarrow l_\rho(\rho) = \int_0^\rho |1 + K \ln \rho'| d\rho'. \quad (2.46)$$

To compute the integral, we need to split the integration into cases when  $\rho < \rho_o$  and  $\rho \geq \rho_o$ . The integration is also affected by the sign of  $K$ . As a result we obtain

$$l_\rho(\rho) = \begin{cases} -\rho(1 - K + K \ln \rho) \operatorname{sgn} K, & 0 < \rho < \rho_o, \\ [\rho(1 - K + K \ln \rho) + 2\rho_o] \operatorname{sgn} K, & \rho \geq \rho_o. \end{cases}$$

The plot (2.1) summarises results for lengths. We can see that radial proper length  $l_\rho$  increases monotonically and has a saddle point at the outer singularity. The proper circumference  $l_\phi$  of circle increases for  $0 < \rho < \rho_c$ , at  $\rho = \rho_c \equiv e^{-1-1/K}$  it has a maximum and then it drops to zero at outer singularity and finally rises above outer singularity. We can calculate the external curvature of a circle with  $\rho$ ,  $z$ , and  $t$  constant, and located between singularities:

$$k \equiv l_\mu^\alpha s_{;\nu}^\mu l_\alpha^\nu = s_\mu s_{;\nu}^\mu s^\nu, \quad (2.47)$$

where  $l_{\mu\nu} = s_\mu s_\nu$  is metric on the line and  $s^\mu = \mathbf{e}_{(\rho)}^\mu$  is a unit vector normal to the curve in  $S$ . We get

$$k = \frac{\rho(1 + K + K \ln \rho)}{(1 + K \ln \rho) \sqrt{(1 + K \ln \rho)^2}}, \quad (2.48)$$

which becomes zero for  $\rho = \rho_c$ . Thus we can interpret the circumference of circle  $\rho = \rho_c$  as the straightest circular line. Circles with of a smaller coordinate radius bend towards the inner singularity, whereas circles with radius  $\rho_o > \rho > \rho_c$  or  $\rho > \rho_o$  bend towards the outer singularity.

We see that  $l_z$  diverges at inner singularity, whereas  $l_\phi$  and  $l_\rho$  go to zero there. This suggest that the inner singularity is a spatially one-dimensional axis, as expected from construction from classical physics. One would expect the same behaviour for outer singularity, but we see that the proper length  $l_z$  goes to zero there. This suggests that the singularity is spatially point-like, which is also seen the from metric, if we fix time and put  $\rho = \rho_o$ .

At the end of the current subsection we summarise results in Figure 2.1, where we plot results in terms of  $\rho/\rho_o$ . The shape of curves is the same for any  $K \neq 0$ .

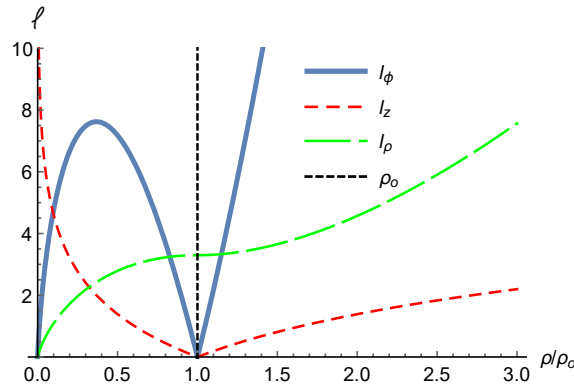


Figure 2.1: Proper length of various curves for  $K = -2, h = 1$ .

### 2.3.2 Proper surface

Another insight into geometry of ECS can be gained by investigating the geometrically privileged surfaces. ECS offers us two such surfaces.

Proper surface of cylinder base, where  $0 \leq \rho' \leq \rho, 0 \leq \phi' \leq 2\pi$  and  $t, z$  are constant, is

$$S_B = \int_0^{2\pi} \int_0^\rho \sqrt{g_{\rho\rho} g_{\phi\phi}} d\rho' d\phi' = \int_0^\rho l_\rho(\rho') l_\phi(\rho') d\rho'. \quad (2.49)$$

After substitution for  $l_\rho, l_\phi$  and integrating over  $\phi$  we get

$$S_B = 2\pi \int_0^\rho \rho' \sqrt{(1 + K \ln \rho')^4} d\rho' = 2\pi \int_0^\rho \rho' (1 + K \ln \rho')^2 d\rho'. \quad (2.50)$$

After some algebra we obtain

$$S_B = \frac{\pi}{2} \rho^2 \left[ 2 - 2K + K^2 - 2K(K - 2) \ln \rho + 2K^2 \ln^2 \rho \right]. \quad (2.51)$$

Proper surface of a cylindrical shell  $0 \leq z \leq h, 0 \leq \phi \leq 2\pi$  and  $t, \rho$  constant is

$$S_S = \int_0^{2\pi} \int_0^h \sqrt{g_{zz}g_{\phi\phi}} dz' d\phi' = l_z(\rho) l_\phi(\rho). \quad (2.52)$$

The computation is simple, as integration reduces to multiplication and we get

$$S_S = 2\pi h \rho (1 + K \ln \rho)^2. \quad (2.53)$$

We see that the proper surface of shell  $S_S$  goes to zero at both singularities, which indicates that the surface is no longer two-dimensional here. The same holds for cylinder base  $S_B$ , as it drops to zero at inner singularity and has a saddle point at outer singularity. The plot of functions is in Figure 2.2.

### 2.3.3 Proper volume

Finally we compute proper volume of static cylinder of coordinate height  $h$

$$V_C = \int_0^h \int_0^{2\pi} \int_0^\rho \sqrt{g_{\rho\rho}g_{\phi\phi}g_{zz}} d\rho' d\phi' dz' = \int_0^\rho l_\rho(\rho') l_\phi(\rho') l_z(\rho') d\rho'. \quad (2.54)$$

After substituting proper lengths, we get

$$V_C = 2\pi h \int_0^\rho \rho' \sqrt{(1 + K \ln \rho')^6} d\rho'. \quad (2.55)$$

Again we need to distinguish, if  $\rho$  is under outer singularity. Then we obtain

$$\frac{4V_C}{\pi h} = \begin{cases} -\rho^2 \left( 4U^3 - 6\rho U^2 U_{,\rho} + 6\rho^2 U U_{,\rho}^2 - 3\rho^3 U_{,\rho}^3 \right) \operatorname{sgn} K, & 0 < \rho < \rho_o, \\ \left[ 3K^3 \rho_o^2 + \rho^2 \left( 4U^3 - 6\rho U^2 U_{,\rho} + 6\rho^2 U U_{,\rho}^2 - 3\rho^3 U_{,\rho}^3 \right) \right] \operatorname{sgn} K, & \rho \geq \rho_o. \end{cases}$$

Since the formula is quite large, we do not write it using explicit form of function  $U$ . The plot of proper volume is in (2.2).

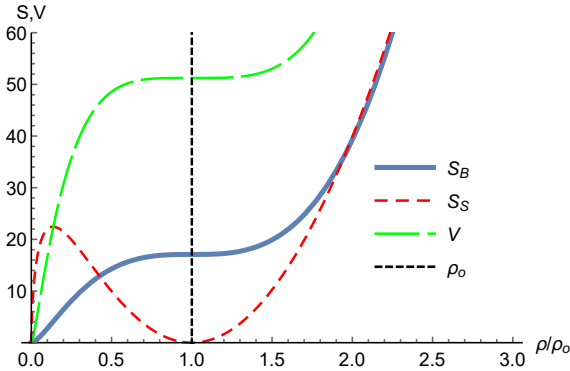


Figure 2.2: Proper surface of cylinder base and shell and proper volume of cylinder for  $K = -2, h = 1$ .





# 3. Mass, energy and charge of ECS

## 3.1 Introduction

In this section we focus on mass (energy) and charge enclosed in static cylinder. However, there is generally no way of determining locally the energy of the gravitational field in general relativity and we thus use several different definitions and compare them. The advantage of ECS is that it is static and is expressed in coordinates, where metric is diagonal and depends only on one coordinate. However, the main disadvantage is that ECS is not asymptotically flat, so for example we cannot use definition of ADM mass. We thus use several different formulae and compare mass (energy) enclosed in coordinate cylinder. Since ECS was constructed from classic string, the linear charge and mass density of which are equal, we expect this behaviour if the formal limit  $K \rightarrow 0$  is applied. At the end of this section we also compute charge enclosed in cylinder, which is defined in straightforward way, based on the flux of the field through the surface of the cylinder.

In the integral definitions  $\Sigma$  means three-volume with two-boundary  $S = \partial\Sigma$ , which encloses  $\Sigma$ . The vector  $n^\mu$  is future oriented timelike normal to  $\Sigma$ , vector  $r^\mu$  is spatial vector from  $\Sigma$  and it is normal to  $S$ , both normals are of unit length. In the following sections we choose  $\Sigma$  in terms of integration variables  $\rho', z', \phi'$  as

$$\Sigma(\rho) = \{t = 0, z' \in [0, h], \rho' \in [0, \rho], \phi' \in [0, 2\pi]\}, \quad (3.1)$$

and thus  $S$  is

$$S(\rho) = S_B(\rho, 0) \cup S_B(\rho, h) \cup S_S(\rho), \quad (3.2)$$

$$S_B(\rho, z) = \{t = 0, \rho' \in [0, \rho], z' = z, \phi' \in [0, 2\pi]\}, \quad (3.3)$$

$$S_S(\rho) = \{t = 0, \rho' = \rho, z' \in [0, h], \phi' \in [0, 2\pi]\}. \quad (3.4)$$

Since the spacetime is static and cylindrically symmetric, tensors depend only on  $\rho$ . Integral over the two bases of the cylinder either vanishes identically or the two contributions cancel each other. Thus integration over  $S$  is reduced only to integration on cylinder shell  $S_S$ . Corresponding volume and surface elements are

$$d\Sigma = \rho\sqrt{U^6}d\rho'd\phi'dz', dS_S = \rho U^2 d\phi'dz'. \quad (3.5)$$

Future-oriented normal  $n^\mu$  to  $\Sigma$  and spatial outer normal  $r^\mu$  to  $S_S$  read

$$n^\mu = e^\mu_{(t)}, r^\mu = e^\mu_{(\rho)} = \frac{1}{\sqrt{x^2 + y^2}} \left( x e^\mu_{(x)} + y e^\mu_{(y)} \right). \quad (3.6)$$

The induced metric on  $\Sigma$  denoted  $h_{\mu\nu}$  and metric on  $S_S$  denoted  $\sigma_{\mu\nu}$  are defined as

$$h_{\mu\nu} \equiv g_{\mu\nu} + n_\mu n_\nu, \sigma_{\mu\nu} \equiv h_{\mu\nu} - r_\mu r_\nu. \quad (3.7)$$

It can be seen that the metric  $h_{\mu\nu}$  on  $\Sigma$  is obtained by putting  $dt = 0$  and the metric  $\sigma_{\mu\nu}$  on surface  $S_S$  is obtained by putting  $d\rho = dt = 0$ .

## 3.2 C-energy

By an appropriate coordinate transformation in  $t, \rho$  the cylindrically symmetric metric can always be transformed to have the form

$$ds^2 = e^{2\gamma-2\psi} (-dt^2 + dR^2) + e^{2\psi} dz^2 + \alpha^2 e^{-2\psi} d\phi^2, \quad (3.8)$$

where  $R$  is radial coordinate,  $\psi, \gamma, \alpha$  are functions of  $t, R$ . The coordinates  $t, \phi, z$  are denoted the same way as in our metric since they are of the desired form with the same meaning and we only need to find a transformation for the radial coordinate. In such new coordinates then the  $C$ -energy enclosed in cylinder of coordinate radius  $R$  and coordinate height  $h$ , is defined as [8]

$$4E_C(t, R) \equiv h \left[ \gamma(t, R) - \ln \sqrt{(\alpha_{,R})^2 - (\alpha_{,t})^2} \right]. \quad (3.9)$$

The  $C$ -energy is a potential for flux vector  $P^\mu$ , which has in coordinates  $t, R$  components

$$P^0 = \frac{e^{2\psi-2\gamma}}{2\pi h \alpha} \frac{\partial E_C}{\partial R}, P^R = -\frac{e^{2\psi-2\gamma}}{2\pi h \alpha} \frac{\partial E_C}{\partial t}, P^\phi = P^z = 0. \quad (3.10)$$

and obeys covariant conservation law

$$P^\mu_{;\mu} = 0 \Rightarrow \int_{\Sigma} P^\mu n_\mu d\Sigma = 0. \quad (3.11)$$

To compute  $C$ -energy for ECS spacetime, we need to find new coordinate  $R$ , giving the metric the desired form. We apply transformation

$$\frac{dR}{d\rho} \equiv U^2(\rho) \Rightarrow R(\rho) = \left[ \rho U^2(\rho) - 2U_{,\rho}(\rho) \rho^2 [U(\rho) - \rho U_{,\rho}(\rho)] \right]. \quad (3.12)$$

From the derivative of  $R$  we see that it is always non-negative and becomes zero for  $\rho = \rho_o$ . Thus it is possible to construct a continuous inverse, i.e. function  $\rho(R)$  and which will be monotonic. The metric then takes form

$$ds^2 = U^{-2}(\rho(R)) (-dt^2 + dR^2) + U^2(\rho(R)) dz^2 + \rho^2(R) U^2(\rho(R)) d\phi^2, \quad (3.13)$$

where  $\rho(R)$  is the inverse of  $R(\rho)$ , which we are not able to express in a closed form. Now the metric has desired form, we can compare it to (3.8) and determine coefficients  $\gamma, \psi, \alpha$ .

$$e^{2\gamma-2\psi} = U^{-2}, U^2 \rho^2 = \alpha^2 e^{-2\psi}, U^2 = e^{2\psi} \Rightarrow \gamma = 0, \alpha^2 = \rho^2 U^4, \psi = \frac{\ln U^2}{2}. \quad (3.14)$$

Once we know the required functions, we can evaluate the expression for  $C$ -energy:

$$E_C(R) = -\frac{h}{8} \ln \left[ \left[ U^2(\rho(R)) + 2\rho(R) U_{,\rho}(\rho(R)) \right] \frac{d\rho}{dR} \right]^2. \quad (3.15)$$

Instead of expressing the result in terms of  $R$ , we can go back to  $\rho$  to obtain

$$E_C(\rho) = -\frac{h}{8} \ln \left[ \frac{U + 2\rho U_{,\rho}}{U} \right]^2 = -\frac{h}{8} \ln \left[ \frac{1 + 2K + K \ln \rho}{1 + K \ln \rho} \right]^2. \quad (3.16)$$

For small  $K$  we get

$$E_C(\rho) \approx h \left[ -\frac{K}{2} + \frac{1}{2} (1 + \ln \rho) K^2 + O(K^3) \right]. \quad (3.17)$$

The function is plotted in Figure 3.1. There are two singularities: one is at outer singularity and the second is on photon orbit. Limit behaviour:

$$\lim_{\rho \rightarrow 0} E_C(\rho) = 0, \lim_{\rho \rightarrow \rho_{ph}} E_C(\rho) = \infty, \lim_{\rho \rightarrow \rho_o} E_C(\rho) = -\infty, \lim_{\rho \rightarrow \infty} E_C(\rho) = 0. \quad (3.18)$$

The  $C$ -energy diverges on photon radius. However, we know that there is no singularity on photon radius and thus the  $C$ -energy diverges there because of coordinate singularity. Therefore it is useful to redefine  $C$ -energy so as to make the new  $C$ -energy  $\mathcal{E}_C$  finite there [8]:

$$\mathcal{E}_C \equiv \frac{h}{8} \left[ 1 - \exp \left( -8 \frac{E_C}{h} \right) \right] = -\frac{K(1 + K + K \ln \rho)}{2(1 + K \ln \rho)^2}. \quad (3.19)$$

The regularized  $C$ -energy  $\mathcal{E}_C$  has same signs as  $E_C$ , but it has different shape. It is positive for  $0 < \rho < \rho_c$  and diverges at outer singularity. As we approach the two singularities or radial infinity the  $C$ -energy behaves as follows:

$$\lim_{\rho \rightarrow 0} \mathcal{E}_C(\rho) = 0, \lim_{\rho \rightarrow \rho_o} \mathcal{E}_C(\rho) = -\infty, \lim_{\rho \rightarrow \infty} \mathcal{E}_C(\rho) = 0. \quad (3.20)$$

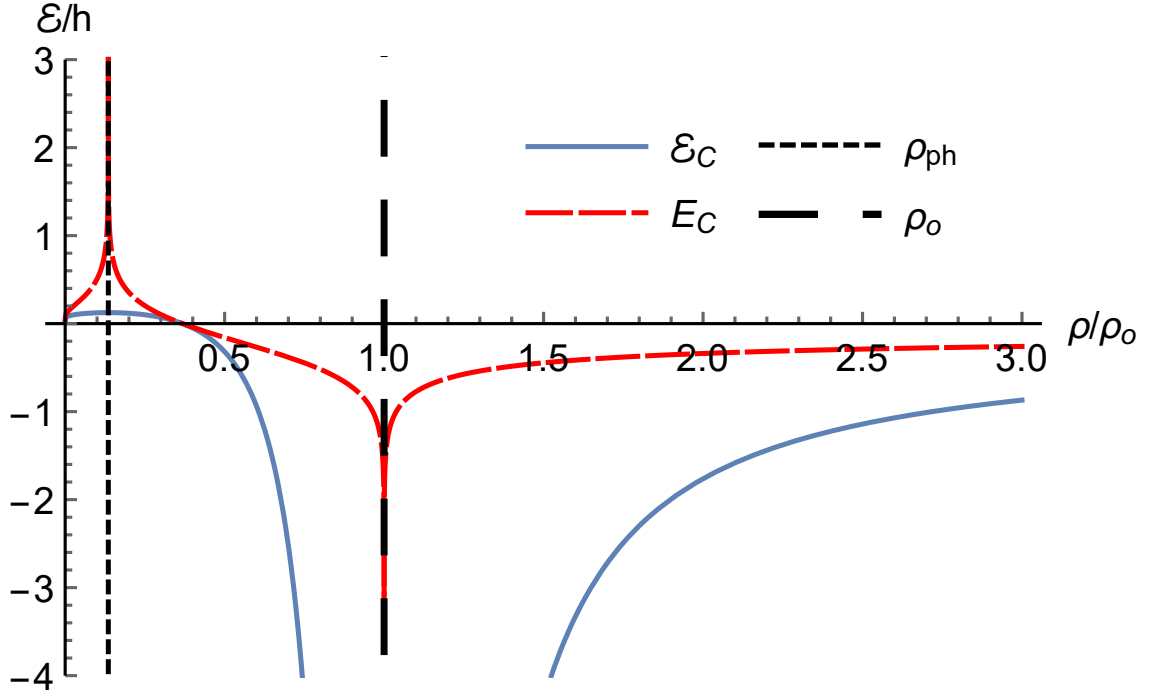


Figure 3.1:  $C$ -energy for  $|K| = 2$ .

### 3.3 Landau-Lifshitz

Landau and Lifshitz derived the conservation law [10]

$$\left[16\pi(-g)(T^{\mu\nu} + t_{LL}^{\mu\nu})\right]_{,\nu} = 0, \quad (3.21)$$

leading to a globally conserved quantity;  $g$  is metric determinant,  $t_{LL}^{\mu\nu}$  is stress–energy–momentum pseudotensor of gravitational field, which is defined as

$$16\pi t_{LL}^{\mu\nu} \equiv g^{-1} \left[ g \left( g^{\mu\nu} g^{\alpha\beta} - g^{\mu\alpha} g^{\nu\beta} \right) \right]_{,\alpha\beta} - [2R^{\mu\nu} + (2\Lambda - R)g^{\mu\nu}]. \quad (3.22)$$

It is possible to find a super-potential  $h^{\mu\nu\lambda}$ , which can be expressed via another potential  $H^{\mu\nu\lambda\kappa}$  to yield a compact form:

$$16\pi(-g)(T^{\mu\nu} + t_{LL}^{\mu\nu}) = h^{\mu\nu\lambda}_{,\lambda}, \quad h^{\mu\nu\lambda} \equiv H^{\mu\nu\lambda\kappa}_{,\kappa}, \quad (3.23)$$

$$H^{\mu\nu\lambda\kappa} \equiv (-g) \left( g^{\mu\nu} g^{\lambda\kappa} - g^{\mu\lambda} g^{\nu\kappa} \right). \quad (3.24)$$

It is thus not necessary to compute  $t_{LL}^{\mu\nu}$ , because the calculation only requires knowledge of  $H^{\mu\nu\lambda\kappa}$ . Then the total four-momentum of gravitational field and matter can be expressed as

$$P^\mu \equiv \int_{\Sigma} (-g) (T^{\mu 0} + t^{\mu 0}) d\Sigma = \frac{1}{16\pi} \oint_S H^{\mu 0 \lambda \kappa}_{,\kappa} r_{\lambda} dS. \quad (3.25)$$

Since  $t_{LL}^{\mu\nu}$  is not a tensor but a pseudotensor (or sometimes called ‘complex’), the equation (3.21) requires some gauge, and we thus compute  $H^{\mu\nu\lambda\kappa}$  in Cartesian coordinates. From the definition of total four-momentum we can see that for ECS only  $P^0$  will be non-trivial since

$$H^{i0\lambda\kappa} = g g^{i\lambda} g^{0\kappa} \Rightarrow H^{i0\lambda\kappa}_{,\kappa} = \left( g g^{i\lambda} g^{00} \right)_{,0} = 0. \quad (3.26)$$

To compute the total energy of system we calculate the integrand in Cartesian coordinates (2.1), at the end we transform back to cylindrical coordinates. Since we integrate over  $\phi$  and  $z$ , but integral depends only on  $\rho$ , the integration reduces only to multiplication. The result for our choice<sup>1</sup> of  $S$  (3.2) is

$$M_{LL} = P^0 = \frac{\hbar}{2} |K| \operatorname{sgn}(\rho_o - \rho) (1 + K \ln \rho)^6. \quad (3.27)$$

We see that  $M_{LL}$  diverges at inner singularity and at infinity, and it changes sign at outer singularity and the behaviour is the same independently of the sign of  $K$ . As we approach the two singularities or radial infinity the  $M_{LL}$  behaves as follows

$$\lim_{\rho \rightarrow 0^+} M_{LL} = \infty, \quad \lim_{\rho \rightarrow \rho_o} M_{LL} = 0, \quad \lim_{\rho \rightarrow \infty} M_{LL} = -\infty. \quad (3.28)$$

---

<sup>1</sup>For  $r^\alpha = e^\alpha_{(z)}$  we get

$$H^{\mu 0 3 \kappa}_{,\kappa} = (-g) (g^{\mu 0} g^{3 \kappa} - g^{\mu 3} g^{0 \kappa})_{,\kappa} = (-g) \left[ (g^{\mu 0} g^{33})_{,3} - (g^{\mu z} g^{00})_{,0} \right] = 0.$$

### 3.4 Brown-York mass

Definition of energy in volume  $\Sigma$ , which has boundary  $S = \partial\Sigma$ , reads [11]

$$M_T = \oint_S g_{\mu\nu} (\mathcal{E}n^\mu + j^\mu) \xi_{(t)}^\nu dS, \quad (3.29)$$

where the quantities used in the calculation are defined as follows

$$k_{\mu\nu} \equiv \sigma_\mu^\alpha \sigma_\nu^\beta r_{\alpha;\beta}, k \equiv k_{\alpha\beta} \sigma^{\alpha\beta}, 8\pi\mathcal{E} \equiv k, \quad (3.30)$$

$$16\pi\sqrt{h}j^\mu \equiv \sigma^{\mu\nu} n^\alpha p_{\nu\alpha}, 16\pi p_{\alpha\beta} \equiv \sqrt{h} (k_{\alpha\beta} - k h_{\alpha\beta}). \quad (3.31)$$

Here  $h_{\mu\nu}$  and  $\sigma_{\mu\nu}$  are metric tensors of (3.7). Tensor field  $k_{\mu\nu}$  is extrinsic curvature,  $p_{\mu\nu}$  is conjugate momentum to  $h_{\mu\nu}$ ,  $k$  is extrinsic curvature scalar. The definition of  $M$  relies on  $\mathcal{E}$ , which is surface density of energy, and  $j^\mu$  which is surface density of momentum on  $S$ . It is clear that  $j_\mu \xi_{(t)}^\mu = 0$ , since  $\xi_{(t)}^\nu$  has only the zero-th component non-vanishing and  $j^0 = 0$  by definition. Thus we do not need to compute conjugate momentum, as it will not contribute in the calculation. Therefore we integrate only

$$M_T = \oint_S \mathcal{E} n_\nu \xi_{(t)}^\nu dS = \frac{1}{8\pi} \oint_S \sigma^{\alpha\beta} r_{\alpha;\beta} n_\nu \xi_{(t)}^\nu dS. \quad (3.32)$$

Result of computation for cylinder surface (3.2) is<sup>2</sup>

$$M_T(\rho) = -h \frac{U + 2\rho U_{,\rho}}{4U} = -h \frac{1 + 2K + K \ln \rho}{4(1 + K \ln \rho)}. \quad (3.33)$$

The series for  $K \rightarrow 0$  is

$$M_T(\rho) \approx -\frac{h}{4} - \frac{hK}{2} + \frac{hK^2}{2} \ln \rho + O(K^3). \quad (3.34)$$

This result agrees with the other definitions, however it has an extra term of zero-th order. To understand this term, we need to look back to computation in article [11], where the background spacetime contribution was subtracted (in that article it was anti-de Sitter). Since in the limit  $K \rightarrow 0$  we ‘formally’ get Minkowski space, we need to subtract contribution measured on two-surface  $S$ . So the correct definition is [12]

$$M_{BY} \equiv M_T - M_0, \quad (3.35)$$

where  $M_0$  is computed as in (3.29) with Minkowski metric

$$ds_0^2 = -dt^2 + d\rho^2 + \rho^2 d\phi^2 + dz^2, \quad (3.36)$$

in cylindrical coordinates. The only non-trivial component of covariant derivative of  $r_\alpha$  in Minkowski (due to curvilinear coordinate system) is

$$r_{\phi;\phi} = \rho \Rightarrow k_0 = \frac{1}{\rho}. \quad (3.37)$$

---

<sup>2</sup>Integration over the cylinder base vanishes, as for choice  $r^\alpha = \mathbf{e}_{(z)}^\alpha$  the corresponding covariant derivative  $r_{\alpha;\beta}$  has only non-zero component  $r_{z;\rho}$ , and the summation in definition of  $k_{\alpha\beta}$  vanishes.

Finally we find the contribution from the background and thus the total mass is

$$M_0 = -\frac{h}{4} \Rightarrow M_{BY}(\rho) = h \left[ \frac{1}{4} - \frac{1 + 2K + K \ln \rho}{4(1 + K \ln \rho)} \right] = \frac{-hK}{2(1 + K \ln \rho)}. \quad (3.38)$$

Series expansion for  $K$  now gives

$$M_{BY} \approx -\frac{hK}{2} + \frac{hK^2}{2} \ln \rho + O(K^3). \quad (3.39)$$

The  $M_{BY}$  mass function vanishes on the central axis and at radial infinity:

$$\lim_{\rho \rightarrow 0^+} M_{BY} = 0, \quad \lim_{\rho \rightarrow \infty} M_{BY} = 0, \quad (3.40)$$

while at outer singularity and photon radius we find

$$\lim_{\rho \rightarrow \rho_{ph}} M_{BY} = \frac{h}{4}, \quad \lim_{\rho \rightarrow \rho_{\bar{o}}} M_{BY} = \infty, \quad \lim_{\rho \rightarrow \rho_{\bar{o}}^+} M_{BY} = -\infty. \quad (3.41)$$

### 3.5 Komar mass

For stationary spacetime the definition of mass enclosed in three-dimensional spacelike surface  $\Sigma$ , which is known as Komar mass [13], is defined as

$$M_K = \frac{1}{4\pi} \oint_S \xi_{(t)}^{\alpha;\beta} r_\alpha n_\beta dS, \quad (3.42)$$

where  $\xi_{(t)}^\beta$  is Killing vector corresponding to time symmetry. Now we plug our choice of  $S$  from (3.2) and the result is

$$M_K(\rho) = \frac{1}{4\pi} \int_0^h \int_0^{2\pi} = -\frac{h\rho U_{,\rho}}{2U}. \quad (3.43)$$

We see that this expression is same as in result from Lemos definition (3.38).

### 3.6 Charge of cylinder

Let us begin with charge, which is defined uniquely. Charge enclosed in area  $S$  is defined as

$$Q \equiv \frac{1}{4\pi} \oint_S *F = \frac{1}{4\pi} \oint_S F_{\alpha\beta} r^\alpha n^\beta dS, \quad (3.44)$$

By integrating over surface of cylinder (3.2) we get

$$Q = \frac{-hK}{2}. \quad (3.45)$$

### 3.7 Summary of results for mass and charge

Summary can be seen in Table 3.1, comparison of functions is in Figure 3.2. We notice that the signs and shape of curves are independent of  $K$ . Furthermore, the integral definitions ( $M_K, M_{BY}, M_{LL}$ ) yield the same signs both below and above the outer singularity.

The integral definitions (3.25), (3.42), (3.29) and (3.35), (3.44) are a useful tool for description of mass and charge of both singularities. These definitions change sign when we change direction of  $r^\mu$ . Since the outer singularity is one-dimensional Figure 2.1, by replacement

$$\Sigma(\rho) \rightarrow \Sigma(\rho_o) \setminus \Sigma(\rho) \Rightarrow r^\mu \rightarrow -r^\mu, \quad (3.46)$$

the integrals yield mass and charge inside cylinder, which surrounds outer singularity in the region between both singularities. Thus the outer singularity will have opposite sign of mass and charge than the inner singularity for observer between both singularities. If we want to compute properties of outer singularity for outer observer, we integrate over  $\Sigma(\rho)$  where  $\rho > \rho_o$  and the cylinder encloses only outer singularity.

Formula	$M$	0	$(0, \rho_c)$	$\rho_c$	$(\rho_c, \rho_o)$	$\rho_o$	$(\rho_o, \infty)$	$\infty$
$C$ -energy	$\mathcal{E}_C$	0	+	0	-	$-\infty$	-	0
Landau-Lifschitz	$M_{LL}$	$\infty$	+	+	+	0	-	$-\infty$
Komar, Brown-York	$M_K$	0	+	+	+	$\pm\infty$	-	0

Table 3.1: Summary of signs for different definitions of mass.

For  $K < 0$ , we see that the charge (3.45) and mass density are positive, and these properties describe the inner singularity. From (3.45) we know that the charge of cylinder with spacelike normal  $r^\mu = e_{(\rho)}^\mu$  is positive. Thus the observer between singularities will measure a positive charge of the inner singularity. If we change direction (3.46), we obtain an outer singularity with a negative charge as observed by an inner observer. Finally, the charge of the outer singularity for an external observer is positive as follows from (3.45).

For  $K > 0$  we use the same arguments and the results yield opposite signs. Thus the inner singularity has a positive mass density and negative charge density, the outer singularity has opposite mass and charge densities than the inner singularity for an inner observer. Finally, the outer singularity has a negative mass and charge density for an outer observer.

For comparison, we give here analogous results for a charged black string on a de Sitter background as found in [11]. The metric and four-potential read

$$ds^2 = -f(\rho) dt^2 + f^{-1}(\rho) d\rho^2 + \rho^2 d\phi^2 + \alpha^2 dz^2, A = -g(\rho) dt. \quad (3.47)$$

where functions  $f, g$  are defined as

$$f(\rho) = \alpha^2 \rho^2 - \frac{b}{\alpha \rho} + \frac{c^2}{\alpha^2 \rho^2}, g(\rho) = \frac{2\lambda}{\alpha \rho}. \quad (3.48)$$

The constants  $\alpha, b, c$  are defined as

$$b = 4\mu, c^2 = 4\lambda^2, \alpha^2 = -\frac{1}{3}\Lambda, \Lambda < 0. \quad (3.49)$$

The paper [11] shows that  $\mu$  and  $\lambda$  correspond to the mass and charge per unit length of the source, respectively. These quantities are constant throughout the spacetime. In ECS only the charge enclosed in any cylinder is constant, but the mass depends on the radial coordinate and varies. We must emphasize however, that the black-string solution involves a negative cosmological constant and thus its radial asymptotics is different from ECS.

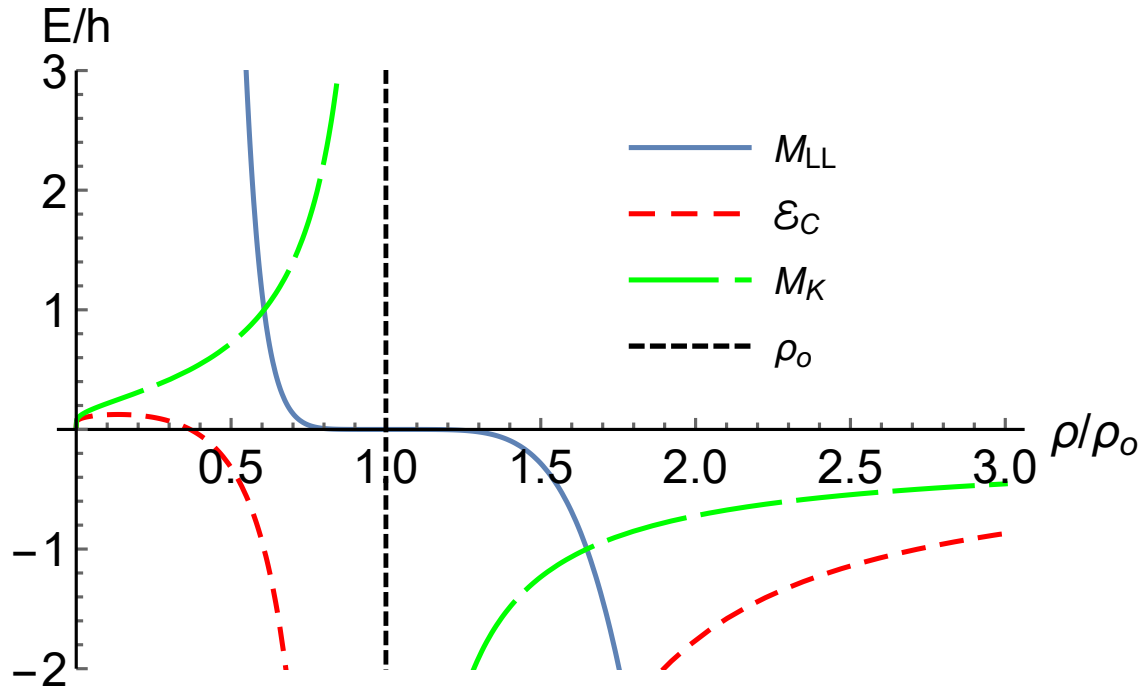


Figure 3.2: Comparison of different definitions of mass for  $|K| = 2$ .



## 4. Equations of motion

The Lagrangian for a charged particle moving on an electrogeodesics is

$$\begin{aligned}\mathcal{L} &= \frac{1}{2}g_{\mu\nu}\dot{x}^\mu\dot{x}^\nu + q\dot{x}^\kappa A_\kappa = \\ &= \frac{1}{2}\left[\left(\rho^2\dot{\phi}^2 + \dot{\rho}^2 + \dot{z}^2\right)U^2 - \frac{\dot{t}^2}{U^2}\right] + q\frac{\dot{t}}{U}.\end{aligned}\quad (4.1)$$

The Lagrangian gives equations of motion

$$\ddot{x}^\mu + \Gamma_{\alpha\beta}^\mu\dot{x}^\alpha\dot{x}^\beta = qF^\mu{}_\nu\dot{x}^\nu, \quad (4.2)$$

where the right hand-side term is the Lorentz force. The Lagrangian does not explicitly depend on  $t, \phi$  and  $z$  yielding the following integrals of motion

$$E \equiv \frac{qU - \dot{t}}{U^2}, L_z \equiv \rho^2\dot{\phi}U^2, N \equiv \dot{z}U^2. \quad (4.3)$$

Thus there remains only one equation, which is not explicitly integrated:

$$\ddot{\rho} - \rho\dot{\phi}^2 - \frac{U_{,\rho}}{U}\left[\rho^2\dot{\phi}^2 - \dot{\rho}^2 + \dot{z}^2\right] + \dot{t}U_{,\rho}\frac{qU - \dot{t}}{U^5} = 0, \quad (4.4)$$

and finally the normalization

$$\left(\rho^2\dot{\phi}^2 + \dot{\rho}^2 + \dot{z}^2\right)U^2 - \frac{\dot{t}^2}{U^2} = \mathcal{U}, \quad (4.5)$$

where  $\mathcal{U}$  is a normalization constant:  $\mathcal{U} = 0$  for photon motion and  $\mathcal{U} = -1$  for timelike motion. The equations of motion are singular, when  $U$  or  $U_{,\rho}$  is singular, diverging thus on the radii  $\rho = 0$  or  $\rho = \rho_o$ .

## 4.1 Static electrogeodesics

For simplicity we begin with static solutions. The equations of motion reduce to

$$-\frac{\dot{t}^2}{U^2} = -1, \ddot{t} = 0, (qU - \dot{t}) \dot{t} = 0. \quad (4.6)$$

The procedure is simple: the last equation yields  $t = qU\tau$  and from the first one we get a restriction on the specific charge. From the condition  $\dot{t} > 0$  we obtain four solutions, which are summarized in Table 4.1 and Figure 4.1.

$K$	$q$	$\rho$	Description of $\rho$ region
$K < 0$	$q = 1$	$0 < \rho < \rho_o$	Between singularities
	$q = -1$	$\rho_o < \rho$	Above outer singularity
$K > 0$	$q = -1$	$0 < \rho < \rho_o$	Between singularities
	$q = 1$	$\rho_o < \rho$	Above outer singularity

Table 4.1: Regions, where static electrogeodesics exist.

The auxiliary tensors describing the properties of the geodesic are as follows

$$\sigma_{\mu\nu} = \Omega_{\mu\nu} = 0, a^\mu = -\frac{U_{,\rho}}{U^3} \mathbf{E}_{(\rho)}^\mu = \frac{-K}{\rho(1 + K \ln \rho)^3} \mathbf{E}_{(\rho)}^\mu, \quad (4.7)$$

and the optical scalars read

$$\Theta = 0, \sigma^2 = \Omega^2 = 0. \quad (4.8)$$

From here we see that the congruence is expansion-free, rotation-free and shear-free. The direction of acceleration, which does not depend on sign of  $K$ , is towards the inner singularity for  $\rho < \rho_o$  and away from outer singularity for  $\rho > \rho_o$ .

Let us discuss the results for static electrogeodesics for  $K < 0$ . Between singularities the condition was  $q = 1$ , which is also an exact solution of Einstein's equations. This suggests the sources may have a charge-to-mass ratio equal to one for the inner observer. Above outer singularity the condition is  $q = -1$ , thus the outer singularity may have a charge-to-mass ratio equal to minus one, so that the particle could be static. The result is summarized in Figure 4.2. Let us continue with case  $K > 0$ , for which the signs of  $q$  change to opposite as compared to  $K < 0$ . Thus the inner and outer singularities have a charge-to-mass ratio equal to minus one for inner observer, and for the outer observer, the charge-to-mass ratio of the outer singularity is equal to one. The signs of the masses and charges is shown in Figure 4.3.

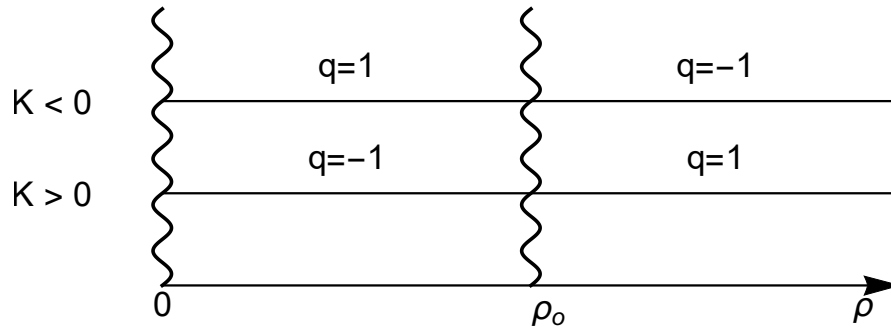


Figure 4.1: Regions, where static electrogeodesics exist for  $K \neq 0$ . Axes are not to scale. The vertical curly lines represent singularities, the horizontal lines represent radial intervals (except singularities), where the static electrogeodesics exist. We also list the required specific charge for a given radial interval and sign of  $K$ .

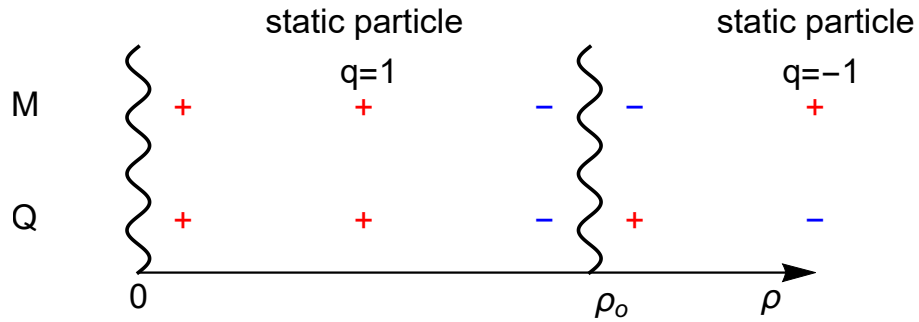


Figure 4.2: Properties of the singularities as indicated by static electrogeodesics for  $K < 0$ . We give the sign of both mass and charge of the singularities and also of the static test particle.

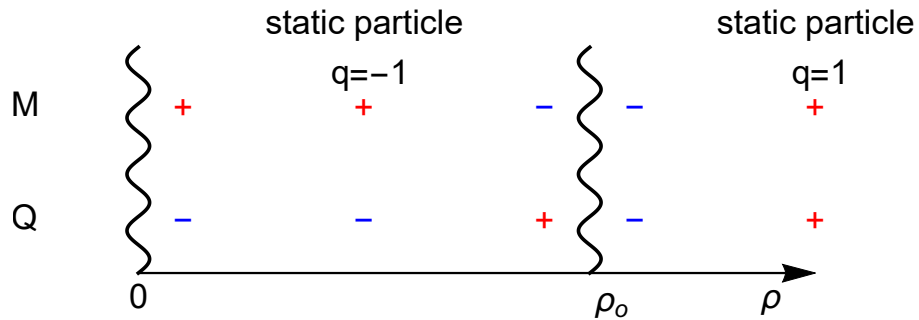


Figure 4.3: Properties of the singularities as indicated by static electrogeodesics for  $K > 0$ .

## 4.2 Radial electrogeodesics

A radial cylindrical electrogeodesics is defined as a world-line, where  $\phi$  and  $z$  are independent of proper time. Then the equations are

$$\dot{\rho}^2 U^2 - \frac{\dot{t}^2}{U^2} = \mathcal{U}, \quad (4.9)$$

$$\frac{qU - \dot{t}}{U^2} = E, \quad (4.10)$$

where the first equation is a normalization condition and the second one comes from conservation of  $E$ .

### 4.2.1 Photon motion

Null geodesics play an important role, as they reveal whether the singularities are covered by horizons. By taking  $q = \mathcal{U} = 0$  the equations (4.9) - (4.10) become equations of motion for photon. We proceed by expressing  $\dot{t}$  from second equation (4.10). From normalization then we obtain equation for  $\rho$ . We thus solve equations

$$\dot{t} = -E(1 + K \ln \rho)^2, \dot{\rho}^2 = E^2. \quad (4.11)$$

From (4.11) we immediately see that  $E < 0$ , so  $\dot{t}$  is positive. For  $E = 0$  the photon would be static. This solution reads

$$\rho_{\pm}(\tau) = r_0 \pm |E| \tau, \quad (4.12)$$

$$t_{\pm}(\tau) = t_i \mp \rho_{\pm} \left\{ 2K^2 - 2KU(\rho_{\pm}(\tau)) + U^2(\rho_{\pm}(\tau)) \right\}, \quad (4.13)$$

where  $r_0$  is the initial radius,  $t_i$  is an integration constant and  $\tau$  is affine parameter. If the photon is emitted in the direction away from the charged line, then the radial dependence is described by  $\rho_+$  and it linearly increases. If the photon is emitted in the opposite direction, then the solution is described by  $\rho_-$ . In both cases, when the photon starts towards one of the singularities, it will hit it, only photons emitted above outer singularity can avoid both singularities. There are also two interesting positions. The first one is where  $\dot{t}$  becomes zero, which happens at coordinate radius  $\rho = \rho_o$ , and the geodesic ends here and cannot be extended. The affine parameter and coordinate time on this radius are

$$\tau_o = \tau(\rho_{\pm} = \rho_o) = \pm \frac{\rho_o - r_0}{|E|}, t(\tau_o) = t_i \mp 2\rho_o K^2, \dot{t}(\tau_o) = 0. \quad (4.14)$$

This means that if a static observer would watch an object falling into the outer singularity, the object would appear to fall faster with decreasing distance from the outer singularity. The second interesting location is when  $\rho$  becomes zero and  $\dot{t}$  becomes infinite, which happens when the photon is emitted between singularities towards the inner singularity. When it reaches radius  $\rho = 0$ , the affine parameter behaves as

$$\tau(\rho_- = 0) = \tau_i = \frac{\rho_0}{E^2}, \lim_{\tau \rightarrow \tau_i} t(\tau) = t_i, \lim_{\tau \rightarrow \tau_i} \dot{t}(\tau) = \infty, \quad (4.15)$$

which also states that the geodesics ends at  $\rho = 0$  with a finite parameter  $\tau$  and cannot be extended. This also means that a static observer between both

singularities will not see the end of the fall of any object into inner singularity, and the falling object will appear to fall slower with decreasing radius. Therefore we have two regions of spacetime which are causally separated, and both singularities have no horizons and are thus naked. For congruence properties we choose a null field

$$l_{\pm}^{\mu} = -\frac{1}{2EU^2} \left( U^2 \mathbf{E}_{(t)}^{\mu} \pm \mathbf{E}_{(\rho)}^{\mu} \right), \quad (4.16)$$

where ‘ $\pm$ ’ corresponds to  $\rho_{\pm}$ . The congruence tensors read

$$a_{\pm}^{\mu} = 0, \Omega_{\pm\mu\nu} = 0, \sigma_{\pm\phi\phi} = \pm \frac{1}{2} E \rho U^2, \sigma_{\pm zz} = -\frac{1}{\rho^2} \sigma_{\pm\phi\phi}, \quad (4.17)$$

and optical scalars read

$$\sigma_{\pm}^2 = \frac{E^2}{4\rho^2}, \Omega_{\pm}^2 = 0, \Theta_{\pm} = \pm E \frac{U + 2\rho U_{,p}}{\rho U}. \quad (4.18)$$

The congruence is thus rotation-free but it is shearing and expanding.

## 4.2.2 Electrogeodesic

The equations for electrogeodesic with  $\mathcal{U} = -1$  can be integrated to

$$\dot{t} = -(1 + K \ln \rho) (E - q + EK \ln \rho), \quad (4.19)$$

$$\dot{\rho}^2 = \frac{(E - q + EK \ln \rho)^2 - 1}{(1 + K \ln \rho)^2}. \quad (4.20)$$

The motion is possible when  $\dot{t} > 0$  and  $\dot{\rho}^2 \geq 0$ , which will give restriction on parameters  $q, E, K$ . By solving  $\dot{\rho} = 0$  for  $\rho$  we obtain two turning points:

$$\rho_{t\pm} = \exp \frac{q - E \pm 1}{EK}, E \neq 0, q \neq \mp 1. \quad (4.21)$$

If  $q = -1$  then  $\rho_{t+}$  becomes outer singularity and  $\rho_{t+}$  is then not turning point, the same holds for  $q = +1 \leftrightarrow \rho_{t-}$ . It is not possible to be static on turnover radii for particles, which do not carry extremal charge, since the acceleration is non-zero here:

$$\ddot{\rho}(\tau : \rho = \rho_{t\pm}) = \pm \frac{KE^3}{\rho_{t\pm} (q \pm 1)^2} \neq 0 \text{ for } q \neq \mp 1. \quad (4.22)$$

As in classical case we can see that acceleration does not change sign thus the particle will reflect at the turning point. If we use ‘trick’ as in (1.17) and prescribe  $\rho(\tau) = \rho_o \exp \mathcal{R}(\tau)$ , the equation for  $\rho$  transform to

$$\mathcal{R}^2 \exp(2\mathcal{R}) \rho_o^2 \dot{\mathcal{R}}^2 = (EK\mathcal{R} - q)^2 - 1. \quad (4.23)$$

However, the equation is more complicated than in classical case and it is hard to find analytical solution. The equations become simpler for  $E = 0$  and read

$$\mathcal{R}^2 \exp(2\mathcal{R}) \rho_o^2 \dot{\mathcal{R}}^2 = q^2 - 1, \dot{t} = qK\mathcal{R}. \quad (4.24)$$

so for  $E = 0$  there are only two possibilities for charge. The solution reads

$$\mathcal{R}_{E=0,\pm}(\tau) = \begin{cases} 1 + W_{-1} \left[ e^{1/K-1} \sqrt{q^2 - 1} (\tau_0 \pm \tau) \right], & 0 < \rho < \rho_o, \\ 1 + W_0 \left[ e^{1/K-1} \sqrt{q^2 - 1} (\tau_0 \pm \tau) \right], & \rho > \rho_o, \end{cases}$$

where  $\tau_0$  is integration constant, ‘ $\pm$ ’ describes whether the radius is increasing or decreasing and  $W$  is Lambert W function (A.4). When the argument of Lambert W function tends to  $-\infty$ , then the radius  $\rho$  tends to zero, when the argument tends to  $e^{-1}$ , it corresponds to  $\rho_o$  and finally, when the argument tends to  $+\infty$ , the radius  $\rho$  tends to  $+\infty$  as well.

Analysing velocity in the radial directions, we can proceed without knowing an explicit analytical solution for the general case. Regions, where the motion is possible for  $K < 0$  are in Table 4.2 and for  $K > 0$  in Table 4.3. The regions are also summarized in Figure 4.4 and Figure 4.5.

We can see the particle’s behaviour as it approaches the inner/outer singularity

$$\lim_{\rho \rightarrow \rho_o} \dot{t} = 0, \lim_{\rho \rightarrow \rho_o} \dot{\rho}^2 = \infty, \lim_{\rho \rightarrow 0} \dot{t}^2 = \infty, \lim_{\rho \rightarrow 0} \dot{\rho}^2 = E^2. \quad (4.25)$$

For particles going to the radial infinity, we find

$$\lim_{\rho \rightarrow \infty} \dot{\rho}^2 = E^2, \lim_{\rho \rightarrow \infty} \dot{t} = \infty. \quad (4.26)$$

In case of uncharged particles following geodesics, we can see from Table 4.2 and Table 4.3 that there are only two admissible regions, which are summarized in Table 4.4.

Congruence properties:

$$a_{\pm}^{\mu} = -qU_{,\rho} \dot{\rho} \mathbf{E}_{(t)}^{\mu} \pm \frac{qU_{,\rho}}{U^4} \dot{t} \mathbf{E}_{(\rho)}^{\mu}, \Omega_{\pm\mu\nu} = 0, \quad (4.27)$$

$$\Omega_{\pm}^2 = 0, \Theta_{\pm} = \mp \frac{\left[ EU (U + \rho U_{,\rho}) - q \right]^2 + (U + \rho U_{,\rho}) (E\dot{t} + 1)}{\rho \dot{\rho} U^3}. \quad (4.28)$$

The shear tensor  $\sigma_{\pm\mu\nu}$  has non-zero components  $\sigma_{\pm t\rho}, \sigma_{\pm\rho\rho}, \sigma_{\pm zz}$  and scalar  $\sigma_{\pm}^2$  is non-zero, but they involve a complicated and lengthy expression and are not presented here. The congruence is thus rotation-free, but shearing.

Let us summarize our results on radial electrogeodesics. Assume a particle with  $E \neq 0$  between singularities for  $K < 0$  on the turning radius  $\rho_{t-}$ . If the particle has a specific charge  $q > 1$ , it is attracted to the outer singularity, for  $q < 1$  it is attracted to the inner singularity. If we put the charged particle above the outer singularity at radius  $\rho_{t+}$ , then it falls into outer singularity if the specific charge  $q < -1$  and it is repulsed for  $q > -1$ . From the classical point of view we can compare electrostatic and gravitational forces. If the sign of both masses in the gravitational force is negative, we get repulsion instead of attraction. We see that the change  $K \rightarrow -K$  leads to  $q \rightarrow -q$  and  $\rho_{t+} \leftrightarrow \rho_{t-}$ . Thus for  $K > 0$  we get the opposite sign of charge to mass ratio for both singularities.

$E$	$q$	$\rho$	Description of $\rho$ region	End of motion
$E = 0$	$q < -1$	$\rho_o < \rho$	Above outer singularity	$\rho_o$ or $\infty$
	$q = -1$	$\rho_o < \rho$	Above outer singularity	Initial radius
	$q > 1$	$0 < \rho < \rho_o$	Between singularities	0 or $\rho_o$
	$q = 1$	$0 < \rho < \rho_o$	Between singularities	Initial radius
$E < 0$	$q \leq -1$	$\rho_o < \rho$	Above outer singularity	$\rho_o$ or $\infty$
	$q < 1$	$0 < \rho \leq \rho_{t-}$	Above inner singularity	0
	$-1 < q$	$\rho_{t+} \leq \rho$	Above outer singularity	$\infty$
	$q \geq 1$	$0 < \rho < \rho_o$	Between singularities	0 or $\rho_o$
$E > 0$	$q > 1$	$\rho_{t-} \leq \rho < \rho_o$	Under outer singularity	$\rho_o$
	$q < -1$	$\rho_o < \rho \leq \rho_{t+}$	Above outer singularity	$\rho_o$

Table 4.2: Regions, where radial electrogeodetic motion is possible for  $K < 0$ .

$E$	$q$	$\rho$	Description of $\rho$ region	End of motion
$E = 0$	$q > 1$	$\rho_o < \rho$	Above outer singularity	$\rho_o$ or $\infty$
	$q = 1$	$\rho_o < \rho$	Above outer singularity	Initial radius
	$q < -1$	$0 < \rho < \rho_o$	Between singularities	0 or $\rho_o$
	$q = -1$	$0 < \rho < \rho_o$	Between singularities	Initial radius
$E < 0$	$1 \leq q$	$\rho_o < \rho$	Above outer singularity	$\rho_o$ or $\infty$
	$-1 < q$	$0 < \rho \leq \rho_{t+}$	Above inner singularity	0
	$q < 1$	$\rho_{t-} \leq \rho$	Above outer singularity	$\infty$
	$-1 \geq q$	$0 < \rho < \rho_o$	Between singularities	0 or $\rho_o$
$E > 0$	$q < -1$	$\rho_{t+} \leq \rho < \rho_o$	Under outer singularity	$\rho_o$
	$1 < q$	$\rho_o < \rho \leq \rho_{t-}$	Above outer singularity	$\rho_o$

Table 4.3: Regions, where radial electrogeodesic motion is possible for  $K > 0$ .

$E$	$K$	$\rho$	End of motion
$E < 0$	$K < 0$	$0 < \rho \leq \rho_{t-}$	0
		$\rho_{t+} \leq \rho$	$\infty$
	$K > 0$	$0 < \rho \leq \rho_{t+}$	0
		$\rho_{t-} \leq \rho$	$\infty$

Table 4.4: Regions, where radial geodesic (i.e.  $q = 0$ ) motion is possible.

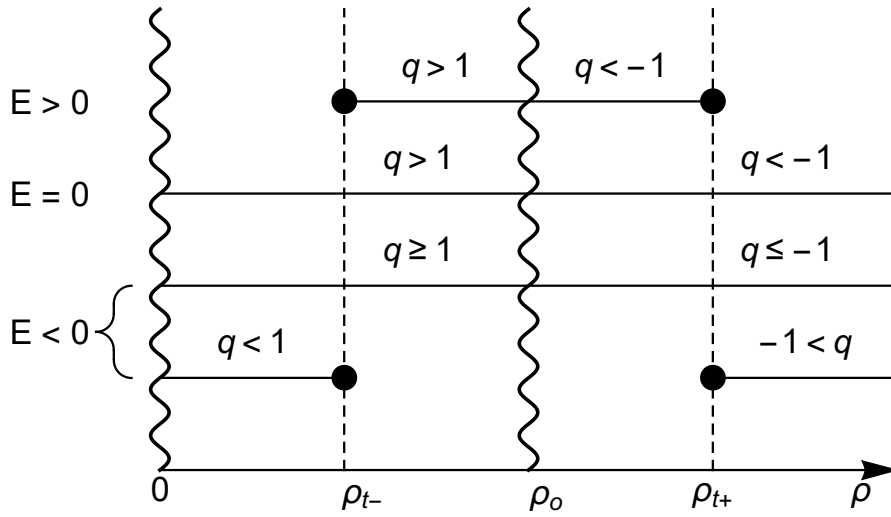


Figure 4.4: Regions, where radial electrogeodesic motion is possible for  $K < 0$ . A black circle indicates the end point is included in the given interval.

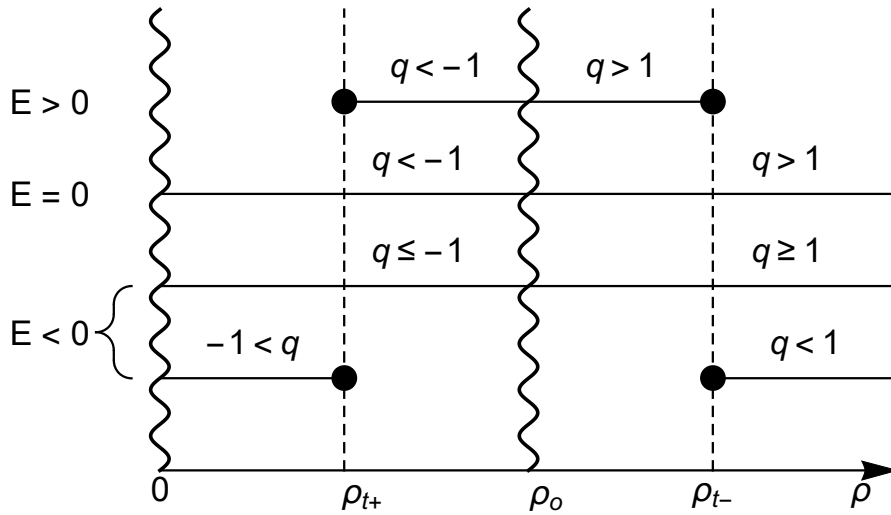


Figure 4.5: Regions, where radial electrogeodesic motion is possible for  $K > 0$ .



### 4.3 Circular electrogeodesics

We investigate circular electrogeodesics, which require  $\rho$  and  $z$  constant. We obtain the following equations:

$$-\frac{\dot{t}^2}{U^2} + U^2 \rho^2 \dot{\phi}^2 = \mathcal{U}, \quad (4.29)$$

$$\ddot{t} = \ddot{\phi} = 0, \quad (4.30)$$

$$\frac{q\dot{t}U_{,\rho}}{U^4} - \frac{\dot{t}^2 U_{,\rho}}{U^5} - \rho \dot{\phi}^2 - \frac{\rho^2 \dot{\phi}^2 U_{,\rho}}{U} = 0. \quad (4.31)$$

We can immediately write  $t = \gamma\tau$ ,  $\phi = \omega\tau$ . Then we have to find  $\gamma$  and  $\omega$ , which do not depend on proper time. However, they depend on radius  $\rho$  and specific charge  $q$ . If we rewrite the equations explicitly, they read

$$-\frac{\gamma^2}{(1 + K \ln \rho)^2} + (1 + K \ln \rho)^2 \rho^2 \omega^2 = \mathcal{U}, \quad (4.32)$$

$$\frac{K\gamma^2}{1 + K \ln \rho} + \rho^2 \omega^2 (1 + K \ln \rho)^3 (1 + K + K \ln \rho) = qK\gamma. \quad (4.33)$$

#### 4.3.1 Photon motion

By putting  $q = \mathcal{U} = 0$  in the previous equations, we obtain the following equation for  $\omega$  and  $\gamma$  for a photon:

$$\rho^2 \omega^2 U^4 - \gamma^2 = 0, \quad (4.34)$$

$$U_{,\rho} \gamma^2 + U^4 \rho \omega^2 (U + \rho U_{,\rho}) = 0, \quad (4.35)$$

which is a linear homogeneous equation in  $\gamma^2, \omega^2$ . A non-trivial solution is obtained, if the determinant of the system is zero. The solution to this condition is

$$U + 2K = 0 \Rightarrow \rho = \rho_{ph} \equiv e^{-2-1/K}, \gamma^2 = 16\rho_{ph}^2 \omega^2 K^4, \omega \neq 0, \quad (4.36)$$

where  $\omega$  is a free non-zero parameter. The auxiliary tensors describing the properties of the null geodesic are as follows

$$l^\mu = \frac{\mathbf{E}_{(t)}^\mu}{2\omega\rho_{ph}} - \frac{\mathbf{E}_{(\phi)}^\mu}{8\omega K^2 \rho_{ph}^2}, a^\mu = 0, \sigma_{\mu\nu} = \Omega_{\mu\nu} = 0, \quad (4.37)$$

and the optical scalars read

$$\Theta = \Omega^2 = \sigma^2 = 0. \quad (4.38)$$

ECS is thus a Kundt spacetime. It is not Ricci-flat (2.21), and it is **Type I** almost everywhere. It is not a VSI<sup>1</sup> (CSI<sup>2</sup>) spacetime due to its non-vanishing (non-constant) Kretschmann scalar (2.17).

<sup>1</sup>Vanishing scalar invariant spacetime

<sup>2</sup>Constant scalar invariant spacetime

### 4.3.2 Charged mass particle

Let us investigate circular motion of a charged massive particle by putting  $\mathcal{U} = -1$ . The equations are quadratic, so we expect two different absolute values of  $\omega$  at most (the change of sign corresponds to a change of trajectory direction). If we look closely at the equations, we find out that the equation for  $\gamma$  can become linear, if  $\rho = \rho_{ph}$ . Then the solution is

$$\rho = \rho_{ph}, \gamma_{\rho_{ph}} = -\frac{2K}{q}, \omega_{\rho_{ph}}^2 = \frac{1 - q^2}{4K^2 \rho_{ph}^2}, \quad (4.39)$$

if  $1 \geq q > 0 \wedge K < 0$  is satisfied or  $-1 \leq q < 0 \wedge K > 0$ . In general case, the solution for  $\gamma$  and  $\omega$  comes from coupled quadratic equations. First we express  $\omega$  from the normalization condition

$$\omega^2 = \frac{\gamma^2 - U^2}{\rho^2 U^4}, \quad (4.40)$$

and substitute in the second equation. The general solution (for  $\rho \neq \rho_{ph}$ ) is

$$\gamma_{\pm} = U \frac{q\rho U_{,\rho} \pm \sqrt{(q^2 + 8)\rho^2 U_{,\rho}^2 + 12\rho U U_{,\rho} + 4U^2}}{2(2\rho U_{,\rho} + U)}, \quad (4.41)$$

$$\omega_{\pm}^2 = U_{,\rho} \frac{\rho U_{,\rho} (q^2 - 4) - 2U \pm q \sqrt{(q^2 + 8)\rho^2 U_{,\rho}^2 + 12\rho U U_{,\rho} + 4U^2}}{2\rho U^2 (2\rho U_{,\rho} + U)^2}. \quad (4.42)$$

The series expansions for  $K \rightarrow 0$  are

$$\omega_{\pm}^2 \approx K \frac{-1 \pm q}{\rho^2} + O(K^2), \gamma_{\pm} \approx \pm 1 + \frac{K}{2} (q \mp 1 \pm 2 \ln \rho) + O(K^2). \quad (4.43)$$

From these circular orbits we can infer an interpretation corresponding to the Newtonian case. If we put  $\mu = \lambda$  in (1.23) and express it using the charge-to-mass ratio, we obtain the Newtonian angular frequency  $\omega_N$ . Comparing this to (4.43) we obtain

$$\omega_N^2 = 2\lambda \frac{1 - q}{\rho^2} \leftrightarrow \omega_{\pm}^2 \approx K \frac{q - 1}{\rho^2} \Rightarrow \lambda = -\frac{K}{2} + O(K^2). \quad (4.44)$$

From this we conclude that to the first order in  $K$ , the linear mass and charge density of the singularity is

$$\frac{M}{h} = \frac{Q}{h} = -\frac{K}{2} + O(K^2). \quad (4.45)$$

Let us investigate existence of solutions. To find out, when solution exists, we have to solve the conditions  $\gamma_{\pm} > 0$  and  $\omega_{\pm}^2 > 0$ . First we investigate solution for  $K < 0$ . We proceed in the same way for  $K > 0$  and we find that a change in the sign of  $K$  effectively corresponds to the change  $q \rightarrow -q$ . Plots of  $\gamma$  and  $\omega$  are in Figure 4.8. Summary of results is in Table 4.5, Figure 4.6 and Figure 4.7. The first column is just notation of the region; the second column describes, which variant of solution is valid ('+', '-' or ' $\rho_{ph}$ ' for photon radius); the third and the

fourth ones contain condition for specific charge of particle, depending on the sign of  $K$ ; the last one describes radial boundaries of the region. The definition of the boundary radius  $\rho_q$  used in the table is

$$\rho_q = \exp\left(-\frac{2 + 3K + K\sqrt{1 - q^2}}{2K}\right). \quad (4.46)$$

We see that there exists a region where both solutions  $\omega_{\pm}$  exist. This is a behavior we have already observed in a previous paper on another MP solution involving two charged black holes [9] and is a result of the quadratic nature of the algebraic form of the equations of motion. The geodesics exist only in the region  $0 < \rho < \rho_{ph}$  with angular velocity  $\omega_+$  for both sings of  $K$ .

#	$\omega$	$K < 0$ $q$	$K > 0$ $q$	$\rho$
$P_{1s}$	$\omega_+ = 0$	$q = 1$	$q = -1$	$0 < \rho < \rho_{ph}$
$F_s$	$\omega_{\rho_{ph}} = 0$	$q = 1$	$q = -1$	$\rho = \rho_{ph}$
$P_{2s}$	$\omega_+ = 0$	$q = 1$	$q = -1$	$\rho_{ph} < \rho \leq \rho_q$
$M_{2s}$	$\omega_- = 0$	$q = 1$	$q = -1$	$\rho_q \leq \rho < \rho_o$
$P_{3s}$	$\omega_+ = 0$	$q = -1$	$q = 1$	$\rho_o < \rho$
$P_1$	$\omega_+$	$q < 1$	$-1 < q$	$0 < \rho < \rho_{ph}$
$F$	$\omega_{\rho_{ph}}$	$0 < q < 1$	$-1 < q < 0$	$\rho = \rho_{ph}$
$P_2$	$\omega_+$	$0 < q < 1$	$-1 < q < 0$	$\rho_{ph} < \rho \leq \rho_q$
$M_1$	$\omega_-$	$0 < q < 1$	$-1 < q < 0$	$\rho_{ph} < \rho \leq \rho_q$
$M_2$	$\omega_-$	$1 < q$	$q < -1$	$\rho_{ph} < \rho < \rho_o$
$P_3$	$\omega_+$	$q < -1$	$1 < q$	$\rho_o < \rho$

Table 4.5: Regions, where circular electrogeodesic motion is possible for  $K \neq 0$ .

For a particle located in region  $P_1$  and approaching the inner singularity:

$$\lim_{\rho \rightarrow 0} \omega_+^2 = \infty, \lim_{\rho \rightarrow 0} \gamma_+ = \infty. \quad (4.47)$$

In region  $P_1$  a particle approaching photon orbit has

$$0 < q^2 < 1 : \lim_{\rho \rightarrow \rho_{ph}^-} \omega_+^2 = \omega_f^2, \lim_{\rho \rightarrow \rho_{ph}^-} \gamma_+ = \gamma_f, \quad (4.48)$$

$$-q \operatorname{sgn} K \leq 0 : \lim_{\rho \rightarrow \rho_{ph}^-} \omega_+^2 = \infty, \lim_{\rho \rightarrow \rho_{ph}^-} \gamma_+ = \infty. \quad (4.49)$$

In region  $P_2$ , it is not possible to overcome  $\rho_q$  for plus variant. If we take  $\rho_{\epsilon} = \rho_q \exp \epsilon$ , then for small positive  $\epsilon$  the square root in  $\gamma_+$  and  $\omega_+$  becomes complex, since interior becomes negative:

$$4U^2 + 12\rho U U_{,\rho} + (8 + q^2) \rho^2 U_{,\rho}^2 \approx -K^2 \epsilon \sqrt{1 - q^2} + O(\epsilon^2). \quad (4.50)$$

At  $\rho_q$ , we obtain

$$\lim_{\rho \rightarrow \rho_q^-} \gamma_+ = \frac{Kq \sqrt{1 - q^2} + 3}{2 \sqrt{1 - q^2} - 1}, \lim_{\rho \rightarrow \rho_q^-} \omega_+^2 = \frac{8 \left( q^2 - 1 + \sqrt{1 - q^2} \right)}{\left[ K \rho_q \left( 2 + q^2 - 2\sqrt{1 - q^2} \right) \right]^2}. \quad (4.51)$$

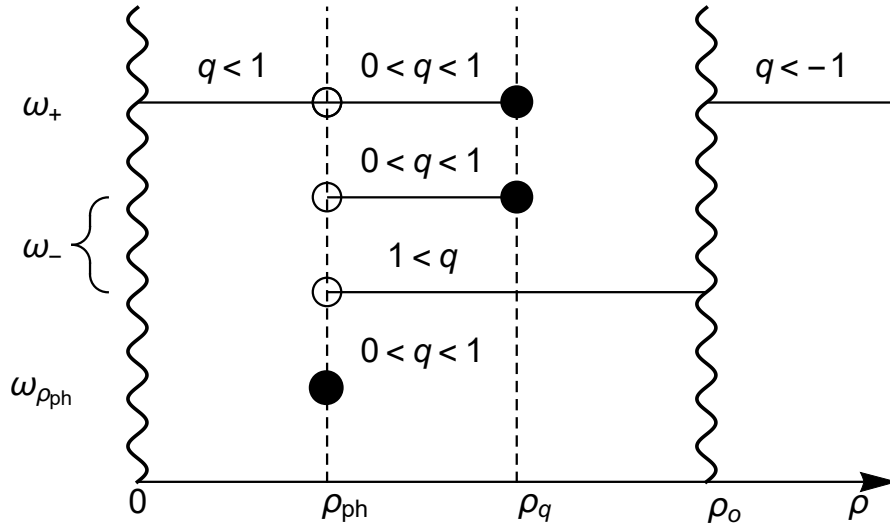


Figure 4.6: Schematic illustration of regions for  $K < 0$ , where circular electrogeodesic motion is possible. Static solutions are excluded. A white circle indicates the end point is not included in the given interval.

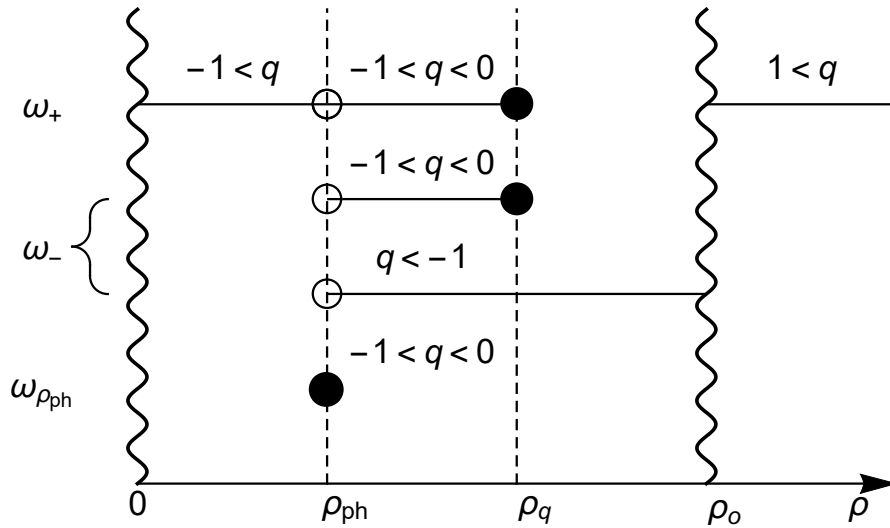


Figure 4.7: Schematic illustration of regions for  $K > 0$  as in the previous case.

In region  $P_3$  approaching outer singularity

$$\lim_{\rho \rightarrow \rho_o^+} \omega_+^2 = \infty, \lim_{\rho \rightarrow \rho_o^+} \gamma_+ = 0. \quad (4.52)$$

In region  $P_3$ , a series expansion for  $\rho \rightarrow \infty$  yields

$$\omega_+^2 \approx \frac{q \operatorname{sgn} K - 1}{K^2 \rho^2 \ln^3 \rho} + O\left(\frac{1}{\rho^2 \ln^4 \rho}\right), \quad (4.53)$$

$$\gamma_+ \approx \frac{qK - |K|}{2} + \operatorname{sgn} K + |K| \ln \rho + O(\ln^2 \rho). \quad (4.54)$$

So the limiting values

$$\lim_{\rho \rightarrow \infty} \omega_+^2 = 0, \lim_{\rho \rightarrow \infty} \gamma_+ = \infty. \quad (4.55)$$

In region  $M_1$  approaching photon radius

$$\lim_{\rho \rightarrow \rho_{ph}^+} \omega_-^2 = \infty, \lim_{\rho \rightarrow \rho_{ph}^+} \gamma_- = \infty. \quad (4.56)$$

In region  $M_1$  it is not possible to have circular orbits beyond  $\rho_q$  with  $0 < q^2 < 1$  due to the same argument as in case of  $P_2$ . The limits at  $\rho_q$  are the same as in case of region  $P_2$ :

$$\lim_{\rho \rightarrow \rho_q^-} \gamma_- = \lim_{\rho \rightarrow \rho_q^-} \gamma_+, \lim_{\rho \rightarrow \rho_q^-} \omega_-^2 = \lim_{\rho \rightarrow \rho_q^-} \omega_+^2. \quad (4.57)$$

In region  $M_2$  near the outer singularity we find

$$\lim_{\rho \rightarrow \rho_o^-} \omega_-^2 = \infty, \lim_{\rho \rightarrow \rho_o^-} \gamma_- = 0. \quad (4.58)$$

Congruence tensors read

$$a^\mu = -\frac{\rho U^3 \omega^2 + U_{,\rho} + 2\rho^2 U^2 \omega^2 U_{,\rho}}{U^3} \mathbf{E}_{(\rho)}^\mu. \quad (4.59)$$

The rotation and shear tensors have only  $t, \rho$  and  $\phi, \rho$  non-zero components, which are quite lengthy. The optical scalars read

$$\sigma^2 = \frac{\rho^2 (\rho U^3 \omega^3 + \omega U_{,\rho} - \omega_{,\rho} U + 2\rho^2 U^2 \omega^3 U_{,\rho})^2}{4\gamma^2}, \Theta = 0, \quad (4.60)$$

$$\Omega^2 = \frac{\left[ \rho^2 U^3 \omega^3 + 3\rho \omega U_{,\rho} + 2\rho^3 U^2 \omega^3 U_{,\rho} + U (2\omega + \rho \omega_{,\rho}) \right]^2}{4\gamma^2}. \quad (4.61)$$

From the behaviour of the circular electrogeodesics listed in Table 4.5 we can see that for  $K < 0$ , a particle with  $q < 1$  can orbit in the vicinity of the inner singularity. This corresponds to the classical case when the particle is attracted to the rod, due to its charge and mass, and repelled by the centrifugal force. The particle between singularities with  $q > 1$  can orbit in the vicinity of the outer singularity, which agrees with a centrifugal force neutralizing the attraction from the outer singularity. Particle with  $q < -1$  above the outer singularity can compensate the electrostatic attraction from the outer singularity in the same way. The change  $K \rightarrow -K$  corresponds to  $q \rightarrow -q$ . Again we see that the opposite  $K$  changes the sign of the charge to mass ratio of both singularities.

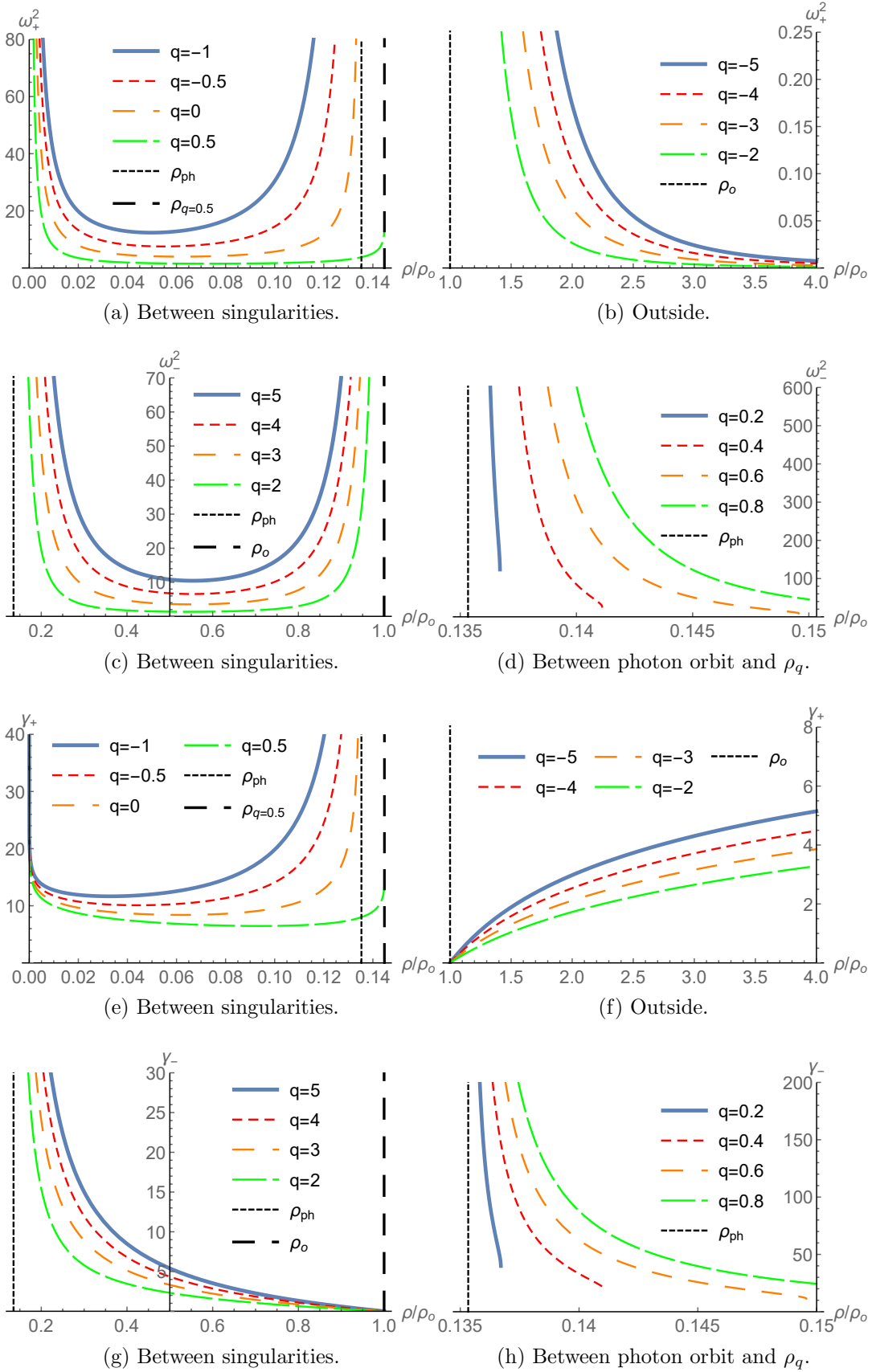


Figure 4.8: Plots of angular velocity  $\omega$  and gamma factor  $\gamma$  for circular motion of test particles of varying specific charge as a function of the radial coordinate,  $K = -2$ .

## 4.4 Electrogeodesics parallel to $z$ -axis

For motion, where  $\rho$  and  $\phi$  are constant, there are following equations

$$-\frac{\dot{t}^2}{U^2} + \dot{z}^2 U^2 = \mathcal{U}, \quad (4.62)$$

$$\ddot{t} = \ddot{z} = 0 \Rightarrow t = \gamma\tau, z = v\tau, \quad (4.63)$$

$$U_{,\rho}(-qtU + \dot{t}^2 + \dot{z}^2 U^4 \rho) = 0. \quad (4.64)$$

If we prescribe  $\mathcal{U} = q = 0$  to search for photon motion, we find that such motion is not possible. We thus search for timelike electrogeodesics only. We follow up the same procedure as in circular electrogeodesics: we find solutions for factors  $\gamma$  and  $v$ :

$$\gamma_{\pm} = \frac{U}{4} \left( q \pm \sqrt{q^2 + 8} \right), v_{\pm} = \sqrt{\frac{q^2 \pm q\sqrt{q^2 + 8} - 4}{8U^2}}. \quad (4.65)$$

Again, the task is to determine where these factors are well defined and real. They do not depend on proper time, but depend on  $\rho$  and  $K$ . In this case the inequalities are straightforward. The condition for  $v$  is found by solving where the argument of the square root is positive, the denominator excludes the outer singularity from solution. In case of  $\gamma$  we check where the product of  $U$  and the bracket is positive. We obtain one region for each solution. The case  $v_{\pm} = 0$  corresponds to static solutions. The results are summarized in Table 4.6 and Figure 4.9. Plot of factors  $v$  and  $\gamma$  is shown in Figure 4.10.

$K$	$v$	$q$	$\rho$	Description of $\rho$ region
$K < 0$	$v_+$	$q > 1$	$0 < \rho < \rho_o$	Between singularities
	$v_+ = 0$	$q = 1$	$0 < \rho < \rho_o$	Between singularities
	$v_-$	$q < -1$	$\rho_o < \rho$	Above outer singularity
	$v_- = 0$	$q = -1$	$\rho_o < \rho$	Above outer singularity
$K > 0$	$v_-$	$q < -1$	$0 < \rho < \rho_o$	Between singularities
	$v_- = 0$	$q = -1$	$0 < \rho < \rho_o$	Between singularities
	$v_+$	$q > 1$	$\rho_o < \rho$	Above outer singularity
	$v_+ = 0$	$q = 1$	$\rho_o < \rho$	Above outer singularity

Table 4.6: Regions, where  $z$ -electrogeodesic motion is possible for  $K \neq 0$ .

For a particle located between singularities and approaching the inner singularity:

$$\lim_{\rho \rightarrow 0^+} \gamma_+ = \infty, \lim_{\rho \rightarrow 0^+} v_+ = 0, \lim_{\rho \rightarrow 0^+} \gamma_- = \infty, \lim_{\rho \rightarrow 0^+} v_- = 0, \quad (4.66)$$

where the first two limits assume  $K < 0$  and the last two  $K > 0$  according to Table 4.6. For the same particle approaching the outer singularity we find

$$\lim_{\rho \rightarrow \rho_o^-} \gamma_+ = 0, \lim_{\rho \rightarrow \rho_o^-} v_+ = \infty, \lim_{\rho \rightarrow \rho_o^-} \gamma_- = 0, \lim_{\rho \rightarrow \rho_o^-} v_- = \infty. \quad (4.67)$$

For a particle located above the outer singularity and approaching the outer singularity:

$$\lim_{\rho \rightarrow \rho_o^+} \gamma_- = 0, \lim_{\rho \rightarrow \rho_o^+} v_- = \infty, \lim_{\rho \rightarrow \rho_o^+} \gamma_+ = 0, \lim_{\rho \rightarrow \rho_o^+} v_+ = \infty, \quad (4.68)$$

and approaching radial infinity

$$\lim_{\rho \rightarrow \infty} \gamma_- = \infty, \lim_{\rho \rightarrow \infty} v_- = 0, \lim_{\rho \rightarrow \infty} \gamma_+ = \infty, \lim_{\rho \rightarrow \infty} v_+ = 0. \quad (4.69)$$

Series expansion for  $K \rightarrow 0$  for  $\gamma$  is trivial, since  $\gamma$  depends linearly on  $K$ . For  $v$  we obtain

$$v_{\pm} \approx \frac{\sqrt{q^2 - 4 \pm \sqrt{q^2 + 8}}}{2\sqrt{2}} (1 - K \ln \rho) + O(K^2). \quad (4.70)$$

Congruence tensors read

$$a_{\pm}^{\mu} = -\frac{qU_{,\rho}\gamma_{\pm}}{U^4} \mathbf{E}_{(\rho)}^{\mu}, \Omega_{\pm\rho t} = \sigma_{\pm\rho t} = \frac{U_{,\rho}\gamma_{\pm}v_{\pm}^2}{U}, \Omega_{\pm\rho z} = \sigma_{\pm\rho z} = \frac{\gamma_{\pm}^2 v_{\pm}}{U}, \quad (4.71)$$

from the optical scalars we obtain that the congruence is expansion-free:

$$\Theta_{\pm} = 0, \sigma_{\pm}^2 = \Omega_{\pm}^2 = U_{,\rho}^2 \frac{\left[ q^2 \left( q \pm \sqrt{q^2 + 8} \right)^2 - 16 \right]}{64U^4}. \quad (4.72)$$

Let us look at the results for electrogeodesics along  $z$ -axis in Table 4.6 for  $K < 0$ . If the particle moves between singularities in  $z$ -direction, it has to have a specific charge  $q > 1$ . The particle is attracted to the outer singularity, as its charge is higher than the equilibrium charge. This attraction is compensated by movement, as the mass of the particle increases (from the point of view of a static observer). The same arguments hold for a particle above the outer singularity: motion along the  $z$ -axis is possible for  $q < -1$  and the particle is attracted to the outer singularity, which is compensated by the motion. For  $K > 0$  the charge to mass ratio of electrogeodesic particles changes, as well as the charge to mass ratio of both singularities.

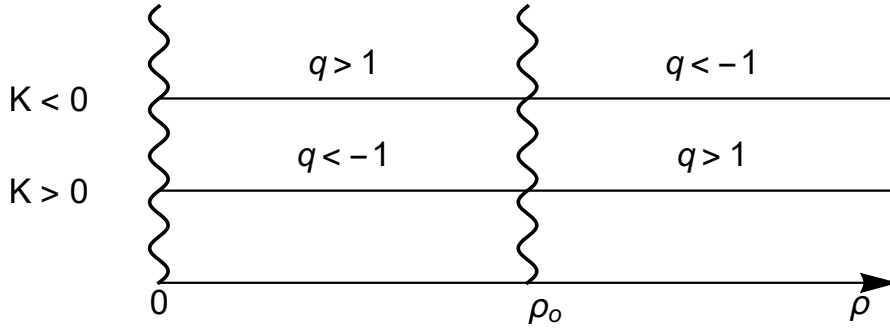


Figure 4.9: Regions, where axial electrogeodesics exist for  $K \neq 0$ .



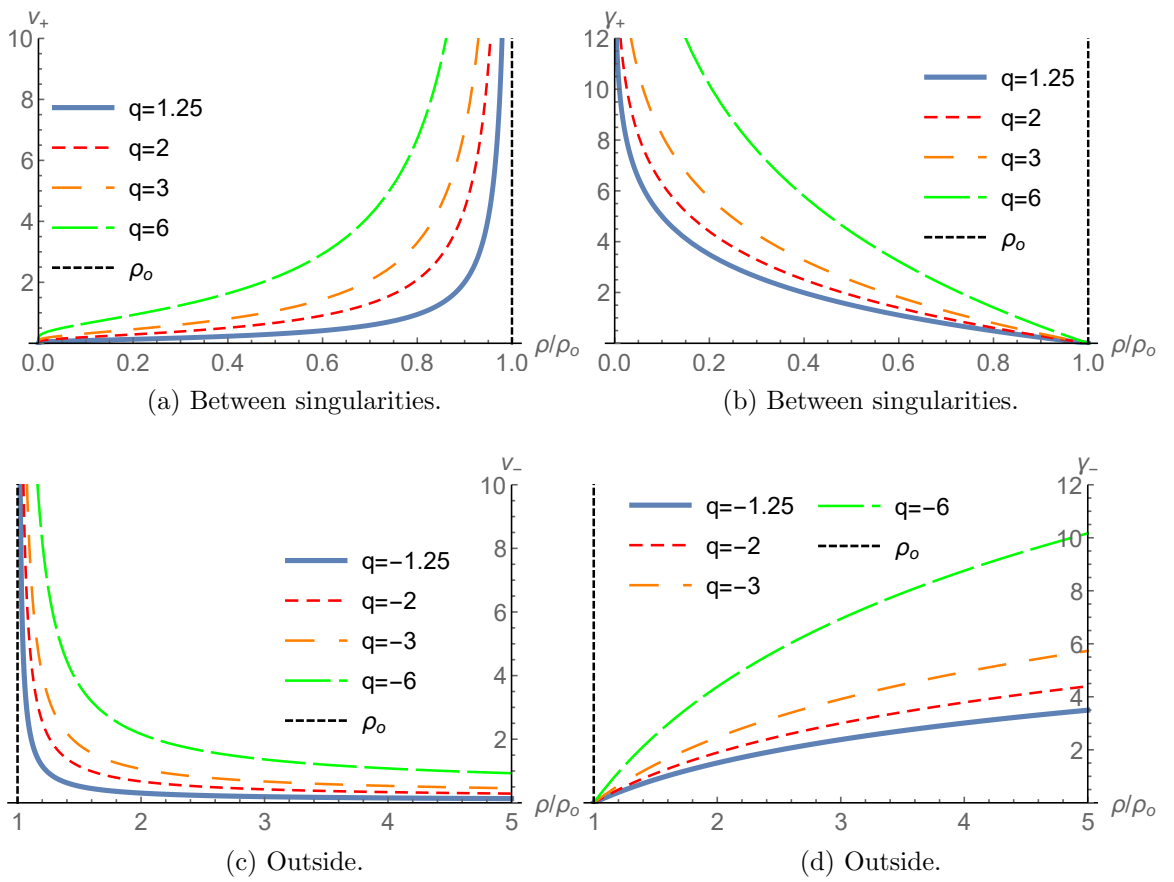


Figure 4.10: Dependence of velocity  $v$  and gamma factor  $\gamma$  for  $K = -2$ .



# 5. The Newtonian limit

In this chapter we discuss the formal limit  $K \rightarrow 0$ . The question is how to do this limit? This is not a physical process but rather a mathematical procedure enabling us to compare various results from GR with their Newtonian analogues. In the previous chapters we often calculated some quantities and expanded them as a series in  $K$  which we then let tend to zero. The lowest term was then compared to the Newtonian expression. This makes sense if the region of spacetime in question approaches flat spacetime for  $K \rightarrow 0$ . Then the Newtonian gravity represents the lowest-order perturbation of the flat spacetime and should correspond to the lowest term in the expansion. One needs to be careful about whether the investigated radius is above or below the outer singularity, which shifts with changing  $K$ . While it is obvious from the metric that ECS becomes Minkowski, however, there is problem with the outer singularity, which has only one-sided limits, and thus only one part of the ECS can become Minkowski. There also arises the question of mass - we computed several formulae for mass and made series expansions for small  $K$ , but what do we get?

## 5.1 $K < 0$

For  $K < 0$  the outer singularity approaches radial cylindrical infinity in the limiting process  $K \rightarrow 0^-$ :

$$\lim_{K \rightarrow 0^-} \rho_o = \infty, \quad \lim_{K \rightarrow 0^-} l_\rho(\rho_o) = \infty, \quad (5.1)$$

where  $l_\rho$  is proper radial cylindrical length from (2.3.1). Thus from the ECS there remains only the inner part, which becomes Minkowski. Therefore, the observer could see only inner singularity and measure its mass and charge. If we look at the Brown-York (3.38) expression and (3.27) we see that for a cylinder enclosing the inner singularity mass is positive. If we enclose outer singularity from inside we get that the mass is negative.

## 5.2 $K > 0$

For  $K > 0$  the outer singularity approaches the inner singularity in the limit process  $K \rightarrow 0^+$ :

$$\lim_{K \rightarrow 0^+} \rho_o = 0, \quad \lim_{K \rightarrow 0^+} l_\rho(\rho_o) = 0. \quad (5.2)$$

Thus from the ECS there remains only the outer part, which becomes Minkowski. Thus the observer can only be outside and see only the outer singularity. Using the same argument as in the previous section, we see that the charge (3.45) and mass densities of the outer singularity are negative.



## 6. Summary of ECS

Let us state our results for ECS. We interpret the ECS spacetime as actually consisting of two independent spacetimes separated by the outer singularity. From the radial electrogeodesics it follows that both singularities are naked and nothing can go through the outer singularity to the other part of the spacetime. Inside, the situation is complicated by the presence of two singularities pulling or pushing test particles in opposite directions, while outside there is only one singularity present in the spacetime. The outer singularity at  $\rho = e^{-1/K}$  always has a negative mass per unit length as observed from both outside and inside. From calculations of proper lengths we see that the outer singularity is spatially point-like. The inner singularity at  $\rho = 0$ , which is spatially one-dimensional, then always has a positive mass. The parameter  $K$  appearing in the metric determines the sign of the charge per unit length of the singularities. For  $K > 0$  the inner singularity has a negative charge. The outer singularity has a negative charge when observed from the outside and a positive charge from the inside. For  $K < 0$  the signs are reversed. For weak fields, i.e., when the limit  $K \rightarrow 0$  is applied, the magnitude of both the mass and charge densities is given by  $K/2$ . The summary of signs of mass and charge is shown in Figure 6.1.

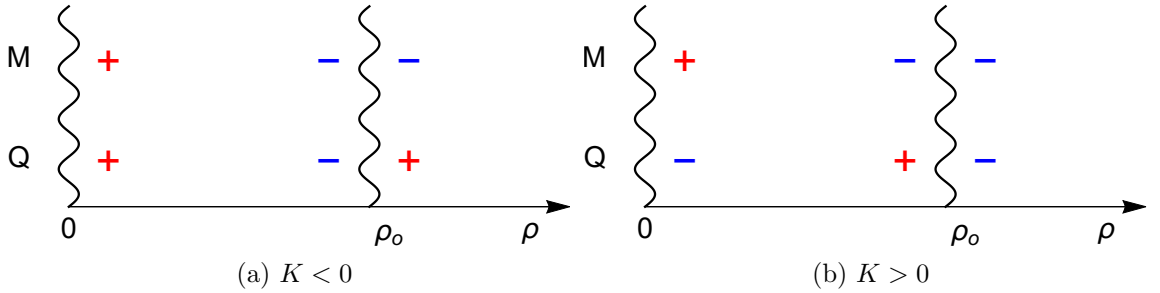


Figure 6.1: Schematic illustration of the sign of linear mass and charge densities of the singularities.



# 7. Geometry of ECS with a cosmological constant

Kastor and Traschen found an extension of the static Majumdar-Papapetrou spacetime, consisting of a finite number of extremal black holes, yielding a dynamical case [4] with a positive cosmological constant  $\Lambda$ , with the limit  $\Lambda \rightarrow 0$  reducing the spacetime to the static case. Static ECS can be extended in the same way, producing a spacetime we call ECSA. We prescribe the metric and electromagnetic four-potential in the following way:

$$ds^2 = -\frac{dt^2}{\Omega^2} + b^2\Omega^2 (d\rho^2 + \rho^2 d\phi^2 + dz^2), \quad (7.1)$$

$$A = \frac{dt}{\Omega}, \Omega = \Omega(t, \rho), b = b(t). \quad (7.2)$$

$$(7.3)$$

Then the electromagnetic tensor and Maxwell invariant read

$$F = \frac{\Omega_{,t}}{\Omega^2} dt \wedge d\rho, \mathcal{F} = -2\frac{\Omega_{,t}^2}{b^2\Omega^4}. \quad (7.4)$$

First we plug the metric tensor and electromagnetic four-potential in Maxwell equations. From the first one we get

$$\rho\Omega_{,t\rho} + \Omega_{,t} = 0 \Rightarrow \Omega(t, \rho) = 1 + c(t) \ln \rho, \quad (7.5)$$

and from the second one we obtain

$$(b\Omega_{,t})_{,t} = 0 \Rightarrow \Omega(t, \rho) = 1 + \frac{K}{b(t)} \ln \rho, \quad (7.6)$$

and the Maxwell equations are thus satisfied. The constant 1 is chosen so<sup>1</sup> that ECSA be consistent with ECS spacetime. The Einstein equations are more complicated. We solve the simplest one:

$$3b'^2 = \Lambda b^2 \Rightarrow b(t) = e^{Ht}, H = \pm\sqrt{\frac{\Lambda}{3}}, \Lambda > 0, \quad (7.7)$$

where the function  $b(t)$  is the same as in [4]. If we plug this function in the remaining equations we find that they are all satisfied. We choose an orthonormal tetrad

$$\mathbf{e}_{(t)}^\mu = \sqrt{\Omega^2} \mathbf{E}_{(t)}^\mu, \mathbf{e}_{(\rho)}^\mu = \frac{1}{b\sqrt{\Omega^2}} \mathbf{E}_{(\rho)}^\mu, \mathbf{e}_{(\phi)}^\mu = \frac{1}{\rho b\sqrt{\Omega^2}} \mathbf{E}_{(\phi)}^\mu, \mathbf{e}_{(z)}^\mu = \frac{1}{b\sqrt{\Omega^2}} \mathbf{E}_{(z)}^\mu. \quad (7.8)$$

Riemann tensor has more complex components than in ECS. The non-zero coordinate and tetrad components vanish neither in the limit  $\rho \rightarrow \infty$ , nor  $Ht \rightarrow \pm\infty$ , so ECSA is not flat in these limits. Ricci curvature is  $R = 12H^2$ , which agrees from the trace of the Einstein equations, thus ECSA is spacetime with constant

---

<sup>1</sup>Einstein equations permit this choice and it simplifies the calculation.

$K$	$H$	$\lim_{t \rightarrow -\infty} \rho_o$	$\lim_{t \rightarrow +\infty} \rho_o$
$K < 0$	$H < 0$	$\infty$	1
	$H > 0$	1	$\infty$
$K > 0$	$H < 0$	0	1
	$H > 0$	1	0

Table 7.1: Movement of the outer singularity in ECSA.

positive curvature. There are only two Killing vectors:  $\mathbf{E}_{(\phi)}^\mu$  and  $\mathbf{E}_{(z)}^\mu$ . ECSA is thus not a subcase of black string (3.47) in [11], as their solution is stationary, featuring a Killing vector field corresponding to time symmetry.

From  $\mathcal{F}$  we see that there are two singularities located at radii

$$\rho_i = 0, \rho_o(t) = \exp \left[ -\frac{\exp(Ht)}{K} \right]. \quad (7.9)$$

We found these singularities in ECS, however here the behaviour is more complicated and depends on both  $H$  and  $K$ . The summary of movement of the outer singularity is shown in Table 7.1.

## 7.1 Algebraic classification

We wish to determine the algebraic class of the spacetime. We proceed in the same way as in ECS. We choose a normalized null tetrad

$$\begin{aligned} k^\mu &= \frac{1}{\sqrt{2}} \left( \mathbf{e}_{(t)}^\mu - \mathbf{e}_{(\rho)}^\mu \right), l^\mu = \frac{1}{\sqrt{2}} \left( \mathbf{e}_{(t)}^\mu + \mathbf{e}_{(\rho)}^\mu \right), \\ m^\mu &= \frac{1}{\sqrt{2}} \left( i\mathbf{e}_{(\phi)}^\mu - \mathbf{e}_{(z)}^\mu \right), \bar{m}^\mu = -\frac{1}{\sqrt{2}} \left( i\mathbf{e}_{(\phi)}^\mu + \mathbf{e}_{(z)}^\mu \right). \end{aligned} \quad (7.10)$$

We compute Weyl scalars as in (2.25) and the non-zero Weyl scalars read

$$\psi_0 = \psi_4 = \frac{\Omega_{,\rho}}{2\rho\Omega^3 b^2}, \psi_2 = \frac{6\rho\Omega_{,\rho}^2 + \Omega(\Omega_{,\rho} - 2\rho\Omega_{,\rho\rho})}{6\rho\Omega^4 b^2}. \quad (7.11)$$

We can see that all Weyl scalars vanish in the limit  $\rho \rightarrow \infty$  or  $Ht \rightarrow \infty$ :

$$\lim_{\rho \rightarrow \infty} \psi_0 = \lim_{\rho \rightarrow \infty} \psi_2 = 0, \lim_{Ht \rightarrow \infty} \psi_0 = \lim_{Ht \rightarrow \infty} \psi_2 = 0. \quad (7.12)$$

This means that ECSA is conformally flat in these limits. For example, for  $Ht \gg 1$  the metric becomes

$$ds^2 \approx -dt^2 + e^{2Ht} (d\rho^2 + \rho^2 d\phi^2 + dz^2), \quad (7.13)$$

which is de Sitter spacetime, which is conformally flat (but not flat) spacetime. We notice that for  $Ht \approx 0$  the metric is close to the static ECS.

To determine the algebraic type of the spacetime we perform the same transformation as in (2.35) and obtain the equation

$$1 + 2\alpha Z^2 + Z^4 = 0, \alpha \equiv \frac{\psi_2}{3\psi_0}, \quad (7.14)$$



which is of the same form as (2.38), but here it also depends on  $t$ . Therefore there are four complex roots in general thus the ECSA spacetime is **type I**. We find that there exist two radii where the spacetime is **type D**. The radii are

$$\rho_{D1,2}(t) = \exp\left(-\frac{(3 \mp 1)b(t) \mp 2K}{K(3 \mp 1)}\right). \quad (7.15)$$

## 7.2 Mass

From the static ECS spacetime we already know the role of the parameter  $K$ . In ECSA we expect that the formulae will be time dependent. Therefore, in the first order we should get an exponential suppression or growth of mass and charge. The ECSA spacetime is not static and has no timelike Killing vectors, so we can not use all definitions as in the static ECS - we can not use Brown-York and Komar formulae. We can thus compute charge and Landau-Lifschitz formulae. One would also want to compute  $C$ -energy. However, it requires complicated transformation of the metric and since we are not able to find an analytical expression for such a transformation, we can not calculate the  $C$ -energy.

To compute the integral definitions of  $M_{LL}$  and  $Q$  we use slightly modified cylinders:

$$\Sigma(\rho) \rightarrow \Sigma(t, \rho), S(\rho) \rightarrow S(t, \rho), \quad (7.16)$$

where  $t$  is general, but constant in the integration. The future-oriented normal  $n^\mu$  to  $\Sigma$  and spatial outer normal  $r^\mu$  to  $S_S$  read

$$n^\mu = \mathbf{e}_{(t)}^\mu, r^\mu = \mathbf{e}_{(\rho)}^\mu = \frac{1}{\sqrt{x^2 + y^2}} \left( x \mathbf{e}_{(x)}^\mu + y \mathbf{e}_{(y)}^\mu \right), \quad (7.17)$$

where the components also depend on time.

### 7.2.1 Landau-Lifschitz

We proceed in the same way as in ECS and use the formula

$$P^\mu = \frac{1}{16\pi} \oint_S H^{\mu 0 \lambda \kappa}{}_{,\kappa} r_\lambda dS. \quad (7.18)$$

However, it seems that the components  $P^x$  and  $P^y$  are non-zero, because the integrand for  $\mu = i$  reads

$$H^{i 0 \lambda \kappa} = g g^{i\lambda} g^{0\kappa} \Rightarrow H^{i 0 \lambda \kappa}{}_{,\kappa} = \left( g g^{i\lambda} g^{00} \right)_{,0}, \quad (7.19)$$

and this expression vanishes in the summation in the integrand only for  $i = z$ . After some algebra we get

$$H^{x t \lambda \kappa}{}_{,\kappa} = \left( g g^{x\lambda} g^{tt} \right)_{,t}, H^{y t \lambda \kappa}{}_{,\kappa} = \left( g g^{y\lambda} g^{tt} \right)_{,t}. \quad (7.20)$$

After expressing the integrand in cylindrical coordinates we see that the integrand in  $P^x$  depends linearly on  $\cos \phi$ . Since we integrate  $\phi$  over the cylinder, the integrand vanishes.  $P^y$  depends linearly on  $\sin \phi$  and the same argument applies. We can thus calmly compute the only non-vanishing component and we obtain

$$M_{LL} = \frac{-hK}{2} b^7 \Omega^5 \sqrt{\Omega^2} \approx \frac{-hK}{2} e^{6Ht} - 3hK^2 e^{5Ht} \ln \rho + O(K^3). \quad (7.21)$$

From this we get that mass changes in time with factor  $e^{6Ht}$  to the first order.

## 7.2.2 Charge

We proceed in the same way as in ECS. We obtain

$$Q = \frac{1}{4\pi} \int_0^{2\pi} \int_0^h F_{\rho t} r^\rho n^t b^2 \Omega^2 \rho dz' d\phi' = -\frac{hK}{2} e^{2Ht}. \quad (7.22)$$

We observe that the charge changes in time with factor  $e^{2Ht}$ . We see that mass changes faster in time than charge. This means that there is a flow of matter and charge in the spacetime along the singularities.

## 8. Grid spacetime

In the previous chapters we constructed a solution describing an extremally charged string. One of interesting questions is whether this solution can be obtained as a limiting case of spacetime, which would consist of an infinite number of extremal black holes. The extremally charged string should be obtained in the limit when the distance from the  $z$ -axis is large compared to the distance between two neighboring point sources. However, there is a problem: we first need to find the corresponding electrostatic potential of such a configuration in classical physics. Thus our goal is to find an electrostatic potential, which would describe an infinite number of point charges situated on the  $z$ -axis, so it can be extended to GR similarly to the ECS spacetime. We investigate two constructions and analyse them.

### 8.1 Superposition of point charges

We prescribe the potential in such a way that it behaves as single point charge if we approach closely to it. We thus sum the potentials of individual point charges. So we prescribe the potential as

$$\varphi = \sum_{n=1}^{\infty} \varphi_n^+ + \sum_{n=1}^{\infty} \varphi_n^- + \varphi_0, \quad (8.1)$$

where

$$\varphi_n^{\pm}(\rho, z) = \frac{1}{\sqrt{\rho^2 + (z \pm n)^2}} - \frac{1}{n}, \quad \varphi_0(\rho, z) = \frac{1}{\sqrt{\rho^2 + z^2}}. \quad (8.2)$$

The meaning of  $\varphi_n^{\pm}$  is the following: it is the potential of a point charge located at  $z = \pm n$  on the  $z$ -axis, the term  $-1/n$  makes the potential  $\varphi_n^{\pm}$  vanish at the origin. It is clear from construction that every  $\varphi_n^{\pm}$  satisfies the Laplace's equation, but it is not clear whether the sums converge uniformly and what the total potential looks like.

We see that  $\varphi$  has mirror symmetry, since  $\varphi_n^+(\rho, z) = \varphi_n^-(\rho, -z)$ . The potential has another important symmetry - it is periodic in  $z$ :

$$\begin{aligned} \varphi(\rho, z+1) &= \quad (8.3) \\ &= \sum_{n=1}^{\infty} \left[ \frac{1}{\sqrt{\rho^2 + (z+1-n)^2}} - \frac{1}{n} \right] + \sum_{n=1}^{\infty} \left[ \frac{1}{\sqrt{\rho^2 + (z+1+n)^2}} - \frac{1}{n} \right] + \frac{1}{\sqrt{\rho^2 + (z+1)^2}} = \\ &= \frac{1}{\sqrt{\rho^2 + z^2}} - \frac{1}{1} + \sum_{n=2}^{\infty} \left[ \frac{1}{\sqrt{\rho^2 + [z-(n-1)]^2}} - \frac{1}{n} \right] + \sum_{n=1}^{\infty} \left[ \frac{1}{\sqrt{\rho^2 + (z+1+n)^2}} - \frac{1}{n} \right] + \varphi_1^+ = \\ &= \varphi_0 - 1 + \sum_{l=1}^{\infty} \left[ \frac{1}{\sqrt{\rho^2 + (z-l)^2}} - \frac{1}{l+1} \right] + \sum_{m=2}^{\infty} \left[ \frac{1}{\sqrt{\rho^2 + (z+m)^2}} - \frac{1}{m-1} \right] + \varphi_1^+ = \\ &= \varphi_0 - 1 + \sum_{l=1}^{\infty} \left[ \varphi_l^- + \frac{1}{l} - \frac{1}{l+1} \right] + \sum_{m=2}^{\infty} \left[ \varphi_m^+ + \frac{1}{m} - \frac{1}{m-1} \right] + \varphi_1^+. \end{aligned}$$

On the third line we separated the first term from the first sum, which gives  $\varphi_0 - 1$ , on the fourth line we substituted  $l = n - 1$  in the first sum and  $m = n + 1$

in the second sum, and on the last line we rewrote zero as  $0 = \frac{1}{l} - \frac{1}{l}$  to restore the terms  $\varphi_l^\pm$ . Since the extra terms in both sums go for large argument as

$$\frac{1}{l} - \frac{1}{l+1} \sim \frac{1}{l^2}, \quad \frac{1}{m} - \frac{1}{m-1} \sim \frac{1}{m^2} \quad (8.4)$$

we see that they converge and can be separated. We thus get

$$\varphi(\rho, z+1) = \varphi_0 + \sum_{l=1}^{\infty} \varphi_l^- + \sum_{l=1}^{\infty} \left[ \frac{1}{l} - \frac{1}{l+1} \right] + \sum_{l=1}^{\infty} \varphi_l^+ + \sum_{m=2}^{\infty} \left[ \frac{1}{m} - \frac{1}{m-1} \right]. \quad (8.5)$$

The separated sums are well-known telescopic sums and they read

$$\sum_{l=1}^{\infty} \left[ \frac{1}{l} - \frac{1}{l+1} \right] = 1, \quad \sum_{m=2}^{\infty} \left[ \frac{1}{m} - \frac{1}{m-1} \right] = -1, \quad (8.6)$$

thus they cancel and we get  $\varphi(\rho, z+1) = \varphi(\rho, z)$ . From the definition we see that  $\varphi(\rho, z)$  diverges in points where the charges are located:

$$\lim_{z \rightarrow \pm n} \varphi(0, z) = \infty, \quad n \in \mathbb{N}_0. \quad (8.7)$$

The periodicity has many advantages. Combining it with mirror symmetry we get

$$\varphi(\rho, 1-z) = \varphi(\rho, z-1) = \varphi(\rho, z), \quad (8.8)$$

which means we can restrict to  $0 \leq z \leq 1/2$ , as the potential has mirror symmetry in every  $z = m/2, m \in \mathbb{Z}$ . From (8.8) it also follows

$$\left. \frac{\partial \varphi(\rho, z)}{\partial z} \right|_{z=1/2} = 0, \quad \rho \neq 0 \Rightarrow \left. \frac{\partial \varphi(\rho, z)}{\partial z} \right|_{z=n} = 0. \quad (8.9)$$

### 8.1.1 Convergence

Let us first look where the terms change sign:

$$\varphi_n^\pm > 0 \Rightarrow \mp 2zn \geq \rho^2 + z^2. \quad (8.10)$$

If we assume on  $z > 0$ , we see that  $\varphi_n^+$  is never positive, as the condition below has no solution for  $n$ . The terms  $\varphi_n^-$  are negative for  $n < n_{max}$ , defined as the highest natural number satisfying the inequality, and then they are always positive. Since  $\varphi_n^+(\rho, z) = \varphi_n^-(\rho, -z)$ , the same holds for  $z < 0$ . Let us inspect the convergence of both sums. Thanks to symmetries we can restrict on  $z \in [0, 1/2]$ . From the definition of  $\varphi_n^\pm$  we can see that the terms will behave for large  $n$  as

$$\varphi_n^\pm \sim n^{-2}, \quad \lim_{n \rightarrow \infty} n^2 \varphi_n^\pm = \mp z, \quad (8.11)$$

and in the plane  $z = 0$  the convergence is even faster and the terms go as  $n^{-3}$ . Thus both sums converge pointwise for every  $\rho$  and for  $z \in [0, 1/2]$ . Plots of  $\varphi$  for fixed  $z$  or  $\rho$  are in Figure 8.1. Figure 8.2 shows where the potential is zero. However, it is not obvious, whether the sums converge uniformly. The terms can be estimated as

$$|\varphi_n^\pm| \leq \frac{1}{n}, \quad \forall \rho \geq 0, \quad z \in \left[ 0, \frac{1}{2} \right], \quad (8.12)$$

which is enough to prove  $\varphi_n^\pm \Rightarrow 0$ , but it is not sufficient for uniform convergence of both sums. If we restrict on  $\rho = 0$  we are able to express  $\varphi$  analytically. For  $0 < z \leq 1/2$  the sums can be rewritten as

$$\varphi(0, z) = \sum_{n=1}^{\infty} \left( \frac{1}{z+n} - \frac{1}{n} \right) + \sum_{n=1}^{\infty} \left( \frac{1}{n-z} - \frac{1}{n} \right) + \frac{1}{z}. \quad (8.13)$$

We can estimate individual terms as

$$\left| \frac{1}{z \pm n} - \frac{1}{n} \right| = \left| \frac{z}{nz \pm n^2} \right| \leq \frac{1}{n^2}, \quad (8.14)$$

so the sums converge absolutely uniformly. Using mathematical software we find that

$$\varphi(0, z) = \frac{1}{z} - H(z) - H(-z), \quad 0 < z \leq 1/2, \quad (8.15)$$

where  $H(z)$  is harmonic number (A.23). The derivatives of  $\varphi_n^\pm$  on the  $z$ -axis can be estimated as

$$\rho = 0 : \frac{\partial \varphi_n^\pm}{\partial z} = \frac{\mp 1}{(n \pm z)^2}, \quad \left| \frac{\partial \varphi_n^+}{\partial z} \right| \leq \frac{1}{n^2}, \quad \left| \frac{\partial \varphi_n^-}{\partial z} \right| \leq \frac{4}{(2n-1)^2} \quad (8.16)$$

so the sums of derivatives of  $\varphi_n^\pm$  converge absolutely uniformly. The second derivatives can be estimated as

$$\rho = 0 : \frac{\partial^2 \varphi_n^\pm}{\partial z^2} = \frac{1}{(z \pm n)^3}, \quad \left| \frac{\partial^2 \varphi_n^+}{\partial z^2} \right| \leq \frac{2}{n^3}, \quad \left| \frac{\partial^2 \varphi_n^-}{\partial z^2} \right| \leq \frac{16}{(2n-1)^3}, \quad (8.17)$$

thus again the sums converge absolutely uniformly, and we can interchange the order of derivatives and sums at the axis. Plots of the potential and its derivatives at the  $z$ -axis is shown in Figure 8.1. However, the rate of convergence of the potential sum is quite low and we thus now proceed to use a different approach based on expanding the solution in terms of fundamental solutions to Laplace's equation.

## 8.2 Separated potential

In this section we assume that the potential is separable:

$$\psi(\rho, z) = R(\rho)Z(z). \quad (8.18)$$

Substituting in Laplace's equation we obtain:

$$\frac{\rho R_{,\rho\rho} + R_{,\rho}}{\rho R} = -\frac{Z_{,zz}}{Z}. \quad (8.19)$$

Since the left side only depends on  $\rho$  and the right side only on  $z$ , the sides equal a constant. Since we require periodicity in  $z$ , it implies the right side to be positive (otherwise the solution for  $Z$  cannot be periodic) and

$$Z_{,zz} + \alpha_n^2 Z = 0 \Rightarrow Z_n = a_n \sin(\alpha_n z) + b_n \cos(\alpha_n z), \quad (8.20)$$

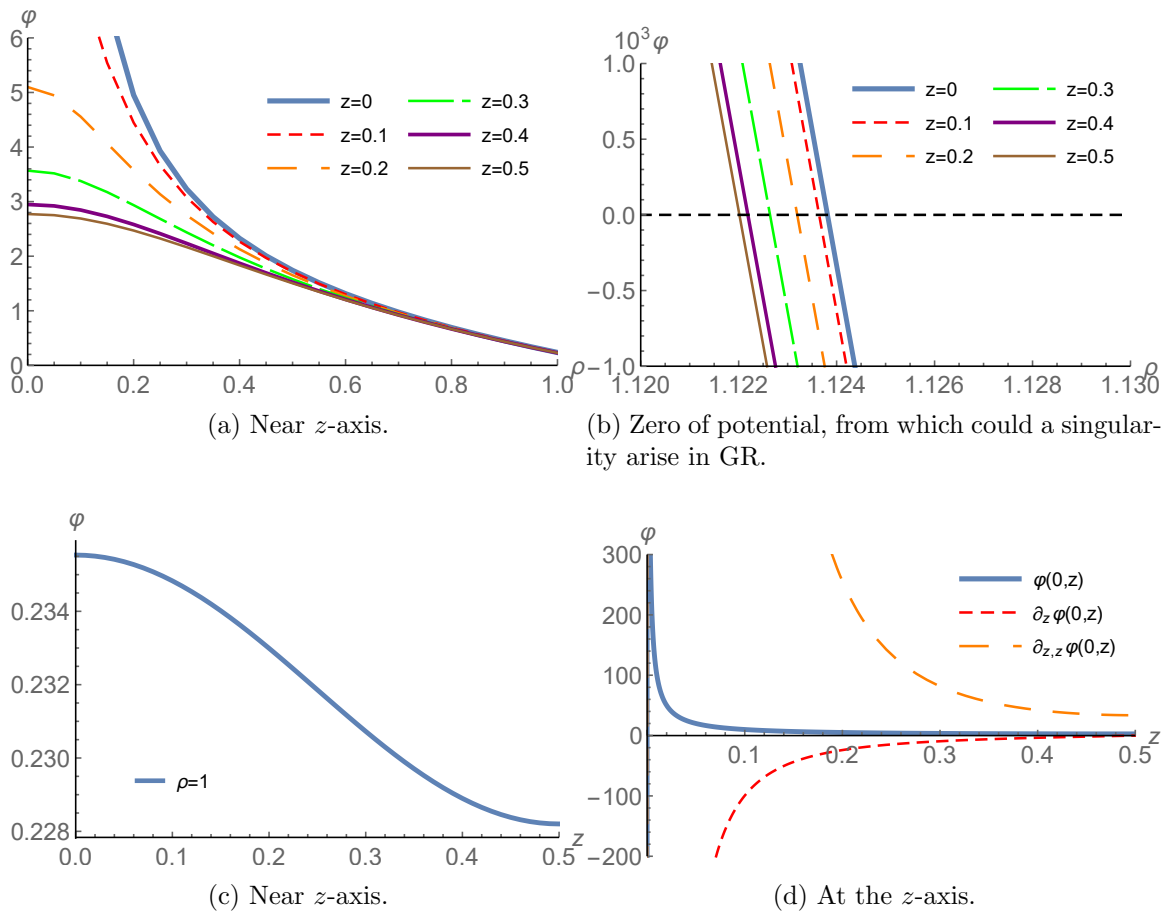


Figure 8.1: Dependence of  $\varphi(\rho, z)$  on  $\rho$  for fixed values of  $z$  (a-b) and  $\rho$  (c-d).

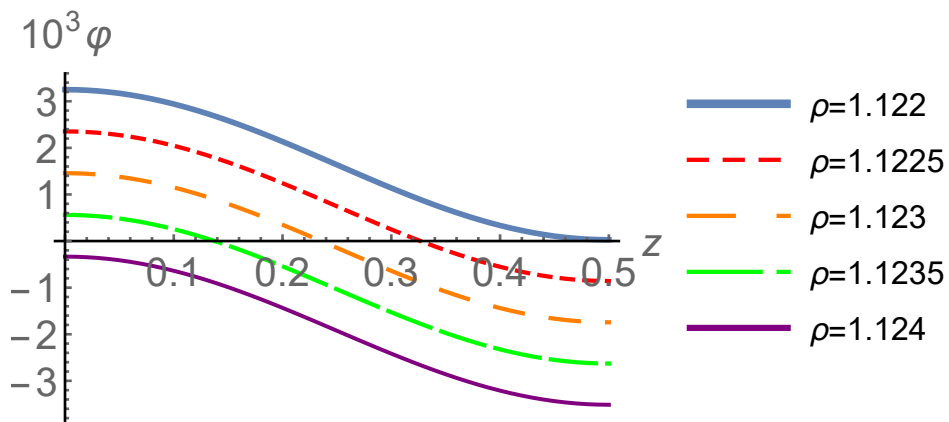


Figure 8.2: Detail of potential  $\varphi$  crossing zero.

where  $\alpha_n$  is a real number. The periodicity requires

$$Z_n(z+k) = Z_n(z) \Rightarrow \alpha_n = \frac{2\pi}{k}n, n \in \mathbb{N}, \quad (8.21)$$

where we restricted to positive frequencies. Let us move to the equation for  $R(\rho)$ . In the special case when  $\alpha_n = 0$  the solution of the equation for  $R(\rho)$  is  $c_1 + c_2 \ln \rho$ . From (8.19) we obtain solution for  $\alpha_n \neq 0$ :

$$R_n(\rho) = AI_0(\alpha_n \rho) + BK_0(\alpha_n \rho), \quad (8.22)$$

where  $A, B$  are constant,  $I_0$  (A.6) and  $K_0$  (A.7) are modified Bessel functions. We construct a general solution in terms of a sum of the fundamental solutions. In view of the desired form of the sources, we choose our potential as

$$\psi(\rho, z) = \psi_0(\rho) + \sum_{n=1}^{\infty} \psi_n(\rho, z), \quad (8.23)$$

where

$$\psi_0(\rho) = -\frac{\ln \rho}{4\pi^2}, \psi_n = \frac{\cos(nz)}{2\pi^2} K_0(n\rho). \quad (8.24)$$

As will be seen below, this corresponds to the correct form of the sources along the axis, with the choice<sup>1</sup>  $k = 2\pi$ ; the factors before logarithm/cosines determine the charge of individual points. The cosines in  $\psi_n$  produce mirror symmetry with respect to the plane  $z = 0$ , the term  $\psi_0$  corresponds to the solution with  $\alpha_n = 0$ . Plots of approximation of  $\psi$  (the first 26 terms) and its derivatives for chosen values of  $\rho$  or  $z$  are shown in Figure 8.3.

## 8.2.1 Convergence

It is obvious that  $\psi_0$  and  $\psi_n$  diverge for  $\rho \rightarrow 0$ . When we restrict on  $\rho \geq \delta > 0$ , using (A.14) we can write

$$|2\pi^2 \psi_n(\rho, z)| \leq |K_0(n\rho)| \leq K_0(\delta) \exp[\delta(1-n)] \equiv c_n, \quad (8.25)$$

from which we get that  $\psi_n \rightarrow 0$ , as  $c_n \rightarrow 0$  in the limit  $n \rightarrow \infty$ . Because the sum  $\sum_n c_n$  is convergent, we also get that the sum  $\sum_n \psi_n$  converges absolutely uniformly. We also notice that derivative with respect to  $z$  keeps the sum convergent because of the exponential suppression. We can also estimate the first derivatives with respect to  $\rho$  as

$$\left| 2\pi^2 \frac{\partial \psi_n}{\partial \rho} \right| \leq |nK_1(n\rho)| \leq K_1(\delta)n \exp[\delta(1-n)], \quad (8.26)$$

as well as the second derivative

$$\left| 2\pi^2 \frac{\partial^2 \psi_n}{\partial \rho^2} \right| \leq |n^2 K_0(n\rho) + n^2 K_2(n\rho)| \leq n^2 c_n + K_2(\delta)n^2 \exp[\delta(1-n)], \quad (8.27)$$

---

<sup>1</sup>For general  $k$  one obtains  $\psi_0 = -\frac{1}{4\pi^2} \ln \rho$ ,  $\psi_n = \frac{1}{2\pi^2} \cos(\alpha_n z) K_0(\alpha_n \rho)$ .

so the sums with first and second derivatives of  $\psi_n$  converge absolutely uniformly for every  $z$  and every  $\rho \leq \delta$ , and we can interchange the order of sums and derivatives/limits/integrals. For  $\rho \gg 1$  we can approximate the sum as

$$2\sqrt{2}\pi^{3/2} \sum_n \psi_n \approx \sum_n \cos(nz) \frac{e^{-n\rho}}{\sqrt{n\rho}} = \frac{\text{Li}_{1/2}(e^{iz-\rho}) + \text{Li}_{1/2}(e^{-iz-\rho})}{\sqrt{\rho}}, \quad (8.28)$$

where  $\text{Li}$  is the polylogarithm function (A.25). We see that terms  $\psi_n$  are exponentially decreasing for large  $\rho$ , and the main contribution in  $\psi$  is  $\psi_0$ . This means that the dependence of  $z$  will disappear. Thus the potential behaves as ECS in the radial cylindrical infinity, with a constant linear density  $\lambda = (8\pi^2)^{-1}$ , where the constant depends on the distance between neighbouring charges.

Let us move now close to the  $z$ -axis. We want to compute charge distribution along the axis. We thus use the integral definition of charge within a cylinder centred at the  $z$ -axis to obtain the linear density:

$$\lim_{\rho \rightarrow 0} 4\pi Q = \int \lambda(z) dz = - \lim_{\rho \rightarrow 0} \oint_S \psi_{,i} n^i dS. \quad (8.29)$$

We rewrite the right-hand side (without the limit) and get

$$4\pi Q = - \iint \psi_{,z} \rho' d\phi' d\rho' - \iint \psi_{,\rho} \rho' d\phi' dz' = q_1 + q_2, \quad (8.30)$$

where  $q_1$  is the first term and  $q_2$  the second one. The term  $q_1$  gives

$$q_1 = \frac{1}{\pi} \sum_{n=1}^{\infty} \int_0^{\rho} n\rho' K_0(n\rho') \sin(nz) d\rho'. \quad (8.31)$$

The function  $K_0$  diverges as logarithm (A.11) for zero argument, but  $\rho K_0(n\rho)$  goes to zero for  $\rho \rightarrow 0$ , so the integrand does not diverge near the axis. We see that the first term in (8.30) vanishes in the limit  $\rho \rightarrow 0$ . The second one gives

$$q_2 = \int \left[ \frac{1}{2\pi} + \frac{1}{\pi} \sum_{n=1}^{\infty} n\rho K_1(n\rho) \cos(nz) \right] dz. \quad (8.32)$$

Since  $K_1(x)$  diverges as  $1/x$  (A.19) for  $x \rightarrow 0$ , we finally get

$$\lim_{\rho \rightarrow 0} 4\pi Q = \int \left[ \frac{1}{2\pi} + \frac{1}{\pi} \sum_{n=1}^{\infty} \cos(nz) \right] dz. \quad (8.33)$$

Using the relation (A.26) we get  $\lambda(z) = \text{III}_{2\pi}(z)$ . For general  $k$  we obtain

$$\lambda(z) = \frac{k}{2\pi} \text{III}_k(z). \quad (8.34)$$

So the charge of the individual sources is  $k(8\pi^2)^{-1}$ . Therefore, for the general case of charges of magnitude  $Q$  located at a distance  $k$  apart, we conclude that the solution must be multiplied by  $8\pi^2 Q/k$  and the asymptotic linear density of



the source is then  $Q/k$ . We thus obtained a sum of distributional charge densities of individual sources along the axis. The total charge density is thus

$$\varrho = \frac{k}{2\pi} \text{III}_k(z) \delta(x) \delta(y) = \frac{k}{4\pi^2 \rho} \text{III}_k(z) \delta(\rho), \quad (8.35)$$

where  $\delta$  is the Dirac delta function. The advantage of the Bessel function expansion consists in the fact that it is easy to see the vanishing of periodicity far away from the axis and approach to the ECS solution. From the behaviour of  $\psi$  we can see that the spacetime is **0** at radial cylindrical infinity, **type D** close to the axis and **type I** far from the axis. It is simple now to construct the corresponding solution of Einstein-Maxwell equations by simply plugging the resulting potential into the general form of the Majumdar-Papapetrou metric. To our knowledge this is the first example of a spacetime with a discrete translational symmetry and in our future work we intend to study its properties further.

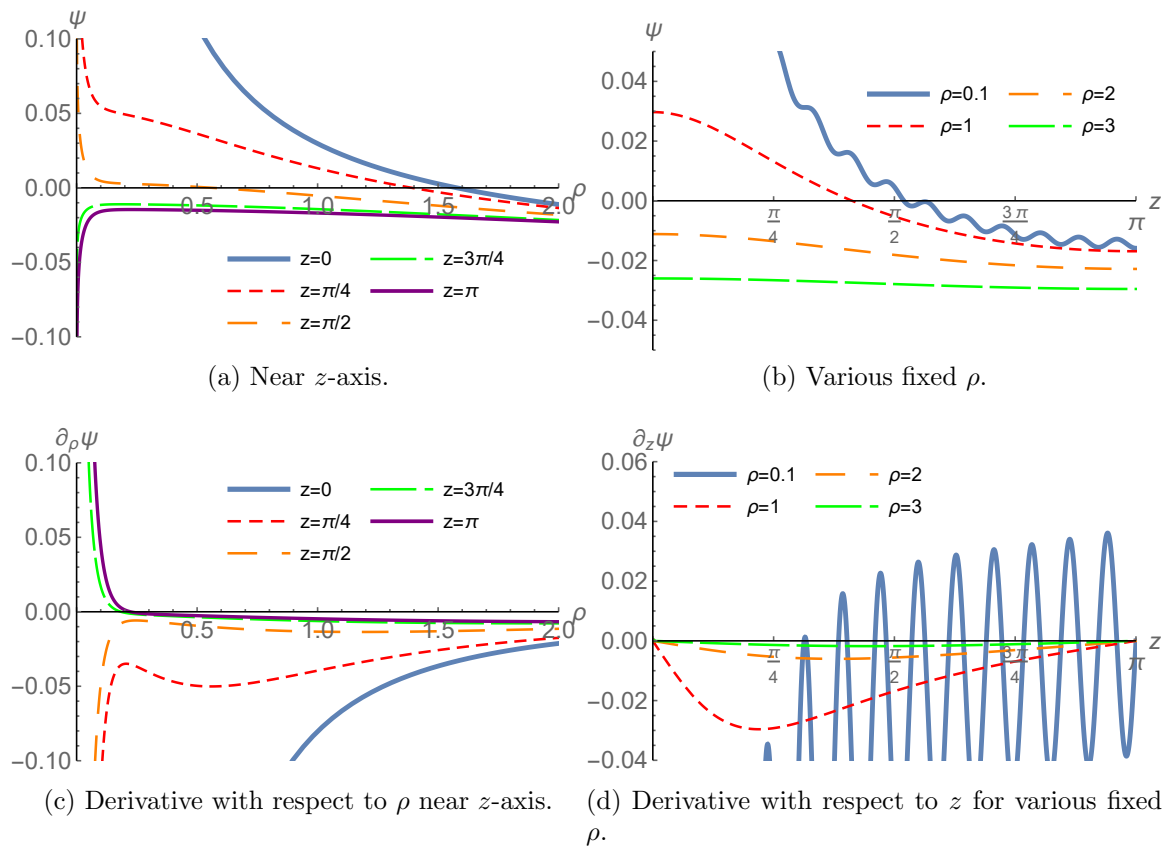


Figure 8.3: Approximation of  $\psi$  - the first 26 terms. One can nicely see that as we move away from the axis the periodicity of the solution fades.

# Conclusion

We investigated the physical properties of a cylindrically symmetric Majumdar-Papapetrou solution of Einstein-Maxwell equations (ECS) sourced by a non-compact, extremally charged linear singularity forming the axis of the spacetime. Based on the form of the metric, we studied geometry of the spacetime and its algebraic classification. From singularities of metric and scalar invariants we discovered that in addition to the axis singularity, the spacetime includes another singularity of different physical properties, which divides the spacetime into two causally separated regions. Since ECS is a solution of electro-vacuum equations both singularities are the only source of the resulting electromagnetic field, which, in turn, produces the gravitational field together with the two singularities. Our goal was to establish their physical parameters — i.e., mass and charge densities per unit length — and geometric characteristics.

We calculated motion of charged test particles moving in preferred directions and compared it to the solution within the framework of classical mechanics. Based on the behavior of radial electrogeodesics, we found that the singularities are not covered by horizons and are thus naked in accordance with [3]. Next, we dealt with static trajectories and gained insight into the specific charge of the singularities. We then determined circular paths and regions where such motion is possible. One interesting result is a range of circular orbit radii and conditions on the spacetime parameters allowing the existence of two electrogeodesics of the same radius but differing angular velocities in the same direction. We then determined the classical limit of the circular velocities to again obtain information about the specific charge of the singularities. We also calculated electrogeodesics parallel to the  $z$ -axis. All solutions of electrogeodesics were summarized in tables and schematic diagrams.

When determining the mass of the sources of ECS, we also proceeded from the total energy of a region of spacetime containing the singularity. However, there is generally no way of determining locally the energy of the gravitational field in GR and we thus used several different definitions — Komar, Brown-York, Landau-Lifschitz and  $C$ -energy formulae — and compared them including the limit to the Newtonian case. Using several independent methods, we thus clarified the meaning of the spacetime's structure and parameters and gained intuition about its physical interpretation. The results will broaden the knowledge of MP spacetimes with non-compact sources, which have not been paid much attention so far.

In Chapter 7 we constructed a solution involving an extremally charged line and a positive cosmological constant (ECSA). We determined its algebraic class and calculated its mass and charge. At the end we compared this solution to the static ECS.

In the last chapter we investigated a classical system consisting of one-dimensional grid of charges. We found the corresponding electrostatic potential and summarized its properties. The solution can be used to construct an analogous system in general relativity.



# Appendix

## Error functions

Error function is defined as

$$\operatorname{erf}(x) \equiv \frac{2}{\sqrt{\pi}} \int_0^x \exp(-t^2) dt. \quad (\text{A.1})$$

The imaginary error function is defined as

$$\operatorname{erfi}(x) \equiv -i \operatorname{erf}(ix) = \frac{2}{\sqrt{\pi}} \int_0^x \exp(t^2) dt. \quad (\text{A.2})$$

The function  $\operatorname{erf}_{-1}$ , resp.  $\operatorname{erfi}_{-1}$ , is the inverse function to  $\operatorname{erf}$ , resp.  $\operatorname{erfi}$ . Function  $\operatorname{erf}_{-1}(x)$  is defined for  $x \in (-1, 1)$  and diverges for  $x \rightarrow \pm 1$ . The function  $\operatorname{erfi}_{-1}(x)$  is defined for  $x \in \mathbb{R}$  and has limit

$$\lim_{x \rightarrow \pm\infty} \operatorname{erfi}_{-1}(x) = \pm\infty. \quad (\text{A.3})$$

Plots of the error functions and their inverses are shown in Figure A.1.

## Lambert W function

Lambert W function (or product log) is defined via relation

$$x = W(x)e^{W(x)}. \quad (\text{A.4})$$

This equation defines  $W(x)$  uniquely only for  $x \geq 0$ , for  $-e^{-1} < x < 0$  there always exist two real solutions:  $W_0(x)$  and  $W_{-1}(x)$ , where  $W_0(x) \geq -1$  and  $W_{-1}(x) \leq -1$ . Function  $W_0(x)$  is defined for  $x \in [-e^{-1}, \infty)$  and function  $W_{-1}(x)$  for  $x \in [-e^{-1}, 0)$ . Plot of both functions is shown in Figure A.2. The series of expansion of  $W_0(x)$  in infinity is

$$W_0(x) \approx \ln x - \ln \ln x + O(1), x \gg 1. \quad (\text{A.5})$$

## Modified Bessel functions

$I_0$  is the modified Bessel function of the first kind, which is defined for  $x \in \mathbb{R}$  as

$$I_0(x) \equiv \frac{1}{\pi} \int_0^\pi \exp(x \cos \theta) d\theta. \quad (\text{A.6})$$

$K_0$  is the modified Bessel function of the second kind, which reads

$$K_0(x) \equiv \int_0^\infty \exp(-x \cosh t) dt, \quad (\text{A.7})$$

and is defined for  $x > 0$ . Plot of these functions is shown in Figure A.2. Both functions are non-negative in their domains. Important limits of these functions read

$$\lim_{x \rightarrow \infty} I_0(x) = \infty, \lim_{x \rightarrow \infty} K_0(x) = 0, \quad (\text{A.8})$$

$$\lim_{x \rightarrow 0} I_0(x) = 1, \lim_{x \rightarrow 0^+} K_0(x) = \infty, \quad (\text{A.9})$$

The series expansion for  $x \ll 1$  are

$$I_0(x) \approx 1 + \frac{x^2}{4} + O(x^4), \quad (\text{A.10})$$

and for  $K_0$

$$K_0(x) \approx \ln 2 - \ln x - \gamma_e + \frac{x^2}{4} (1 - \gamma_e + \ln 2 - \ln x) + O(x^3), \quad (\text{A.11})$$

where  $\gamma_e \approx 0.5772$  is the Euler–Mascheroni constant,  $\ln 2 > \gamma_e$ . For  $x \gg 1$  we get the following series expansion:

$$I_0(x) \approx \sqrt{\frac{2}{\pi}} e^x \left( \frac{1}{2\sqrt{x}} + \frac{1}{16\sqrt{x^3}} \right) + O\left(\frac{1}{x^{5/2}}\right), \quad (\text{A.12})$$

$$K_0(x) \approx \sqrt{2\pi} e^{-x} \left( \frac{1}{2\sqrt{x}} - \frac{1}{16\sqrt{x^3}} \right) + O\left(\frac{1}{x^{5/2}}\right). \quad (\text{A.13})$$

Following bound [14] holds for  $K_\nu$ :

$$\frac{K_\nu(x)}{K_\nu(y)} > e^{y-x}, 0 < x < y, \quad (\text{A.14})$$

where  $K_\nu$  is defined as

$$K_\nu(x) \equiv \int_0^\infty \exp(-x \cosh t) \cosh(\nu t) dt. \quad (\text{A.15})$$

The Bessel functions  $I_1, K_1$  can be expressed in terms of derivatives of  $I_0$  and  $K_0$ :

$$\frac{dI_0}{dx} = I_1(x), \quad \frac{dK_0}{dx} = -K_1(x). \quad (\text{A.16})$$

Their limit behaviour is

$$\lim_{x \rightarrow \infty} I_1(x) = \infty, \quad \lim_{x \rightarrow \infty} K_1(x) = 0, \quad (\text{A.17})$$

$$\lim_{x \rightarrow 0} I_1(x) = 0, \quad \lim_{x \rightarrow 0^+} K_1(x) = \infty. \quad (\text{A.18})$$

The series expansion for  $x \ll 1$  are

$$I_1(x) \approx \frac{x}{2} + \frac{x^3}{16} + O(x^5), \quad K_1(x) \approx \frac{1}{x} + \frac{x}{4} \left( 2\gamma_e - 1 + 2 \ln \frac{x}{2} \right) + O(x^3). \quad (\text{A.19})$$

For  $x \gg 1$  we get the series expansion

$$I_1(x) \approx \frac{e^{2x}}{\sqrt{2\pi}} \left( \frac{1}{\sqrt{x}} + \frac{3}{8\sqrt{x^3}} \right) + O\left(\frac{1}{x^{5/2}}\right), \quad (\text{A.20})$$

$$K_1(x) \approx \sqrt{\pi} e^{-x} \left( \frac{1}{2\sqrt{x}} + \frac{3}{8\sqrt{2x^3}} \right) + O\left(\frac{1}{x^{5/2}}\right). \quad (\text{A.21})$$

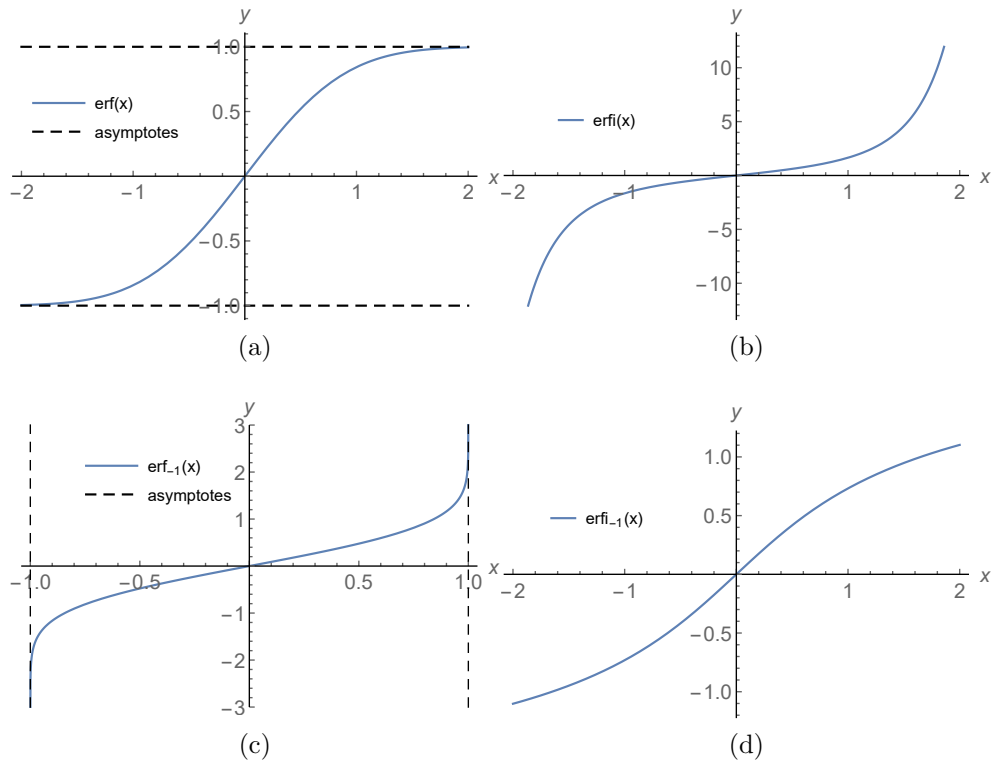


Figure A.1: Plots of the (a) error function, (b) imaginary error function, (c) inverse error function, (d) inverse imaginary error function.

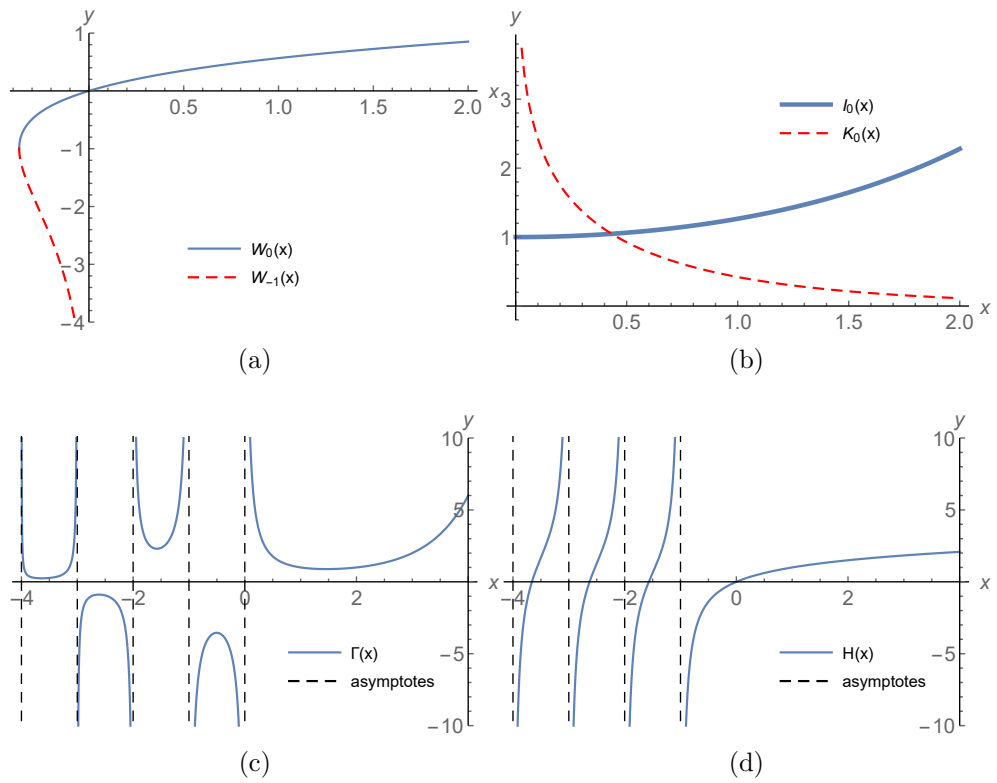


Figure A.2: Plots of the (a) product log functions, (b) Bessel functions, (c) gamma function, (d) harmonic number.

## Other special functions

The well-known Euler gamma function  $\Gamma$  is defined as

$$\Gamma(z) = \int_0^{\infty} x^{z-1} e^{-x} dx, \quad (\text{A.22})$$

where the definition for positive integers reduce to  $\Gamma(z) = (z-1)!$ . The harmonic number is defined as

$$H(z) = \gamma_e + \psi(z+1), \psi(z) = \frac{1}{\Gamma(z)} \frac{d\Gamma(z)}{dz}, \quad (\text{A.23})$$

where  $\psi(z)$  is the digamma function. For positive integers the harmonic number can be expressed as

$$H(n) = \sum_{k=1}^n \frac{1}{k}, n \in \mathbb{N}. \quad (\text{A.24})$$

Plot of harmonic number and gamma function is shown in Figure A.2. The polylogarithm function  $\text{Li}_n$  is defined as

$$\text{Li}_n(z) \equiv \sum_{k=1}^{\infty} \frac{z^k}{k^n}, \quad (\text{A.25})$$

and has a branch cut discontinuity in the complex  $z$  plane running from 1 to  $\infty$ .

## Dirac comb

Dirac comb is a periodic tempered distribution defined as

$$\text{III}_T(t) \equiv \sum_{n \in \mathbb{Z}} \delta(t - nT) = \frac{1}{T} \sum_{n \in \mathbb{Z}} e^{2\pi i n t / T} = \frac{1}{T} + \frac{2}{T} \sum_{n=1}^{\infty} \cos\left(\frac{2\pi n t}{T}\right). \quad (\text{A.26})$$

In the second step we used that  $\text{III}$  is periodic and wrote it as Fourier series and in the last step we rewrote it in terms of real functions. The distribution  $\text{III}_T(t)$  behaves as the Dirac delta function  $\delta$  at every  $t = nT, n \in \mathbb{Z}$ .



# Extremally charged line

Jiří Ryzner & Martin Žofka

Institute of Theoretical Physics, Charles University in Prague

E-mail: j8.ryzner@gmail.com, zofka@mbox.troja.mff.cuni.cz

**Abstract.** We investigate the properties of a static, cylindrically symmetric Majumdar-Papapetrou-type solution of Einstein-Maxwell equations. We locate its singularities, establish its algebraic type, find its asymptotic properties and weak-field limit, study the structure of electrogeodesics, and determine the mass and charge of its sources. We provide an interpretation of the spacetime and discuss the parameter appearing in the metric.

PACS numbers: 04.40.Nr, 04.20.Jb

*Keywords:* Majumdar-Papapetrou spacetime, line singularities, electrogeodesics

Submitted to: *Class. Quantum Grav.*

## 1. Introduction

The Majumdar-Papapetrou solution [1, 2] representing an arbitrary set of stationary, extremally charged black holes in equilibrium is well known. The spacetime arises as a solution of Laplace equation. Hartle and Hawking [3] assumed a flat spatial infinity and showed that any solution to the Laplace equation with non point-like sources must contain a naked singularity. There are, however, interesting classes of solutions of different asymptotics. In this paper, we assume a line source that extends to infinity along a straight line and we thus do not have a flat spatial infinity. Although it does contain a naked singularity it is of interest in itself and, generally, non-asymptotically flat MP solutions may involve horizons. The importance of the solution consists in the fact that it has an obvious classical analog we can compare it to. We investigate the properties of the spacetime and also compare it to the charged black string [4], which however requires a non-zero cosmological constant. We interpret the parameter of the metric using electrogeodesics, integral definitions of mass and charge, and Israel formalism for various shell sources replacing the singularities of the solution. We first derive the physical properties of the non-relativistic counterpart of the solution to be later able to compare it to the full solution. In Chapter 3, we present the studied spacetime and its basic geometrical characteristics. In Chapters 4 and 5, we determine the mass and charge of the singular line sources using integral definitions of energy and the Israel formalism, respectively. In Chapter 6, we finally investigate motion of both charged and uncharged massive particles and photons and compare them to the Newtonian case.

## 2. Newtonian analog

We review the classical analog of the infinite charged string. We first write the gravitational and electrostatic potentials,  $\varphi_G$  and  $\varphi_E$ , in the standard cylindrical coordinates  $\rho, \phi, z$  as follows

$$\varphi_G = 2\mu \ln \frac{\rho}{P}, \quad \varphi_E = -2\lambda \ln \frac{\rho}{P}, \quad (1)$$

with  $\mu$  the mass and  $\lambda$  charge per unit length of the string.  $P$  is a normalization constant defining the cylindrical surface of vanishing potential<sup>‡</sup>. We now rescale the radial and azimuthal coordinates so that  $\rho/P \rightarrow \rho, z/P \rightarrow z$ . The classical Lagrangian per unit mass of a massive and charged test particle of specific charge  $q = Q/M$  then reads

$$\mathcal{L} = \frac{1}{2} \left( \dot{\rho}^2 + \rho^2 \dot{\phi}^2 + \dot{z}^2 \right) - (q\varphi_E + \varphi_G). \quad (2)$$

The Lagrangian does not depend on  $\phi$  and  $z$  and does not explicitly depend on  $t$ , so we have the following integrals of motion

$$E \equiv \sum_i \frac{\partial \mathcal{L}}{\partial \dot{q}^i} \dot{q}^i - \mathcal{L} = \frac{1}{2} \left( \dot{\rho}^2 + \rho^2 \dot{\phi}^2 + \dot{z}^2 \right) + \varphi_G + q\varphi_E, \quad (3)$$

<sup>‡</sup> We chose both potentials to vanish at the same radius so that they are proportional to each other; we may always do so as the two constants only appear as a constant in the Lagrangian (2).

$$L_z \equiv \frac{\partial \mathcal{L}}{\partial \dot{\phi}} = \dot{\phi} \rho^2, \quad (4)$$

$$p_z \equiv \frac{\partial \mathcal{L}}{\partial \dot{z}} = \dot{z}. \quad (5)$$

The only remaining equation of motion is

$$2(q\lambda - \mu) + \rho^2 \dot{\phi}^2 - \rho \ddot{\rho} = 0. \quad (6)$$

### 2.1. Static solution

If the test particle is to be in equilibrium at a given point we must have

$$\mu - q\lambda \equiv \mathcal{A} = 0, E = p_z = L_z = 0. \quad (7)$$

Thus, the particle can only remain at rest if it is made of the same material as the source as regards its specific charge and in such a case it can stay still at any point. In fact, the potential part of the Lagrangian then cancels out and we have a particle moving along straight lines at a constant velocity. Also, free-particle motion is the only case admitting purely axial motion (with  $E, p_z \neq 0$ ).

### 2.2. Radial motion

For radial motion, with  $z$  and  $\phi$  constant, we obtain a single equation

$$E = \frac{1}{2} [\dot{\rho}^2 + 4\mathcal{A} \ln \rho], \quad (8)$$

which can be rewritten as

$$\dot{\rho}^2 = 2[E - 2\mathcal{A} \ln \rho]. \quad (9)$$

Motion is only possible if the right-hand side is non-negative. Omitting the above case of a freely moving particle with  $\mathcal{A} = 0$ , we then have two cases depending on the sign of  $\mathcal{A}$ : unbound orbits reaching the radial infinity with  $\mathcal{A} < 0$  and bound orbits intersecting the source otherwise. Motion can be expressed explicitly in terms of the error function.

### 2.3. Circular motion

For circular orbits with  $\rho$  and  $z$  constant, we find the following equations

$$0 = \rho^2 \dot{\phi}^2 - 2\mathcal{A} \quad (10)$$

$$L_z = \rho^2 \dot{\phi}, p_z = 0 \quad (11)$$

$$E = \frac{1}{2} [\rho^2 \dot{\phi}^2 + 4\mathcal{A} \ln \rho] \quad (12)$$

This yields a constant angular velocity

$$\omega = \frac{\sqrt{2\mathcal{A}}}{\rho}. \quad (13)$$

Circular motion can occur at any radius but only for  $\mathcal{A} > 0$ , which means that gravity is stronger than the electromagnetic force.

### 3. Geometry of the spacetime

The investigated general relativistic solution stems from the same Laplace equation as the classical field of Chapter 2. Based on this analogy, we shall refer to it as the extremally charged string or ECS, for short. However, the gravitational and electromagnetic fields are not independent here and are given by the same function. One integration constant,  $P > 0$ , can be scaled away by introducing dimensionless cylindrical coordinates,  $\rho/P \rightarrow \rho, z/P \rightarrow z, t/P \rightarrow t$ . The investigated spacetime is then described by the rescaled metric

$$d\bar{s}^2 = \frac{ds^2}{P^2} = -\frac{dt^2}{U^2} + U^2 (d\rho^2 + \rho^2 d\phi^2 + dz^2), \quad (14)$$

with

$$U(\rho) = 1 + K \ln \rho, \quad (15)$$

where  $K$  is the other integration constant the meaning of which is one of our goals. The form of the potential  $U$  is chosen in such a way that the limit  $K \rightarrow 0$  corresponds to the Minkowski space as discussed below. The electromagnetic four-potential is

$$A = \frac{dt}{U}, \quad (16)$$

yielding the following Maxwell tensor

$$F = \frac{U_{,\rho}}{U^2} dt \wedge d\rho, \quad (17)$$

describing a purely radial electric field  $E_\rho = -K/\rho(1 + K \ln \rho)^2$ , which vanishes at radial infinity. The spacetime is static and cylindrically symmetric, admitting only these three Killing vectors.

The Kretschmann scalar reads

$$R_{\mu\nu\kappa\lambda} R^{\mu\nu\kappa\lambda} = \frac{8K^2 [2K^2 \ln^2 \rho + 7K^2 + 2(3K + 2)K \ln \rho + 6K + 2]}{\rho^4 (K \ln \rho + 1)^8}, \quad (18)$$

and vanishes far away from the axis,  $\rho \rightarrow \infty$ , as do also all tetrad components of the Riemann tensor. The spacetime thus has two singularities: one located at  $\rho = 0$  while the outer one has  $\rho \equiv \rho_o = \exp(-1/K)$ . The spacetime thus splits in two independent regions separated by the outer singularity.

The spacetime is generally of type I apart from two special cylindrical surfaces where it is type D. Additionally, at radial infinity, it approaches type O as all Weyl scalars vanish in the limit  $\rho \rightarrow \infty$ .

Lemos and Zanchin [4] found a spacetime also describing the field of a charged and massive infinite straight string. Their solution, however, requires the presence of a negative cosmological constant balancing the field. Therefore, the asymptotics of the solution far away from the axis approach that of anti-de Sitter. The string itself is singular but it always has a horizon making sure the cosmic censorship conjecture holds. The mass and charge densities are independent. These are all points of difference between the two solutions. If there are any closer similarities they might be revealed due

to the fact that our solution can also be generalized to contain a positive cosmological constant, which will change its asymptotics and cancel the static nature of the spacetime. In our future work we will study the cosmological solution in more detail.

### 3.1. Proper lengths

Let us now investigate the proper length of some special curves. Let us begin with the proper circumference of a circle of constant  $\rho$

$$dl_\phi^2 = \rho^2 U^2(\rho) d\phi^2 \Rightarrow l_\phi(\rho) = 2\pi\rho|1 + K \ln \rho|. \quad (19)$$

The circumference of the hoops vanishes at  $\rho = 0$  then grows to its maximum value at  $\rho_c = \exp(-1 - 1/K) = \rho_0/e < \rho_0$  and vanishes again at  $\rho = \rho_0$ . The outer singularity thus behaves as another axis of the spacetime, see Figure 1. The proper length of the coordinate segment  $(0, h)$  along the  $z$ -axis is

$$dl_z^2 = U^2(\rho) dz^2 \Rightarrow l_z(\rho) = h|1 + K \ln \rho|. \quad (20)$$

The outer singularity thus contracts along its length as well and appears to be a point rather than a cylindrical surface. The proper distance from  $\rho = 0$  is given by

$$dl_\rho^2 = U^2(\rho) d\rho^2 \Rightarrow l_\rho(\rho) = \int_0^\rho |1 + K \ln \rho'| d\rho'. \quad (21)$$

To compute the integral, we need to split the integration into cases when  $0 < \rho < \rho_0$  and  $\rho \geq \rho_0$ . We obtain

$$l_\rho(\rho) = \begin{cases} -\rho(1 - K + K \ln \rho) \operatorname{sgn} K, & 0 < \rho < \rho_0, \\ [\rho(1 - K + K \ln \rho) + 2K\rho_0] \operatorname{sgn} K, & \rho \geq \rho_0. \end{cases} \quad (22)$$

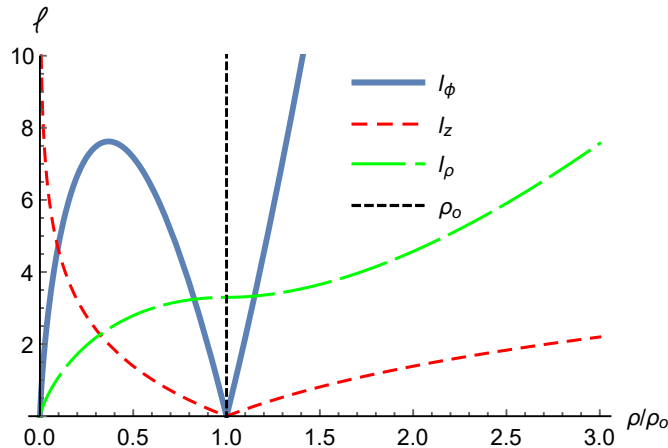


**Figure 1.** Proper length of various curves for  $K = -2$ . The form of the curves is the same also for  $K > 0$ .

For  $K > 0$  and in the limit  $K \rightarrow 0^+$ , the spacetime yields the Minkowski spacetime above  $\rho_0$  while the inner region shrinks with the proper distance from the axis to  $\rho_0$  vanishing and from  $\rho_0$  to infinity diverging as  $\rho$ . For  $K < 0$  and in the limit  $K \rightarrow 0^-$ , we find Minkowski below  $\rho_0$  with the proper distance from the axis to  $\rho_0$  infinite.

#### 4. Mass and charge of ECS

In this section we focus on the total energy enclosed within a static cylinder of constant radius,  $\rho$ . The advantage of ECS is that it is static and expressed in coordinates where the metric is diagonal. However, ECS is not asymptotically flat so we cannot use, for example, the ADM mass. We thus apply several other definitions of mass (energy) enclosed within a coordinate cylinder and compare them. Finally, we also calculate the charge enclosed in the respective cylinders. Since ECS is a special case of Majumdar-Papapetrou spacetimes with equal linear charge and mass densities we expect a similar behavior at least in the weak-field limit of  $K \rightarrow 0$ .

##### 4.1. C-energy

We cast the metric as

$$ds^2 = U^{-2} (-dt^2 + dR^2) + U^2 dz^2 + \rho^2 U^2 d\phi^2, \quad (23)$$

corresponding to the canonical form required to determine the C-energy [5]. After regularization, we obtain

$$\mathcal{E}_C(\rho) = \frac{h}{8} \left[ 1 - \left( \frac{U + 2\rho U_{,\rho}}{U} \right)^2 \right] = -\frac{h}{2} K \frac{1 + K + K \ln \rho}{(1 + K \ln \rho)^2}. \quad (24)$$

In the limit  $K \rightarrow 0$ , we get

$$\mathcal{E}_C(\rho) \approx -\frac{hK}{2} + \frac{h}{2} (-1 + \ln \rho) K^2 + O(K^3). \quad (25)$$

For a plot of the resulting function, refer to Figure 2. It diverges at the outer singularity and vanishes both at  $\rho = 0$  and at the radial infinity.

##### 4.2. Landau-Lifshitz

Landau and Lifshitz derived a conservation law [6]

$$[16\pi (-g) (T^{\mu\nu} + t_{LL}^{\mu\nu})]_{,\nu} = 0, \quad (26)$$

with  $g$  the determinant of the metric and based on the stress-energy pseudotensor of the gravitational field,  $t_{LL}^{\mu\nu}$ , defined as follows

$$16\pi t_{LL}^{\mu\nu} \equiv g^{-1} [g (g^{\mu\nu} g^{\alpha\beta} - g^{\mu\alpha} g^{\nu\beta})]_{,\alpha\beta} - [2R^{\mu\nu} + (2\Lambda - R) g^{\mu\nu}]. \quad (27)$$

In our calculation we determined the corresponding super-potential (see [6]) and obtained a relation for the mass

$$M_{LL}(\rho) = P^0 = \frac{h}{2} |K| \text{sgn}(\rho_o - \rho) (1 + K \ln \rho)^6. \quad (28)$$

For  $K \rightarrow 0$ , we find

$$M_{LL}(\rho) \approx -\frac{hK}{2} - 3K^2 h \ln \rho + O(K^3). \quad (29)$$

For a plot of the resulting function, refer to Figure 2 where we can see that  $M_{LL}(\rho)$  diverges at  $\rho = 0$  and radial infinity and vanishes at  $\rho = \rho_o$ . It changes sign at the outer singularity and its behavior is independent of the sign of  $K$ .

### 4.3. Brown-York

Energy is defined as an integral over the boundary  $S$  of a volume  $\Sigma$  and one needs to subtract the contribution of a selected background spacetime [7]. Since in the limit  $K \rightarrow 0$  we obtain Minkowski, we subtract the contribution of flat spacetime [4]. From the relation

$$M_{BY} = \int_S g_{\mu\nu} (\mathcal{E}n^\mu + j^\mu) \xi_{(t)}^\nu dS, \quad (30)$$

with appropriate definition of the terms appearing in the integral (see [4]). After some algebra, we conclude

$$M_{BY}(\rho) = \frac{-hK}{2(1 + K \ln \rho)}. \quad (31)$$

For  $K \rightarrow 0$ , we find

$$M_{BY}(\rho) \approx -\frac{hK}{2} + \frac{hK^2}{2} \ln \rho + O(K^3). \quad (32)$$

For a plot of the resulting function, refer to Figure 2 where we can see that for  $K < 0$   $M_{BY}$  is always non-negative, whereas for  $K > 0$  it is positive up to  $\rho = e^{-1-1/K}$  and then it is only negative. Brown-York mass is always finite at  $\rho = 0$  and at infinity while diverging at  $\rho = \rho_o$ .

### 4.4. Komar mass

For a stationary spacetime, Komar defines the mass enclosed in a three-dimensional spacelike surface  $\Sigma$  [8] as

$$M_K = \frac{1}{4\pi} \oint_S \xi_{(t)}^{\alpha;\beta} r_\alpha n_\beta dS \quad (33)$$

where  $\xi_{(t)}^\beta$  is the Killing vector corresponding to the time symmetry. Now we plug in our choice of integration surface to yield

$$M_K(\rho) = -\frac{h\rho U_{,\rho}}{2U}. \quad (34)$$

We see that this expression is identical to the Brown-York definition (31).

### 4.5. Overview of results for mass

We summarize our results for various definitions of mass in Figure 2. Generally, they are consistent with the singularity at  $\rho = 0$  having a positive linear mass density equal to  $-K/2$  at least for small negative values of  $K$ , while the outer singularity at  $\rho = \rho_o$  has a negative linear mass density equal to  $-K/2$  at least for small positive values of  $K$ . This is due to the fact that the Minkowski limit can only be applied in these regions and the corresponding signs of  $K$ , see the last paragraph of Chapter 3. If we shift the origin of coordinate  $\rho$  to  $\rho_o$  and calculate the energy within a cylinder centered at  $\rho = \rho_o$ , we find that the total mass switches sign.

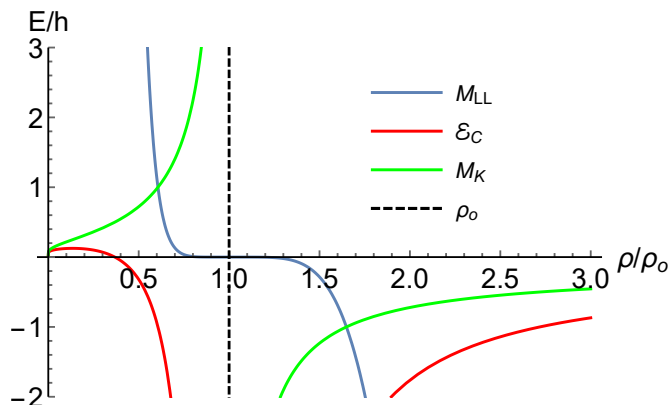


**Figure 2.** Comparison of different definitions of mass for  $K = \pm 2$ .

#### 4.6. Charge

We now calculate the charge within a closed area  $S$

$$Q \equiv \frac{1}{4\pi} \oint_S *F = \frac{1}{4\pi} \oint_S F_{\alpha\beta} r^\alpha n^\beta dS = \frac{-hK}{2}, \quad (35)$$

where  $F$  is the Maxwell tensor and  $*$  denotes the Hodge dual. Similarly to the previous subsections on energy, if we calculate the charge enclosed by a cylindrical surface around the outer axis, the expression switches its sign. We thus conclude that the singularity at  $\rho = 0$  has a linear charge equal to  $-K/2$  just like the outer singularity when observed from the outside. However, when we consider the outer singularity from below, its linear charge density is  $K/2$ . Overall, the linear charge and mass densities of the singularities are of the same magnitude as expected.

### 5. Shell sources

We now apply the Israel formalism [9] generalized to non-vacuum spacetimes involving electromagnetic fields by Kuchař [10]. Instead of relying on non-unique definitions of local energy density, we replace the singular regions of the spacetime by flat space and study the mass and charge of matter induced on the interface between the newly introduced Minkowski sections and the original ECS outside. For the sake of brevity, we just give the results here.

We first replace the singularity at  $\rho = \rho_o$  and thus take  $\rho > \rho_o$ . We have a Minkowskian cylinder of finite radius restricted by an infinitely thin cylindrical surface of induced matter, beyond which ECS stretches on to radial infinity. For  $K > 0$  we must have  $U > 0$  and for the mass and charge induced per unit length of the cylindrical interface we find  $M_1 = Q_1 = -\frac{1}{2}\frac{K}{U} < 0$ . There is zero induced pressure along the  $z$  and  $\phi$  directions. The lowest-order expansion yields  $M_1 = Q_1 = -K/2$  as expected. Taking  $K < 0$  now, we have  $U < 0$  and the induced mass is of the form  $M_1 = \frac{1}{2}(1 + \frac{K}{U}) > 0$  and the induced charge is  $Q_1 = \frac{1}{2}\frac{K}{U} > 0$ . We cannot apply the limit  $K \rightarrow 0$  here, since



we could not keep the cylinder radius constant in the limiting process to stay above the outer singularity. Additionally, there is also induced tension along the  $z$ -direction.

Let us look now at the singularity located at  $\rho = 0$ . For  $K > 0$  we need  $U < 0$  and find  $M_1 = \frac{1}{2}(1 + \frac{K}{U})$  and  $Q_1 = \frac{1}{2}\frac{K}{U} < 0$ . There is again tension induced along the  $z$  direction. The induced mass is positive below the radius of largest circumference,  $\rho_c$  (see text below (19) and Figure 1), and negative above it. There is no Minkowski limit. Taking  $K < 0$  now, we need  $U > 0$  and the induced mass is of the form  $M_1 = Q_1 = -\frac{1}{2}\frac{K}{U} > 0$ . The lowest-order expansion yields  $M_1 = Q_1 = -K/2$  in the Minkowski limit as expected. The induced cylinder has no pressure or tension in any direction.

Finally, we now replace the outer singularity—located at  $\rho_o$  and forming the other spacetime axis with a vanishing circumference (see Figure 1)—by a cylindrical region of Minkowski and continue across a cylindrical surface inside, towards  $\rho = 0$ . Let us first take  $K > 0$  and thus  $U < 0$ . We have  $M_1 = Q_1 = -\frac{1}{2}\frac{K}{U} > 0$ , with no pressure or tension. We cannot do the Minkowski limit here. For  $K < 0$  and  $U > 0$  we obtain  $Q_1 = \frac{1}{2}\frac{K}{U} < 0$  and  $M_1 = \frac{1}{2}(1 + \frac{K}{U})$ , which is negative if we are above  $\rho_c$ . There is again tension along the  $z$ -direction. We cannot do the Minkowski limit since the cylinder radius would fall below  $\rho_c$  and we would end up with two sections of Minkowski pasted together inside out with two axes present in the resulting spacetime.

The cases admitting a Minkowski limit are consistent with the findings of Chapter 4, for an overview, see Conclusions and summary.

## 6. Equations of motion

Finally, we will study motion of test particles in the spacetime to compare to the results from the previous sections. The Lagrangian for a charged particle of specific charge  $q$  and moving in an electromagnetic field is

$$\begin{aligned} \mathcal{L} &= \frac{1}{2}g_{\mu\nu}\dot{x}^\mu\dot{x}^\nu + q\dot{x}^\kappa A_\kappa = \\ &= \frac{1}{2}\left[\left(\rho^2\dot{\phi}^2 + \dot{\rho}^2 + \dot{z}^2\right)U^2 - \frac{\dot{t}^2}{U^2}\right] + q\frac{\dot{t}}{U}. \end{aligned} \quad (36)$$

The Lagrangian does not explicitly depend on  $t$ ,  $\phi$  and  $z$ , so the integrals of motion read

$$E \equiv \frac{qU - \dot{t}}{U^2}, L_z \equiv \rho^2\dot{\phi}U^2, N \equiv \dot{z}U^2. \quad (37)$$

There is thus a single equation remaining, which is not explicitly integrated:

$$\ddot{\rho} - \rho\dot{\phi}^2 - \frac{U_{,\rho}}{U}\left[\rho^2\dot{\phi}^2 - \dot{\rho}^2 + \dot{z}^2\right] + \dot{t}U_{,\rho}\frac{qU - \dot{t}}{U^5} = 0. \quad (38)$$

And finally the normalization

$$\left(\rho^2\dot{\phi}^2 + \dot{\rho}^2 + \dot{z}^2\right)U^2 - \frac{\dot{t}^2}{U^2} = \mathcal{U}, \quad (39)$$

where  $\mathcal{U}$  is a normalization constant,  $\mathcal{U} = 0$  for photon motion and  $\mathcal{U} = -1$  for timelike motion. The equations of motion are singular if  $U$  or  $U_{,\rho}$  are singular and they diverge at  $\rho = 0$  or  $\rho = \rho_o$ .

### 6.1. Static electrogeodesics

First we will investigate static solutions. The equations reduce to

$$-\frac{\dot{t}^2}{U^2} = -1, \ddot{t} = 0, (qU - \dot{t}) \dot{t} = 0. \quad (40)$$

The solution only exists between the singularities for  $q = -\text{sgn}K$  and outside for  $q = \text{sgn}K$ . Accepting our previous results on the charge of the singularities, we see that for  $K > 0$  a test particle located between the singularities with  $q = -1$  is repelled outward so the linear mass density of the two singularities must be positive at  $\rho = 0$  and negative at  $\rho = \rho_o$  at least in the weak-field limit. Moreover, their magnitude must be the same as this is the case for the particle. If we are outside where  $q = 1$ , the particle is attracted inwards by the charge so it must be repelled by a negative mass density. Following the same line of reasoning for  $K < 0$ , we find that the signs of mass densities of the singularities are in fact the same as for  $K > 0$  and their magnitude is again equal to the charge density.

### 6.2. Radial motion

Radial cylindrical electrogeodesics are defined as world-lines where  $\phi$  and  $z$  are independent of proper time. They are governed by the equations

$$\dot{\rho}^2 U^2 - \frac{\dot{t}^2}{U^2} = \mathcal{U}, \quad (41)$$

$$\frac{qU - \dot{t}}{U^2} = E, \quad (42)$$

where the first equation is the normalization condition and the second one comes from conservation of  $E$ .

*6.2.1. Photon motion* Taking  $q = \mathcal{U} = 0$ , (41)–(42) become equations of motion for photon. We proceed by expressing  $\dot{t}$  from (42). From normalization we then obtain an equation for  $\rho$ . We thus need to solve

$$\dot{t} = -E(1 + K \ln \rho)^2, \dot{\rho}^2 = E^2. \quad (43)$$

From (43) we immediately see that  $E < 0$  for  $\dot{t}$  to be positive. For  $E = 0$  the photon would be static. This solution reads

$$\rho(\tau) = r_0 \pm |E|\tau, \quad (44)$$

where  $r_0$  is the initial radius and  $\tau$  is the affine parameter. If the photon starts towards one of the singularities, it will hit it, only photons emitted above outer singularity can avoid both singularities. The geodesic cannot be continued across the singularities and, therefore, we have two regions of spacetime which are causally separated.

6.2.2. *Electrogeodesic* The equations for electrogeodesic can be integrated to yield

$$\dot{t} = -(1 + K \ln \rho) (E - q + EK \ln \rho), \quad (45)$$

$$\dot{\rho}^2 = \frac{(E - q + EK \ln \rho)^2 - 1}{(1 + K \ln \rho)^2}. \quad (46)$$

We find two turning points

$$\rho_{t\pm} = \exp \frac{q - E \pm 1}{EK}, E \neq 0, q \neq \mp 1. \quad (47)$$

Radial acceleration at these radii reads

$$\ddot{\rho}(\tau : \rho = \rho_{t\pm}) = \pm \frac{KE^3}{\rho_{t\pm} (q \pm 1)^2} \neq 0 \text{ for } q \neq \mp 1. \quad (48)$$

We summarize our results for radial electrogeodesics in Figure 3.

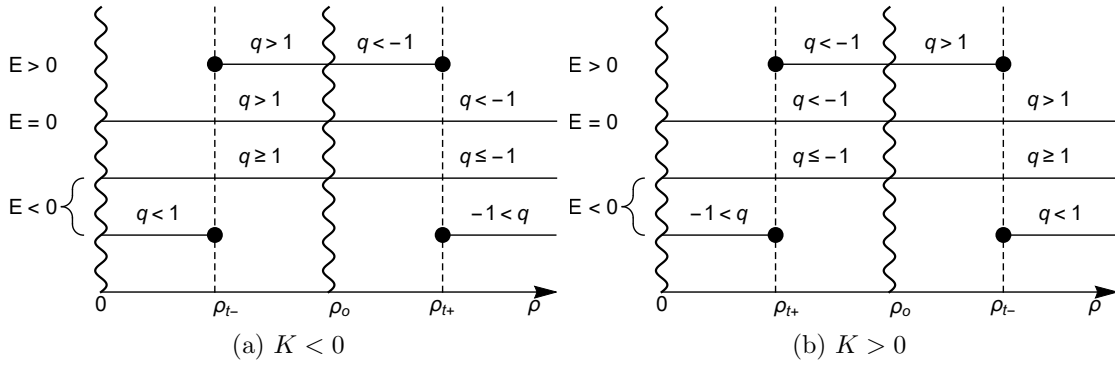


**Figure 3.** Regions, where radial electrogeodesic motion is possible.

### 6.3. Circular electrogeodesics

We investigate circular electrogeodesics with  $\rho$  and  $z$  constant and governed by

$$-\frac{\dot{t}^2}{U^2} + U^2 \rho^2 \dot{\phi}^2 = \mathcal{U}, \quad (49)$$

$$\ddot{t} = \ddot{\phi} = 0, \quad (50)$$

$$\frac{q \dot{t} U_{,\rho}}{U^4} - \frac{\dot{t}^2 U_{,\rho}}{U^5} - \rho \dot{\phi}^2 - \frac{\rho^2 \dot{\phi}^2 U_{,\rho}}{U} = 0. \quad (51)$$

We can immediately write  $t = \gamma\tau, \phi = \omega\tau$  and insert this into the above equations to give

$$-\frac{\gamma^2}{(1 + K \ln \rho)^2} + (1 + K \ln \rho)^2 \rho^2 \omega^2 = \mathcal{U}, \quad (52)$$

$$\frac{K \gamma^2}{1 + K \ln \rho} + \rho^2 \omega^2 (1 + K \ln \rho)^3 (1 + K + K \ln \rho) = qK\gamma. \quad (53)$$

6.3.1. *Photon motion* Setting  $q = \mathcal{U} = 0$  in the previous equations, we obtain

$$\rho^2 \omega^2 U^4 - \gamma^2 = 0, \quad (54)$$

$$U_{,\rho} \gamma^2 + U^4 \rho \omega^2 (U + \rho U_{,\rho}) = 0, \quad (55)$$

which yields the radius,  $\rho_{ph}$ , of the photon orbit

$$U + 2K = 0 \Rightarrow \rho = \rho_{ph} \equiv e^{-2-1/K}, \gamma^2 = \rho^2 \omega^2 K^2, \quad (56)$$

where  $\omega$  is a free parameter.

6.3.2. *Charged massive particle* We now investigate charged massive particles with  $\mathcal{U} = -1$ . The equations are quadratic, so we expect two different absolute values of  $\omega$  at most (the opposite sign corresponds to the opposite direction). First we express  $\omega$  from the normalization condition

$$\omega^2 = \frac{\gamma^2 - U^2}{\rho^2 U^4} \quad (57)$$

and substitute back into the second equation. The general solution (for  $\rho \neq \rho_f$ ) is

$$\gamma_{\pm} = U \frac{q\rho U_{,\rho} \pm \sqrt{(q^2 + 8)\rho^2 U_{,\rho}^2 + 12\rho U U_{,\rho} + 4U^2}}{2(2\rho U_{,\rho} + U)}, \quad (58)$$

$$\omega_{\pm}^2 = U_{,\rho} \frac{\rho U_{,\rho} (q^2 - 4) - 2U \pm q\sqrt{(q^2 + 8)\rho^2 U_{,\rho}^2 + 12\rho U U_{,\rho} + 4U^2}}{2\rho U^2 (2\rho U_{,\rho} + U)^2}. \quad (59)$$

Plots of the angular velocities for a range of specific charges are given in Figure 5.

To compare these trajectories to the Newtonian case, we calculate a series expansion of the angular velocity for  $K \rightarrow 0$

$$\omega_{\pm}^2 \approx K \frac{-1 \pm q}{\rho^2} + O(K^2). \quad (60)$$

We need to set  $\mu = \lambda$  in (7) to have an extremally charged source of the field and express the angular velocity,  $\omega_N$ , using the charge-to-mass ratio

$$\omega_N^2 = 2\lambda \frac{1 - q}{\rho^2}. \quad (61)$$

Therefore,  $\omega_+$  approaches the Newtonian velocity if we identify the parameters of the field as follows

$$\frac{M}{h} = \frac{Q}{h} = -\frac{K}{2}. \quad (62)$$

The regions where circular motion is possible are summarized in Figure 4. There are regions admitting both  $\omega_{\pm}$  unlike the Newtonian case which only allows a single angular velocity at any given radius. This is a behavior we have already observed in a previous paper on another MP solution involving two charged black holes [11] and is a result of the quadratic nature of the algebraic form of the equations of motion. The value  $\rho_q$  used in the figures is

$$\rho_q = \exp\left(-\frac{2 + 3K + K\sqrt{1 - q^2}}{2K}\right). \quad (63)$$

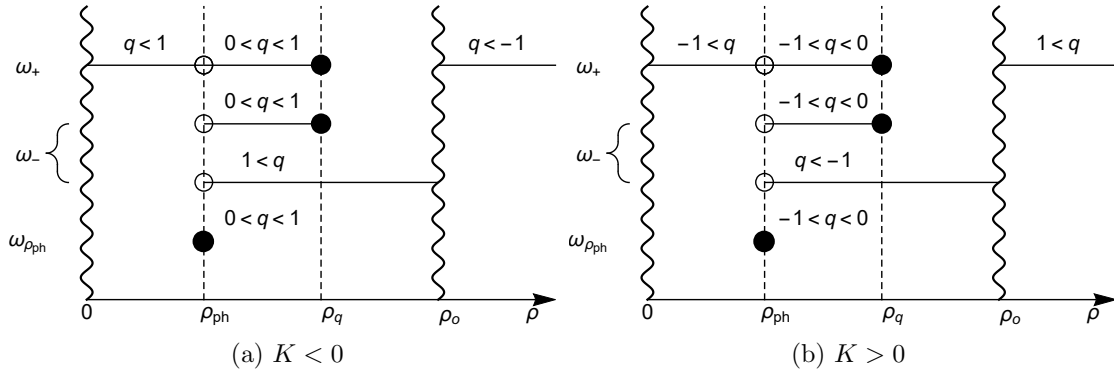


**Figure 4.** Schematic illustration of regions where circular electrogeodesic motion is possible. The diagrams are not to scale, static solutions are excluded. The photon orbit radius  $\rho_{ph}$  admits a special frequency  $\omega_{\rho_{ph}}^2 = (1 - q^2)/4K^2\rho_{ph}^2$ .

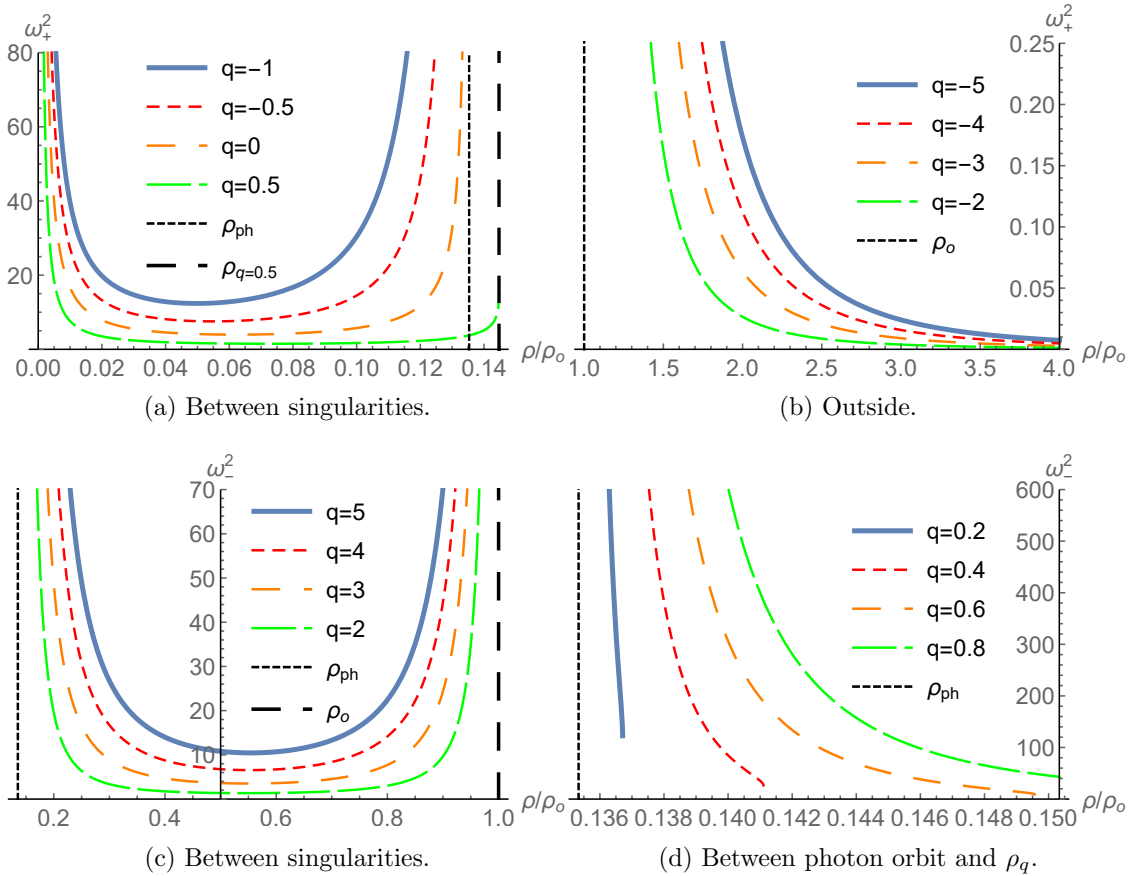


**Figure 5.** Plots of angular velocity for circular motion of test particles of varying specific charge as a function of the radial coordinate,  $K = -2$ .

#### 6.4. Electrogeodesics parallel to the axis

Unlike in the Newtonian case, motion parallel to the axis is possible in GR. It is governed by the following equations

$$-\frac{\dot{t}^2}{U^2} + \dot{z}^2 U^2 = \mathcal{U}, \quad (64)$$

$$\ddot{t} = \ddot{z} = 0 \Rightarrow t = \gamma\tau, z = v\tau, \quad (65)$$

$$U_{,\rho}(-qtU + \dot{t}^2 + \dot{z}^2U^4\rho) = 0. \quad (66)$$

Null geodesics parallel to the  $z$ -axis are not possible. For charged massive particles we determine their Lorentzian factor,  $\gamma$ , and their velocity parallel to the axis,  $v$ . We again find two distinct solutions

$$\gamma_{\pm} = \frac{U}{4} \left( q \pm \sqrt{q^2 + 8} \right), v_{\pm} = \sqrt{\frac{q^2 \pm q\sqrt{q^2 + 8} - 4}{8U^2}}. \quad (67)$$

The regions admitting solutions are summarized in Figure 6.

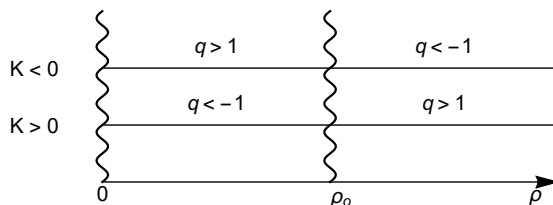


**Figure 6.** Regions, where  $z$ -electrogeodesic motion is possible for  $K \neq 0$

## 7. Conclusions and summary

Let us first state our results. We interpret the spacetime as actually consisting of two independent spacetimes separated by the outer singularity. Inside, the situation is complicated by the presence of two singularities pulling or pushing test particles in opposite directions, while outside there is only one singularity present in the spacetime. The outer singularity always has a negative mass per unit length as observed from both the outside and the inside. The inner singularity at  $\rho = 0$  then always has a positive mass. The parameter  $K$  appearing in the metric determines the sign of the charge per unit length of the singularities. For  $K > 0$  the inner singularity has a negative charge. The outer singularity has a negative charge when observed from the outside and a positive charge from the inside. For  $K < 0$  the signs are reversed. For weak fields,  $K \rightarrow 0$ , the magnitude of both the mass and charge densities is given by  $K/2$ , see Figure 7.

We investigated the physical properties of a cylindrically symmetric Majumdar-Papapetrou solution of Einstein-Maxwell equations (ECS) sourced by a non-compact, extremally charged linear singularity forming the axis of the spacetime.

Based on the form of the metric, we discovered that in addition to the axis singularity, the spacetime includes another singularity of different physical properties, which divides the spacetime into two causally separated regions. Since ECS is a solution of electro-vacuum equations both singularities are the only source of the resulting gravitational and electromagnetic fields. Our goal was to establish their physical parameters—i.e., mass and charge densities per unit length—and geometric characteristics.

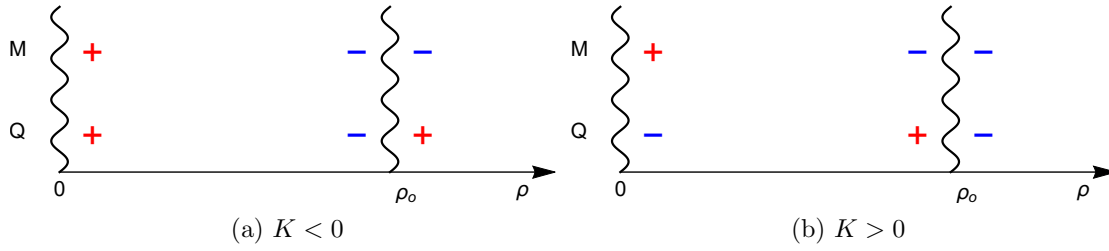


**Figure 7.** Schematic illustration of the sign of linear mass and charge densities of the singularities.

We calculated motion of charged test particles moving in preferred directions and compared it to the solution within the framework of classical mechanics. Based on the behavior of radial electrogeodesics, we found that the singularities are not covered by horizons and are thus naked in accordance with [3]. Next, we dealt with static trajectories and gained insight into the specific charge of the singularities. We then determined circular paths and regions where such motion is possible. One interesting result is a range of circular orbit radii and conditions on the spacetime parameters allowing the existence of two electrogeodesics of the same radius but differing angular velocities in the same direction. We then determined the classical limit of the circular velocities to again obtain information about the specific charge of the singularities.

When determining the mass of the sources of ECS, we also proceeded from the total energy of a region of spacetime containing the singularity. However, there is generally no way of determining locally the energy of the gravitational field in GR and we thus used several different definitions and compared them.

Using Israel formalism, we then regularized the spacetime by replacing the regions containing the singularities with flat space and continuing with ECS outside the respective cylindrical hypersurfaces, which then become the source of the gravitational and electromagnetic fields. We determined their charge and mass and compared them again for various spacetime parameters and also with the classical solution.

Using several independent methods, we thus clarified the meaning of the spacetime's structure and parameters and gained intuition about its physical interpretation. The results will broaden the knowledge of MP spacetimes with non-compact sources, which have not been paid much attention so far.

## Acknowledgements

JR was supported by Student Faculty Grant of Faculty of Mathematics and Physics, Charles University in Prague and by grant No. 504616 of Charles University Grant Agency. MZ was supported by Albert Einstein Center, Project of Excellence No. 14-37086G funded by the Czech Science Foundation.

## References

- [1] Majumdar S D 1947 *Phys. Rev.* **72** 930
- [2] Papapetrou A 1947 *Proc. Roy. Irish Acad.* **A51** 191
- [3] Hartle J B and Hawking S W 1972 *Communications in Mathematical Physics* **26** 87
- [4] Lemos J P S and Zanchin V T 1996 *Phys. Rev. D* **54** 3840
- [5] Thorne S 1964 *Phys. Rev.* **138** 251
- [6] Landau L D and Lifshitz E M 1980 *The Classical Theory of Fields*, Butterworth-Heinemann
- [7] Brown J D and York J W 1993 *Phys. Rev. D* **47** 1407
- [8] Poisson E 2007 *A Relativist's Toolkit: The Mathematics of Black-Hole Mechanics*, Cambridge University Press
- [9] Israel W 1966 *Nuov. Cim.* **44** 1, 1967 *ibid.* **48** 463
- [10] Kuchař K 1968 *Czech J. Phys.* B **18** 435
- [11] Ryzner J and Žofka M 2015 *Class. Quantum Grav.* **32** 205010



# Bibliography

- [1] Majumdar S D 1947 *Phys. Rev.* **72**, 930
- [2] Papapetrou A 1947 *Proc. Roy. Irish Acad.* **A51**, 191
- [3] Hartle J B and Hawking S W 1972 *Communications in Mathematical Physics.* **vol. 26**, issue 2, p. 87-101
- [4] Kastor D and Traschen J 1993 *Physical Review D* **vol. 47**, issue 12, p. 5370-5375
- [5] Griffiths J B and Podolsky J 2009 *Exact Space-Times in General Relativity*
- [6] Kuchař K 1968 *Základy obecné teorie relativity*
- [7] Lee J M 1997 *Riemannian Manifolds: An Introduction to Curvature*
- [8] Thorne S 1964 *Phys. Rev.* **138** 251-266
- [9] Ryzner J and Žofka M 2015 *Class. Quantum Grav.* **32** 205010
- [10] Landau L D and Lifshitz E M 1975 *The Classical Theory of Fields*
- [11] Lemos P S J and Zanchin V T 1996 *Phys.Rev.* **D54** 3840-3853
- [12] Brown J D and York J W 1993 *Quasilocal energy and conserved charges derived from the gravitational action* *Phys.Rev.* **D47** 1407-1419
- [13] Poisson E 2007 *A Relativist's Toolkit: The Mathematics of Black-Hole Mechanics*, Cambridge University Press
- [14] Laforgia A 1991 *Bounds for modified Bessel functions* *Journal of Computational and Applied Mathematics* **vol. 34**, issue 3, p. 263-267

